Appendix 1. Geohydrologic Framework

This appendix contains two sections. The first briefly discusses the framework of glacial deposition during the Quaternary period. The second summarizes the geohydrology by model subregion, with emphasis on the bedrock hydrostratigraphy.

1.1 Quaternary Framework at Regional Scale

The advances and retreats of the southern Laurentide Ice Sheet are responsible for the glacial deposition in the Upper Midwest of the United States. Figure 1–1, adapted from Mickelson and Colgan (2004), shows the major lobes in the vicinity of Lake Michigan that advanced during the last glaciation (from about 25,000 to 8,000 years ago). Each lobe is associated with multiple types of deposition environments (for example, tills, coarse stratified deposits, lacustrine and deltaic deposits, outwash plains). The distribution of surficial tills is one indicator of the dominant texture of glacial material in different parts of the model domain. Figure 1–2, adapted from Mickelson and others (1983), shows the general pattern. Concentrations of clayey till are evident along the rim of most of Lake Michigan, southwest of Green Bay, and in eastern Michigan. Sandier tills are present south of Lake Superior and in much of the western Lower Peninsula of Michigan, extending into parts of northern Indiana. In some areas, the surficial deposits are underlain by very thick glacial sequences, notably in parts of the northern Lower Peninsula of Michigan, where total thicknesses can exceed 1,000 ft. Much of this material is probably fine stratified drift associated with large deltas (Kevin Kincare, formerly Michigan State Geological Survey, now U.S. Geological Survey, oral commun., March 9, 2007). Glacial deposits are not the only unconsolidated deposits that mantle the bedrock. Alluvial sediments fill narrow stream valleys, and coastal dunes are prominent along Lake Michigan's southeast shoreline.

As part of the LMB modeling study, a database and GIS coverage of the unconsolidated stratigraphy was prepared in terms of the distribution of coarse and fine deposits (see section 4 of the main text, "Model Construction"). The coverage is consistent with the regional overview, but it uses more fine-scaled mapping and a vast number of water-well driller logs to provide detail in both the horizontal and vertical dimensions.

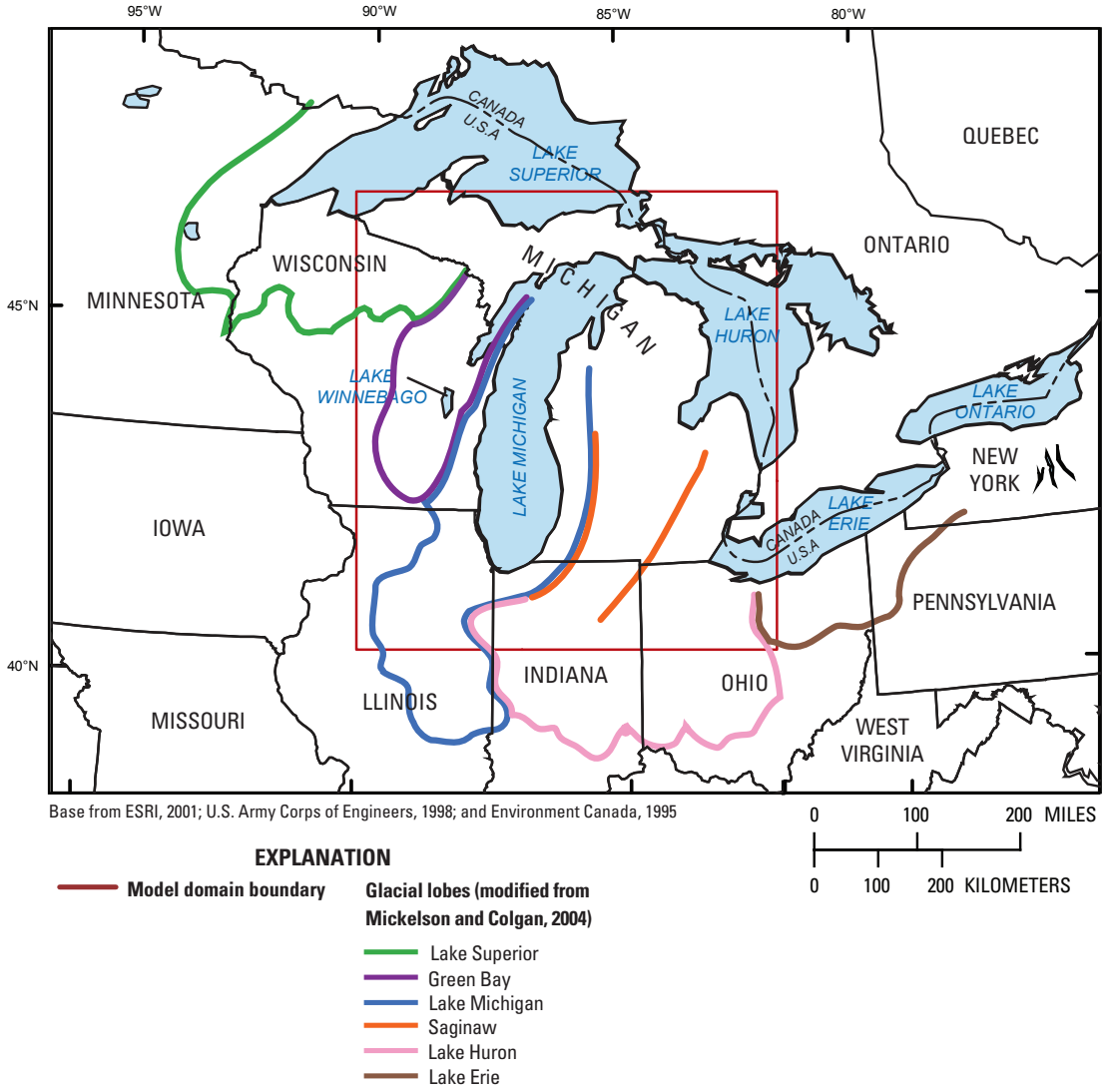

Figure 1–1. Glacial lobes in model area.

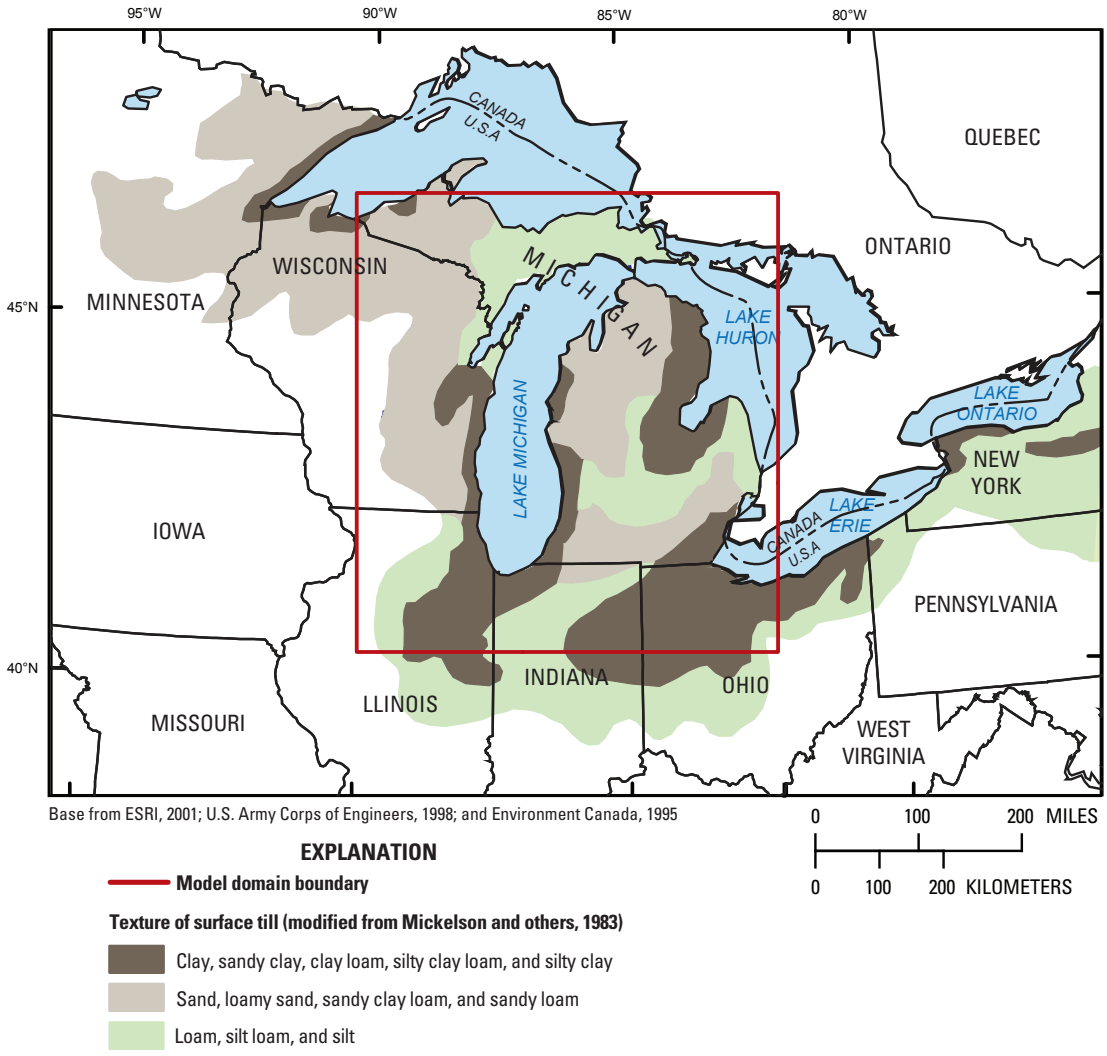

Figure 1–2. Texture of surficial tills.

1.2 Geohydrologic Framework by Model Subregion

The geologic information presented in this section is, in large measure, abridged from the following references. Formal nomenclature of the rock-stratigraphic units described differs somewhat from state to state:

3. Northeastern Illinois: Meyer and others (2009)
4. Southeastern Wisconsin: Feinstein and others (2005)
5. Northeastern Wisconsin: Krohelski (1986)
6. Northern Indiana: Eberts and George (2000)
7. Southern and Northern Lower Peninsula, Michigan: Westjohn and Weaver (1998)

1.2.1 Northeastern Illinois

(see schematic in fig. 12 of the main the main report text)

The sedimentary Paleozoic geology in northeastern Illinois consists of sandstone, siltstone, shale, and carbonate units that thicken and dip gently to the east from the Kankakee Arch toward the Michigan Basin. This section briefly describes these units, beginning with the oldest Paleozoic rocks.

The Mount Simon Sandstone (Cambrian) underlies all of northeastern Illinois and parts of southern Wisconsin. It is primarily fine- to coarse-grained sandstone. Although the Mount Simon Sandstone (or Formation) supplies fresh groundwater to wells in southern Wisconsin, its use in Illinois is limited by the presence of water with dissolved concentrations of 10,000 mg/L or more within the aquifer unit (Visocky and others, 1985).

The Eau Claire Formation (Cambrian) consists of fine- to medium-grained sandstone with some interbedded gray shale; dolomite, sometimes sandy, with interbedded greenish gray shale; and dolomitic siltstone with interbedded shale. In northeastern Illinois, sandy materials occur in the lower Elmhurst Sandstone Member, but use of this member as an aquifer is limited in northeastern Illinois by the presence of saline water (Visocky and others, 1985). More generally, the Eau Claire Formation is a confining unit in northeastern Illinois that limits movement of groundwater between the overlying Ironton-Galesville aquifer and the underlying Mount Simon aquifer.

The Ironton and Galesville Sandstones (Cambrian) are generally fine to medium grained and are locally silty and dolomitic. These sandstones become finer grained southward and eastward from the Kankakee Arch area, grading into finer grained siliciclastic rocks and dolomite in central Illinois, central and eastern Indiana, and central Michigan. The Ironton-Galesville Sandstones constitute a productive aquifer that furnishes significant quantities of potable water to wells in southern Wisconsin and northern Illinois, but the groundwater within it is too saline for most purposes in central Illinois, Indiana, and Michigan (Visocky and others, 1985).

The Franconia Formation (Cambrian) consists of poorly sorted, fine-grained siliciclastic sediments and dolomite that grade southward and eastward from the Kankakee Arch area to purer dolomite (Willman and others, 1975; Young, 1992). Equivalent lithostratigraphic units include the Tunnel City Group of Wisconsin (Ostrom, 1966; Young and Siegel, 1992) and the Franconia Sandstone (Munising Group) of Indiana and Michigan. In northeastern Illinois, the Franconia Sandstone is overlain by the Potosi Formation, which is a fairly pure dolomite throughout its distribution in Illinois; however, sand content increases northward (Buschbach, 1964), and the largely dolomitic rocks of the equivalent rocks in Wisconsin contain greater quantities of sand, silt, and clay (Young and Siegel, 1992). In Indiana and Michigan, the relatively pure dolomite correlating to the Potosi Dolomite and overlying Eminence Formation in Illinois are not distinguishable, and the two units are therefore lumped as the Potosi Dolomite in Indiana and as the Trempealeau Formation in Michigan (Droste and Patton, 1985; Catacosinos and Daniels, 1991). The Potosi-Franconia Formation is the oldest of the hydrostratigraphic units exposed at bedrock surface in Illinois, where it forms the bedrock surface in a limited area of north-central Illinois on the south side of the Sandwich Fault Zone (fig. 8*B* in the main report text) (Willman and others, 1975; Kolata and others, 1978). Where exposed at bedrock surface, the presence of secondary porosity in these materials probably increases well yields somewhat; but, in general, the Potosi-Franconia Formation is a confining throughout the extent of the LMB model in northeastern Illinois.

The Prairie du Chien Group (Ordovician) in northeastern Illinois is underlain by the Eminence Formation (Cambrian). The Eminence Formation is a sandy dolomite that becomes less sandy southward and eastward from the Kankakee Arch area so that it is distinguished with difficulty from overlying and underlying dolomites in central Illinois, Indiana, and Michigan (Willman and others, 1975; Droste and Patton, 1985; Catacosinos and Daniels, 1991). The sandy dolomites of the Eminence Formation grade northwestward into a sandstone unit, known as the Jordan Sandstone in Illinois and the Jordan Formation in Wisconsin. The Prairie du Chien Group consists primarily of finely to coarsely crystalline, cherty dolomite with lenses of sandstone. The Prairie du Chien-Eminence complex is most accurately characterized as a confining unit in northeastern Illinois, despite the fact that the Jordan Sandstone and other lenses of sandstone within the predominantly dolomitic unit may be important aquifers where present. These sandstones are not well developed in northeastern Illinois, however. Where exposed at the bedrock surface, secondary porosity permits small groundwater supplies to be obtained from the carbonates of this unit.

The St. Peter Formation is a sandstone unit within the Ancell Group (Ordovician) of Illinois. In northern Illinois the upper St. Peter grades laterally into the silty Glenwood Formation. Where the St. Peter Sandstone is present in northern Illinois, it is an important aquifer supplying many large municipal wells, often in combination with the Ironton-Galesville Sandstones.

The Sinnipee Group is represented by dolomites of the Galena and Platteville Formations in Illinois and is present over most of the northeastern part of the State. These rocks consist of relatively pure limestone and dolomite with subordinate amounts of shaly limestone and dolomite. Small to moderate supplies of groundwater are obtained from the upper 50–100 ft of the Galena-Platteville in areas where the unit is exposed at bedrock surface and permeability has been increased through development of secondary porosity.

The Maquoketa Group of Illinois consists predominantly of dolomitic shale, argillaceous dolomite, and argillaceous limestone. Correlative lithostratigraphic units include the Maquoketa Group in Indiana (Shaver and others, 1986) and the Maquoketa Formation in Wisconsin. The Maquoketa Group is generally considered an important confining unit in the region, although its more carbonate-rich facies—where present within 50–100 ft of the bedrock surface—provide small groundwater supplies, owing to secondary porosity (Csallany and Walton, 1963). Like the Sinnipee Group, the entire Maquoketa Group is a confining unit in places where there is no interval of secondary-porosity development near bedrock surface. The subcrop of the unit crosses northeastern Illinois. The absence of the unit due to erosion over the northern and western parts of the subregion exercises an important control on regional groundwater flow.

A series of Silurian carbonates is present in the eastern and southern parts of northeastern Illinois. These rocks consist largely of dolomite; but lesser amounts of shale are present, and the dolomites may be argillaceous, silty, and clean. Secondary porosity in the 50–100 ft of the Silurian underlying the bedrock surface provides small to moderately large quantities of groundwater to wells in the subregion (Csallany and Walton, 1963).

Quaternary deposits consist of tills and of sand, gravel, clay, and silt. Most of these materials were deposited during glaciation of the area during the Pleistocene, but postglacial sand, lacustrine clays and silts, and anthropogenic fill are present in some areas, including the bottom of Lake Michigan (Gross and others, 1970). Where they are thick and laterally extensive, sand and gravel deposits within the Quaternary deposits can provide large groundwater supplies, and till, clay, and silt beds function as confining units.

1.2.2 Southeastern Wisconsin

(see schematic in fig. 12 of the main report text)

The bedrock hydrostratigraphy of southeastern Wisconsin (Eaton and others, 1999) consists of Paleozoic sedimentary units generally thickening to the east. In most places, Pleistocene deposits of till, sand and gravel, or lake sediment cover the bedrock units, and bedrock outcrops are rare. Cambrian-Ordovician units rest on the Precambrian crystalline basement rocks, which transmit little water and form the bottom boundary to the aquifer system. In ascending order, the major water-producing units of the deep aquifer are sandstones of the Mount Simon Formation, the Wonewoc Formation (equivalent to the Ironton and Galesville Sandstones in northeastern Illinois), and the St. Peter Formation.

Between the Mount Simon Formation and the Wonewoc Formation lies the Eau Claire Formation, composed of shale and sandstone. A laterally extensive shaly zone within the Eau Claire Formation forms a confining unit over much of southern Wisconsin. Rocks between the Wonewoc and St. Peter Formations are identified with the Trempeleau and Tunnel City Groups (correlated with the Franconia Formation in northeastern Illinois). They can also form a leaky confining unit and are made up of interbedded sandstone, shale, siltstone, and dolomite. Overlying the St. Peter Formation, dolomite of the Sinnipee Group and shale of the Maquoketa Formation together make up a major confining unit between deep and shallow aquifers. The hydraulic properties of the Sinnipee Group dolomite depend on whether it is overlain by the Maquoketa. Where it is not, and forms the uppermost bedrock unit, it is highly weathered and relatively permeable. Deep wells are generally cased through the Maquoketa Formation and open from the Sinnipee Group to the St. Peter Formation or lower in the deep part of the flow system. The Silurian-Devonian aquifer (predominately dolomite) and the unlithified Pleistocene materials (till, sand and gravel, and lake sediment from several glacial lobes) constitute important shallow sources of public and domestic water supply.

The Mount Simon Formation, which is absent to very thin in the northern part of southeastern Wisconsin thickens to more than 1,500 ft at the Illinois State line to the south. Much of this thickening occurs abruptly along a southwest-northeast fault zone (fig. 8*B*). This feature is commonly called the Waukesha Fault zone, but its geometry and characteristics are poorly understood. In the thickened section of the Mount Simon, geophysical logs suggest the presence of a fine-grained interval that extends from about 500 to 800 ft below the top of the unit over much of southeastern Wisconsin. The overlying Eau Claire Formation, the Wonewoc Formation (Ironton and Galesville Sandstones), and the Prairie du Chien Group are not continuous throughout the study area. In contrast, the St. Peter Formation varies in thickness but is generally continuous. It is commonly capped by the silty Glenwood Formation.

All southeastern Wisconsin sedimentary rocks dip gently to the east and south, and erosion at the bedrock surface has truncated the uppermost units so that the Maquoketa Formation and overlying rocks are present in only the eastern part of southeastern Wisconsin. Unlithified Quaternary deposits blanket these rocks at thicknesses of less than 25 ft to more than 400 ft and are thicker in areas where the bedrock surface is incised. Ancient drainage cut down through the shallowest bedrock—penetrating the Silurian-Devonian dolomite, the shale of the Maquoketa Formation, and the dolomite of the Sinnipee Group—resulting in buried valleys filled with Quaternary deposits. Where dolomite of the Sinnipee Group is the uppermost bedrock unit in the west, it forms a minor part of the deep aquifer system. Quaternary deposits can form aquifers in areas where they are sufficiently thick and are dominated by sand and gravel, but they act as confining units near Lake Michigan, where they are primarily clays and silts.

1.2.3 Northeastern Wisconsin

(see schematic in fig. 12 of the main report text)

Northeastern Wisconsin is underlain by Paleozoic sedimentary rocks that range in age from Cambrian to Silurian. The Paleozoic rocks and the Precambrian surface slope to the east under Lake Michigan toward the Michigan Basin at about 30 to 40 ft/mi. Erosion has removed the Silurian rocks and the Maquoketa Formation in the central and western part of the area. The total thickness of the Paleozoic rocks ranges from zero in the west, where Precambrian rocks are at or near land surface, to almost 2,000 ft along the Lake Michigan shoreline.

The basal unit of the Cambrian is the Elk Mound Group, which overlies the Precambrian. The group normally comprises (from bottom to top) the Mount Simon, Eau Claire, and Wonewoc Formations (equivalent to the Ironton and Galesville Sandstones). The group name is used because the Eau Claire Formation cannot be identified in much of northeastern Wisconsin, and the sandstones of the Mount Simon and Wonewoc Formations commonly cannot be distinguished from one another. In areas where they can be distinguished, the Mount Simon Formation consists of poorly cemented, subangular, fine to very fine grained sandstone, which locally may be silty. The Wonewoc Formation consists of poorly cemented, subrounded, medium- to coarse-grained sandstone. As a whole, the Elk Mound Group is an important aquifer in this area.

The Cambrian Trempeleau and Tunnel City Groups overlie the Elk Mound Group. They can be roughly correlated with the Franconia Formation and Potosi Dolomite to the south. Both groups contain siltstone, sandstone, and dolomite layers, which as a whole allow lateral flow but resist vertical flow.

At the bottom of the Ordovician System is the Prairie du Chien Group, which is generally dolomite with varying amounts of chert. Although karst has been identified in the Prairie du Chien, it does not generally function as an aquifer. Overlying the Prairie du Chien Group is the Ancell Group, consisting of the St. Peter and Glenwood Formations. The Glenwood is a silty sandstone, whereas the St. Peter consists of a poorly cemented fine- to medium-grained sandstone with a lower sandy shale member. The St. Peter Formation varies areally in thickness because of erosion of the Prairie du Chien strata in pre-St. Peter times, but it can be more than 200 ft thick and serves as an important aquifer.

The Ancell Group is overlain by the Ordovician Sinnipee Group which includes the Platteville, Decorah, and Galena Formations. The Platteville and Galena Formations consist of dolomite and shaly layers. The Galena is distinguished from the Platteville by its chert content. The Decorah Formation is predominantly shale. The Ordovician Maquoketa Formation overlies the Sinnipee Group roughly east of a line that extends along the centerline of Green Bay to the south. This formation consists of dolomitic shale and dolomite. It is a confining unit of very low permeability.

Also east of a line that extends along the strike of Green Bay to the south are rocks of Silurian age. They are composed of massive dolomite which, where weathered or fractured, forms an important aquifer unit.

Quaternary deposits of variable thickness overlie the Paleozoic rocks. Tills and fluvial sands and gravels were deposited by a succession of glacial episodes, whereas large volumes of generally fine-grained lacustrine deposits spreading southeast of Green Bay are associated with the action of ice-dammed lakes. Modern sediments deposited by wind and water and by the accumulation of organic matter also are present. The sand and gravel deposits are typically used as aquifers.

1.2.4 Upper Peninsula, Michigan

(see schematic in fig. 13 of the main report text)

The geologic sequence found in northeastern Wisconsin of slightly dipping Paleozoic sedimentary layers underlain by crystalline rocks and overlain by glacial deposits is also present in the Upper Peninsula of Michigan. However, some distinctive features affect the groundwater system in the UP_MI subregion. Toward the northwestern and northern edges of the model domain, rocks correlative to the Mount Simon sandstone are underlain not by Precambrian crystalline rocks but by Precambrian sedimentary layers, notably the Jacobsville Sandstone (see fig. 11 in the main report text). The Jacobsville was formed by aeolian and alluvial sands infilling the Midcontinental Rift zone, which formed 1.1 billion years ago along an axis stretching between present-day Lake Superior and Kansas (Chase and Gilmer, 1973). It serves as bedrock aquifer, along with the package of overlying sedimentary rocks which in the UP_MI are called the Munising Group, and correlate with the sequence of Mount Simon Sandstone, Eau Claire Formation, and Ironton and Galesville Sandstones to the south (Dorr and Eschmann, 1970). The Precambrian and Cambrian-Ordovician sedimentary rocks dip generally southeast into the Michigan Basin. Silurian dolomites overlie the Cambrian-Ordovician rocks but are limited in extent to a rim close to the Lake Michigan shoreline. The cover of glacial material deposited between about 2 million and 11,000 years ago defines a hummocky topography marked by ponds, swamps, bogs, and rivers. In places, especially north of Green Bay, the glacial cover is thin and the bedrock is very near or at the land surface.

1.2.5 Northern Indiana

(see schematic in fig. 14 of the main report text)

The sedimentary rocks in northern Indiana lie at the southern boundary of the Michigan Basin and the northern boundary of the Findlay and Kankakee Arches. They dip to the north and range in age from Precambrian through Mississippian and correlate with the units to the west in northeastern Illinois. The bedrock units of primary interest range in age from Ordovician through Devonian-Mississippian units.

The bedrock units of Ordovician age consist predominantly of shale with some limestone. They are stratigraphically equivalent to the Maquoketa Group to the west in Illinois and act as a confining unit. This unit is overlain by limestones and dolomites of Silurian and Devonian age, which also contain evaporite deposits. They thicken to the north, reaching 2,500 ft in thickness at the border with southeastern Michigan. The carbonate rocks are overlain mostly by shales of Devonian and Mississippian age. The carbonate and fractured shales of the bedrock sequence are capable of sustaining low-yielding wells.

The bedrock is overlain by Quaternary glacial deposits resulting from multiple glacial advances. These deposits bury numerous valleys in the bedrock surface. The glacial sediments include ground- and end-moraine deposits, ice-contact stratified drift, glaciolacustrine deposits, and outwash deposits. Surficial glaciolacustrine deposits are present in the lowlands adjacent to Lake Michigan and Lake Erie and are the product of glacial lakes that formed along the margins of retreating ice. Because they are dominated by lake-bottom silts and clays, the lake deposits act chiefly as confining units, although minor sands and gravels mark the beaches of ancient shorelines. Outwash deposits, which commonly fill the ancient drainage systems, serve as aquifers.

1.2.6 Southern Lower Peninsula and Northern Lower Peninsula, Michigan

(see schematic in fig. 15 of the main report text)

Mississippian and younger geologic units form a regional system of aquifers and confining units in the central Lower Peninsula of Michigan. Bedrock aquifers and confining units are overlain by surficial glaciofluvial aquifers, which are complexly intercalated with confining beds composed of glacial till and fine-grained lacustrine deposits.

The Coldwater Shale of Early Mississippian age is the basal unit of the Michigan Basin regional aquifers. The Coldwater Shale consists primarily of gray to dark-gray shale and acts as a major confining unit.

The Marshall Sandstone of Early Mississippian age overlies the Coldwater Shale in most of the Lower Peninsula. Sandstone forms only part of the formation; it is commonly interbedded with limestone, dolomite, siltstone, and shale. The composite thickness of units that form the Marshall Sandstone ranges from 130 to 360 ft (Monnett, 1948; Ells, 1979; Harrell and others, 1991). Two relatively thick, stratigraphically continuous blanket sandstones constitute the bulk of the formation in most areas. The upper sandstone is formally named the Napoleon Sandstone Member (commonly referred to as the "Upper Marshall sandstone"); the lower sandstone has no formal name. The composite thickness of the blanket sandstones is typically 75 to 200 ft. Freshwater is present in the Marshall aquifer only in areas where it is a subcrop beneath glacial material.

The Michigan Formation of Late Mississippian age is an interbedded sequence of shale, limestone, dolomite, gypsum or anhydrite, siltstone, and sandstone (listed in order of decreasing abundance). Cumulative thickness of all Michigan Formation lithologies is typically 300 to 400 ft (Harrell and others, 1991). Geophysical logs show that thickness of individual Michigan Formation strata is typically less than 20 ft. Typically, 6 to 10 gypsum beds are intercalated with shale and (or) limestone and (or) dolomite. Some sandstones at or near the base of the Michigan Formation are currently or were formerly natural-gas reservoirs. Typically, these elongate, discontinuous sandstone bodies are thin (typically less than 10 ft, but as thick as 30 ft) and are intercalated with evaporite, dolomite, limestone, and shale. Regionally, the Michigan Formation functions as a confining unit.

The Bayport Limestone of Late Mississippian age consists of sparsely fossiliferous to highly fossiliferous limestone, dolostone, sandy limestone, cherty limestone, and sandstone (Bacon, 1971; Lasemi, 1975; Ciner, 1988). In the center of the Michigan Basin the thickness of the Bayport Limestone is typically 50 to 100 ft (Cohee and others, 1951; Harrell and others, 1991). It yields water to wells.

The Parma Sandstone, which consists of medium- to coarse-grained sandstone, is typically less than 100 ft thick (Cohee and others, 1951). Because the Parma Sandstone seems to interfinger with the Bayport Limestone in many areas of the central part of the Michigan Basin, these units may be time-stratigraphic equivalents (Westjohn and Weaver, 1996). Where present, it serves as an aquifer. The Parma, like the Bayport Limestone, contains freshwater only in subcrop areas where it is in direct hydraulic connection with glacial deposits.

Pennsylvanian rocks in the Michigan Basin have been formally subdivided into the Parma Sandstone (Lower Pennsylvanian), the Saginaw Formation (Lower Pennsylvanian) and the Grand River Formation (Middle Pennsylvanian). These Pennsylvanian units consist mostly of alluvial and deltaic deposits (Wanless and Shideler, 1975). The Saginaw Formation, which constitutes the bulk of the Pennsylvanian rock sequence, consists of interbedded sandstone, siltstone, shale, coal, and limestone. The depositional sequence of these rock units is rhythmic in many areas of the basin; deposits are typical of cyclothem-type strata, which are characteristic of Pennsylvanian-age sediments in other areas of the United States (Weller, 1930).

The Saginaw Formation acts as as confining unit in locations where it is predominantly shale, separating the aquifer constituted by the sandstone-rich Grand River Formation and Saginaw sandstone horizons from the deeper Parma Sandstone and Bayport Limestone aquifers. The thickness of the Saginaw confining unit in the central part of the Michigan Basin typically ranges from 50 to 250 ft.

In places, the Grand River Formation and Saginaw sandstone horizons are separated from glacial deposits by 100 to 150 ft of overlying Jurassic red beds. The assemblage of plant microfossils in Jurassic red beds indicates that these sediments were probably deposited in ephemeral lakes that periodically occupied shallow, arid to semiarid desert-lake basins (Shaffer, 1969). The red beds are a confining unit, and the Saginaw aquifer contains saline water where it is overlain by these deposits.

Quaternary glacial deposits cover bedrock units almost everywhere in the Lower Peninsula of Michigan. Glacial deposits are probably products primarily of the Wisconsin stage of the Pleistocene Epoch, although deposits from older stages (Illinoian or pre-Illinoian) may underlie them (Eschman, 1985). The distinct lobate character of late Wisconsin glacial ice resulted in a landscape distinguished by multiple recessional moraines and outwash aprons in front of these moraines. These glacial landforms mark stillstand positions of different ice lobes. Glacial deposits in the study area can be separated into three general provinces: (1) Glacial deposits in the southern part are primarily recessional moraines and outwash deposits that formed at the front of retreating ice lobes. (2) Surficial deposits in the eastern lowlands are primarily basal-lodgment tills and fine-grained lacustrine sediments that were deposited in former proglacial lakes. (3) Glacial deposits of the northern half of the study area are primarily glaciofluvial deposits and some coarse-textured till (Farrand and Bell, 1982).

Very thick sequences of Paleozoic rock lie below the Coldwater Shale in the Michigan Basin. Devonian, Silurian, Ordovician, and Cambrian rocks can be identified in oil and gas logs and can be correlated with units updip of the basin associated with the Wisconsin/Kankakee Arches (Catacosinos, 1973; Catacosinos and others, 1990, 2001; Meyer and others, 2009; see also fig. 10 in the main report text). Some Devonian and Silurian units are tapped by water wells at the southern and northern ends of the Lower Peninsula at the edge of the Michigan Basin "bowl," but the other units are too deep and too saline to serve as aquifers. One distinctive feature of the very thick sequence of Silurian rocks is the prevalence of evaporite beds. These deposits tend to occur toward the middle and top of the Silurian sequence and are associated with the Salina Group.

References

Bacon, D.J., 1971, Chert genesis in a Mississippian sabhka environment: East Lansing, Mich., Michigan State University, M.S. thesis, 47 p.

Buschbach, T.C., 1964, Cambrian and Ordovician strata of Northeastern Illinois: Urbana, Ill., Illinois State Geological Survey Report of Investigation 218, 90 p.

Catacosinos, P.A., 1973, Cambrian lithostratigraphy of Michigan Basin: American Association of Petroleum Geologists Bulletin, v. 57, no. 12, p. 2404–2418.

Catacosinos, P.A., Daniels, P.A., Jr., and Harrison, W.B., III, 1990, Structure, stratigraphy, and petroleum geology of the Michigan Basin, *in* Leighton, M.W., Kolata, D.R., Oltz, D.F., and Eidel, J.J., eds., Interior cratonic basins: Tulsa, Okla., American Association of Petroleum Geologists Memoir 51, p. 561–601.

Catacosinos, P.A., and Daniels, P.A., Jr., 1991, Stratigraphy of Middle Proterozoic to Middle Ordovician formations of the Michigan basin, *in* Catacosinos, P.A., and Daniels, P.A., eds., Early sedimentary evolution of the Michigan Basin: Boulder, Colo., Geological Society of America Special Paper 256, p. 53–71.

Catacosinos, P.A.; Westjohn, D.B.; Harrison W.B., III; Wollensak, M.S.; and Reynolds, R.F., 2001, Stratigraphic lexicon for Michigan: Michigan Department of Environmental Quality, Geological Survey Division Bulletin 8, 56 p.

Chase, C.G., and Gilmer, T.H., 1973, Precambrian plate tectonics—The midcontinent gravity high: Earth and Planetary Science Letters, v. 21, p. 70–78.

Ciner, A.T., 1988, Stratigraphic and depositional environment of the Bayport Limestone of the southern Michigan Basin: Toledo, Ohio, University of Toledo, M.S. thesis, 133 p.

Cohee, G.V.; Burns, R.N.; Brown, Andrew; Brant, R.A; and Wright, D., 1950, Coal resources of Michigan: U.S. Geological Survey Circular 77, 56 p.

Csallany, Sandor, and Walton, W.C., 1963, Yields of shallow dolomite wells in northern Illinois: Illinois State Water Survey Report of Investigation 46, 44 p.

Dorr, J.A., and Eschman, D.F., 1970, Geology of Michigan: Ann Arbor, Mich., University of Michigan Press, 476 p.

Droste, J.B., and Patton, J.B., 1985, Lithostratigraphy of the Sauk Sequence in Indiana: Indiana Department of Natural Resources Geological Survey Occasional Paper 47, 24 p.

Eaton, T.T., Bradbury, K.R., and Evans, T.J., 1999, Characterization of the hydrostratigraphy of the deep sandstone aquifer in southeastern Wisconsin—Final report to the Wisconsin Deptartment of Natural Resources: Wisconsin Geological and Natural History Survey Open-File Report 1999–02, 30 p.

Eberts, S.M., and George, L.L., 2000, Regional ground-water flow and geochemistry in the Midwestern Basins and Arches aquifer system: Indiana, Ohio, Illinois, and Michigan: U.S. Geological Survey Professional Paper 1423–C, 103 p.

Ells, GD., 1979, The Mississippian and Pennsylvanian (Carboniferous) Systems in the United States—Michigan: U.S. Geological Survey Professional Paper 1110–J, p. 1–17.

Eschman, D.F., 1985, Summary of the Quaternary history of Michigan, Ohio, and Indiana: Journal of Geological Education, v. 33, p. 161–167.

Farrand, W.R., and Bell, D.L., 1982, Quaternary geology of southern Michigan: Ann Arbor, Mich., University of Michigan, Department of Geological Sciences, map sheet, scale 1:500,000.

Feinstein, D.T., Eaton, T.T., Hart, D.J., Krohelski, J.T., and Bradbury, K.R., 2005. Regional aquifer model for southeastern Wisconsin, Report 1—Data collection, conceptual model development, numerical model construction, and model calibration: Administrative report to the Southeastern Wisconsin Regional Planning Commission, 81 p.

Gross, D.L., Lineback, J.A., White, W.A., Ayer, N.J., Collinson, C., and Leland, H.V., 1970, Preliminary stratigraphy of unconsolidated sediments from the southwestern part of Lake Michigan: Illinois State Geological Survey Environmental Geology Note 30, 20 p.

Harrell, J.A., Hatfield, C.B., and Gunn, G.R., 1991, Mississippian System of the Michigan Basin—Stratigraphy, sedimentology, and economic geology, *in* Catacosinos, P.A, and Daniels, P.A, Jr., eds., Early sedimentary evolution of the Michigan Basin: Geological Society of America Special Paper 256, p. 203–219.

Kolata, D.R., Buschbach, T.C., and Treworgy, J.D., 1978, The Sandwich Fault Zone of northern Illinois: Illinois State Geological Survey Circular 505, 26 p.

Krohelski, J.T., 1986, Hydrogeology and ground-water use and quality, Brown County, Wisconsin: Wisconsin Geological and Natural History Survey Information Circular 57, 42 p.

Lasemi, Y., 1975, Subsurface geology and stratigraphic analysis of the Bayport Formation in the Michigan Basin: East Lansing, Mich., Michigan State University, M.S. thesis, 54 p.

Meyer, S.C., Lin, Y.-F., Roadcap, G.S., and Walker, D.D., 2009, Kane County Water Resources Investigations—Simulation of groundwater flow in Kane County and northeastern Illinois: Illinois State Water Survey Contract Report 2009–07, 425 p.

Mickelson, D.M.; Clayton, Lee; Fullerton, D.S.; and Borns, H.W., Jr.,1983, Late glacial record of the Laurentide Ice Sheet in the United States, *in* Wright, H.E., Jr., ed., Late Quaternary environments of the United States—Volume 1 (Porter, S.C., ed.), The Late Pleistocene: Minneapolis, University of Minnesota Press, p. 3–37.

Mickelson, D.M., and Colgan, P.M., 2004, The southern Laurentide ice sheet in the United States—What have we learned in the past 40 years?, *in* Gillespe, A.R., Porter, S.C., and Atwater, B.F., eds., Advances in research in Quaternary geology of the United States: New York, Elsevier, p. 1–16.

Monnett, V.B., 1948, Mississippian Marshall Formation of Michigan: American Association of Petroleum Geologists Bulletin, v. 32, p. 629–688.

Ostrom, M.E., 1966, Cambrian stratigraphy in western Wisconsin: Wisconsin Geological and Natural History Survey Information Circular 7, 79 p.

Shaffer, B.L., 1969, Palynology of the Michigan "Red Beds": East Lansing, Mich., Michigan State University, unpublished Ph.D. dissertation, 250 p.

Shaver, R.H.; Ault, C.H.; Burger, A.M.; Carr, D.D.; Droste, J.B.; Eggert, D.L.; Gray, H.H.; Harper, Denver; Hasenmueller, N.R.; Hasenmueller, W.A.; Horowitz, A.S.; Hutchison, H.C.; Keith, B.D.; Keller, S.J.; Patton, J.B.; Rexroad, C.B.; and Wier, C.E., 1986, Compendium of Paleozoic rock-unit stratigraphy in Indiana—A revision: Indiana Department of Natural Resources Geological Survey Bulletin 59, 229 p.

Visocky, A.P., Sherrill, M.G., and Cartwright, Keros, 1985, Geology, hydrology, and water quality of the Cambrian and Ordovician Systems in northern Illinois: Illinois State Geological Survey and Illinois State Water Survey Cooperative Groundwater Report 10, 136 p.

Wanless, H.R., and Shideler, G.L., 1975, Michigan Basin region, *in* McKee, E.D., and Crosby, E.J., coordinators, Paleotectonic investigations of the Pennsylvanian System in the United States: U.S. Geological Survey Professional Paper 853, Part I, Introduction and regional analyses of the Pennsylvanian System: p. 63–70.

Weller, J.M., 1930, Cyclical sedimentation of the Pennsylvanian Period and its significance: Journal of Geology, v. 38, p. 97–135.

Westjohn, D.B., and Weaver, T.L., 1996, Hydrogeologic framework of Pennsylvanian and Late Mississippian rocks in the central Lower Peninsula of Michigan: U.S. Geological Survey Water-Resources Investigations Report 94–4107, 44 p.

Westjohn, D.B., and Weaver, T.L., 1998, Hydrogeologic framework of the Michigan Basin regional aquifer system, central Lower Peninsula of Michigan: U.S. Geological Survey Professional Paper 1418, 47 p.

Willman, H.B.; Atherton, E.; Buschbach, T.C.; Collinson, C.; Frye, J.C.; Hopkins, M.E.; Lineback, J.A.; and Simon, J.A,. 1975, Handbook of Illinois stratigraphy: Illinois State Geological Survey Bulletin 95, 261 p.

Young, H.L., 1992, Summary of ground-water hydrology of the Cambrian-Ordovician aquifer system in the Northern Midwest, United States: U.S. Geological Survey Professional Paper 1405–A, 55 p.

Young, H.L., and Siegel, D.I., 1992, Hydrogeology of the Cambrian-Ordovician aquifer system in the northern Midwest, United States: U.S. Geological Survey Professional Paper 1405–B, 55 p.

Appendix 2. Inland Surface-Water Network

This appendix supplements the discussion of surface-water features in the main text. It gives details on the construction of the network of streams (major rivers and their tributaries) and water bodies (lakes and wetlands) that constitute the inland surface-water network for the LMB model. It also includes notes on the uncertainties and limitations that arise from mapping the real surface-water network to the simplified representation permitted by a coarse model grid.

2.1 Overview

The surface-water network was built from 64 nearfield and farfield drainage areas (or watersheds) defined for the Great Lakes Aquatic Gap Analysis Program (GAP) (U.S. Geological Survey, Great Lakes Science Center, 2004; Brenden and others, 2006)[1]. The watersheds (known as GAP processing units) are listed in the table 2–1.

The procedure consisted of intersecting GIS coverages of streams and other surface-water bodies from GAP databases with the LMB model grid. Water-body stages were extracted directly from elevations in the GAP databases. The locations of the stream arcs were matched with Digital Elevation Model (DEM) land-surface elevations to assign stages to stream arcs. Hydraulic conductance for a stream or water-body feature was computed as the product of the hydraulic conductivity of the bed material and the cross-sectional area of the water body divided by the thickness of the bed material. Inputs needed to specify the conductance terms for streams and for water bodies were assembled by grid cell. The stages and conductance terms of multiple surface-water elements in any grid cell were combined to generate a single representative stage and conductance for the cell, which in turn were identified with a single RIV boundary condition in the LMB model. The process involved the following steps:

1. Geographic Information Systems (GIS) datasets for 71 GAP watersheds that are wholly or partly in the Lake Michigan Basin model domain were assembled for both streams and water bodies, which include lakes/ponds and wetlands (swamps and marshes). GIS features include linear elements representing rivers, called stream arcs, and areal elements representing lakes and wetlands, called water-body polygons.
2. Average DEM elevations along the trace of stream arcs were assigned as stream stage; elevations in the GAP datasets were assigned to water-body polygons.
3. Stream arcs were analyzed and adjusted so that they preserve proper tributary relations according to information contained in the GAP databases.
4. The stages assigned stream arcs were interpolated to enforce the correct downstream routing of flow so that stage elevations decreased in the downstream direction.
5. Arbolate sums were employed to calculate stream width as a function of length of all upstream arcs. (Arbolate sums are discussed below in section A2.4.)
6. Stream arcs within the nearfield part of the model were censored such that only stream arcs with a calculated width greater than a specified threshold (8 ft) were simulated; nearfield water bodies also were censored to only permit bodies with a minimum area (20 acres).
7. For each cell containing at least one qualifying stream arc, stream conductance was calculated as the sum of arc contributions according to the expression

[arc Length]*[WIDTH]*[Bed K] / [Bed THK],

where

- arc Length is the length of the stream arc,
- WIDTH is the width of the stream arc,
- Bed K is the hydraulic conductivity of the streambed (Bed K =5 ft/d for all cases), and
- Bed THK is the thickness of the streambed material (Bed THK=1 ft for all cases).
- For each cell containing at least one qualifying water body, water-body conductance was calculated as the sum of polygon contributions according to the expression:

[polygon perimeter]*[Width of active area of exchange] *[Bed K] / [Bed THK],

where

- polygon perimeter is the perimeter of the water-body polygon,
- width of active area of exchange is assumed to be 20 ft for all water-body polygons,
- Bed K is the hydraulic conductivity of the bed of the water body (Bed K of Lake/Pond polygon = 2 ft/d; Bed K of Swamp/Marsh polygon = 0.5 ft/d; Bed K of Reservoir or Canal/Ditch polygon = 0.0 ft/d, and, therefore, these last elements are excluded from the input), and
- Bed THK is the thickness of the water-body bed material (Bed THK=1 ft for all cases).

8. If only streams were present in a cell, then the cell stage was set equal to the conductance-weighted average of the qualifying stream with the highest Strahler stream order (Strahler, 1952)[2]. For example, if the cell contained second- and third-order qualifying stream arcs, only the third-order arcs were used to compute the stage. If there were two third-order arcs and one had twice the conductance of the other, then its stage was weighted twice as much in the calculation.

[1] The GAP program, undertaken by the USGS in collaboration with state agencies and university researchers, combined bilogical and hydrological analyses to evaluate biological diversity of aquatic species and their habitats, and it identified gaps in the distribution and protection of these species and their habitats within the Great Lakes Basin.

[2] The Strahler stream order is a way to classify streams on the basis of a hierarchy of tributaries. First-order streams have no tributaries. When two first-order streams come together, they form a second-order stream. When two second-order streams come together, they form a third-order stream. When two streams of different order come together, they form a stream of maximum order of both (MATLAB Central, 2009).

Table 2–1. Surface-water network database organized by GAP processing units.

Processing unit code	Processing unit name	Processing state	Hydrologic unit	Hydrologic unit code (cataloging unit)
AUSAB	Au Sable	MI	Lake Huron	04070007
BADRI	Bad River	WI	Lake Superior	04010302
BIRCH	Birch	MI	Lake Huron	04080104
BOARD	Boardman	MI	Lake Michigan	04060105
BREVO	Brevoort	MI	Lake Michigan	04060107
CARPR	Carp	MI	Lake Huron	04070002
CEDAR	Cedar - MI	MI	Lake Michigan	04030109
CHEBO	Cheboygan	MI	Lake Huron	04070004, 04070005
CHIPP	Chippewa	WI	Upper Mississippi	0705001, 0705002, 07050003, 07050004, 07050005, 07050006, 07050007
CHOCO	Chocolay	MI	Lake Superior	04020201
CLINT	Clint	MI	Lake Erie	04090003
COOPE	Cooper	IL	Upper Mississippi	07080101
DEADR	Dead River	MI	Lake Superior	04020105
DETRO	Detroit	MI	Lake Erie	04090004
DOORP	Door Peninsula	WI	Lake Michigan	04030102
EDWAR	Edwards	IL	Upper Mississippi	07080104
ESCAN	Escanaba	MI	Lake Michigan	04030110
FISHD	Fishdam	MI	Lake Michigan	04030112
FXWLF	Fox Wolf	WI	Lake Michigan	04030201, 04030202, 04030203, 04030204
GALIE	Galien	MI	Lake Michigan	04040001
GRAND	Grand - MI	MI	Lake Michigan	04050004, 04050005, 04050006, 04050007
HURON	Huron - MI	MI	Lake Erie	04090005
ILLIN	Illinois	IL	Upper Mississippi	07120001, 07120002, 07120003, 07120004, 07120005, 07120006, 07120007,
				07130001, 07130002, 07130003, 07130004, 07130005, 07130006, 07130007, 07130008,
				07130009, 07130010, 07130011, 07130012
KALAM	Kalamazoo	MI	Lake Michigan	04050003
KAWKA	Kawkawlin	MI	Lake Huron	04080102
KEWEE	Keeweenaw	MI	Lake Superior	04020103
LSTCL	Lake St. Clair	MI	Lake Erie	04090002
MACAT	Macatawa	MI	Lake Michigan	04050002
MANIQ	Manistique	MI	Lake Michigan	04060106
MANIS	Manistee	MI	Lake Michigan	04060103
MAUME	Maumee	OH	Lake Erie	04100003, 04100004, 04100005, 04100006, 04100007, 04100008, 04100009
MENOM	Menominee	WI	Lake Michigan	04030106, 04030107, 04030108
MLWKE	Milwaukee	WI	Lake Michigan	04040003
MUSKE	Muskegon	MI	Lake Michigan	04060102

Table 2–1. Surface-water network database organized by GAP processing units.—Continued

Processing unit code	Processing unit name	Processing state	Hydrologic unit	Hydrologic unit code (cataloging unit)
OCNTO	Oconto	WI	Lake Michigan	04030104
OCQUE	Ocqueoc	MI	Lake Huron	04070003
ONTON	Ontonagon	MI	Lake Superior	04020102
OTTAW	Ottawa	MI	Lake Erie	04100001
PENDK	Pensaukee Duck	WI	Lake Michigan	04030103
PEREM	Pere Marquette	MI	Lake Michigan	04060101
PESHT	Peshtigo	WI	Lake Michigan	04030105
PIGEO	Pigeon	MI	Lake Huron	04080103
PIKER	Pike	WI	Lake Michigan	04040002
PLATT	Platte	MI	Lake Michigan	04060104
PRESQ	Presque Isle	MI	Lake Superior	04020101
PRTGE	Portage	OH	Lake Erie	04100010
RAISN	Raisin	MI	Lake Erie	04100002
RIFLE	Rifle	MI	Lake Huron	04080101
ROCKR	Rock River	WI	Upper Mississippi	07090001, 07090002, 07090003, 07090004, 07090005, 07090006, 07090007
SAGIN	Saginaw	MI	Lake Huron	04080201, 04080202, 04080203, 04080204, 04080205, 04080206
SHMAN	Sheboygan Manitowoc	WI	Lake Michigan	04030101
SINWA	Sinsinawa	WI	Upper Mississippi	07060005
SNDSK	Sandusky	OH	Lake Erie	04100011
STCLR	St. Clair	MI	Lake Erie	04090001
STJOM	St. Joseph - MI	MI	Lake Michigan	04050001
STMAR	St. Marys	MI	Lake Huron	04070001
STURG	Sturgeon	MI	Lake Superior	04020104
TAHQU	Tahquamenon	MI	Lake Superior	04020202
THUND	Thunder	MI	Lake Huron	04070006
TNMLE	Ten Mile	OH	Lake Erie	04100001
WABAS	Wabash	IL	Ohio	05120113
WAISK	Waiska River	MI	Lake Superior	04020203
WHITE	White	MI	Lake Michigan	04030111
WISCN	Wisconsin	WI	Upper Mississippi	07070001, 07070002, 07070003, 07070004, 07070005, 07070006

9. If only water bodies were present in a cell, then the cell stage was set equal to the conductance-weighted average of all the qualifying water bodies.
10. If both streams and water bodies were present in a cell, then the cell stage was set equal to the conductance-weighted average of the highest-order qualifying stream arcs only.
11. Nearfield cells with only streams or both streams and water bodies were set to RIV cells, with the parameter RIVBOT set 1 ft below stage elevation.
12. Nearfield cells with only water bodies were set to RIV cells, with RIVBOT set to the same elevation as the river stage to ensure that water bodies act only as drains and do not act as a source to groundwater.
13. For farfield cells, no censoring by minimum stream width or water-body area was done.
14. Stages for farfield cells were calculated according to same formulas as for nearfield stages (but all streams and water bodies qualified).
15. Any farfield cell containing a surface-water feature (the great majority) was set to a constant head equivalent to the average stage of the highest order stream, or if no stream, the largest water body.

Some of these steps are discussed in more detail in the following paragraphs.

2.2 Assembly of Geographic Information Systems (GIS) Datasets

GIS coverages of surface-water features were used in conjunction with a Digital Elevation Model (DEM) to calculate stage elevations for streams and water bodies to simulate the surface-water component of the LMB model. By use of ArcInfo GIS software, stream centerlines and water-body polygons were attributed with elevation values from a Digital Elevation Model (DEM) specified on 30-m (98-ft) centers.

The source of the surface-water feature coverage was the medium-resolution (1:100,000 scale) National Hydrography Dataset (NHD) (U.S. Geological Survey, 2009). The medium-resolution NHD is a seamless hydrography spatial dataset available for the entire United States. The various surface-water data were obtained by eight-digit Hydrologic Unit Code (HUC). An eight-digit HUC is a class in a standard watershed classification scheme based on a topographically defined set of drainage areas organized in a nested hierarchy by size. Nationally, the average size of an eight-digit HUC is approximately 1,400 mi^2. Once the data were gathered, they were merged to represent the major river drainage from the headwaters to the terminus for the drainage basins within the model area. Stream features were extracted from the NHD and converted to an arc coverage representing stream centerlines. The water-body features were also extracted from the NHD to create a polygon coverage consisting of lakes, wetlands, and double-bank streams (large streams may be very wide and can be represented as a polygon in the NHD such that instead of a centerline representing the stream, two lines or a double-bank stream results).

Taking advantage of existing Great Lakes Aquatic GAP databases, a hydrologically correct, drainage-enforced DEM was derived from the 1:24,000-scale National Elevation Dataset (NED). By using a multiresolution interpolation algorithm in ArcInfo called TOPOGRID (Environmental Systems Research Institute, 2003), the DEM surface was altered to reflect the locations of stream valleys and lakes in the NHD. The result of running TOPOGRID was a new elevation surface that accurately mapped the flow of water across the landscape by removing sinks that were largely artifacts as a result of the methods used to generate the source elevation data. The new elevation surface accounts for the flow of streams and the location of water bodies in the NHD. This adjustment to the elevation data is important to ensure that flow in the surface-water network is correctly routed from upstream locations to downstream locations. Also, as part of the Great Lakes Aquatic GAP, the NHD centerlines were edited to remove secondary flow lines; examples are lines that loop back on themselves, producing a circular flow, and areas where multiple lines diverge from a confluence into a series of braids. The representation of stream reaches was altered slightly from the source NHD data in that the edited stream line coverage followed a confluence-to-confluence rule, meaning individual stream reaches were always split at stream junctions regardless of the size of a contributing tributary. Additionally, stream reaches that overlay water bodies were split where the reach flows into and out of the water body. Stream reaches and water bodies were assigned unique identifiers, and stream reaches were attributed with Strahler stream order.

The NHD water-body reaches were intersected with a polygon coverage representing the LMB model grid to divide the NHD water-body reaches into unique reaches within each model cell. The centroid for each new water-body polygon was then calculated within ArcInfo. The elevation value at the centroid was then assigned from the hydrologically correct DEM to the water-body polygon.

Stream centerline stages and lengths within each model cell were exported from the GIS coverages and edited externally for further smoothing of downstream stage. Also, stages for water bodies and the areas within each model cell were exported from GIS for external editing. Finally, the x and y coordinates for the upstream and downstream ends of each stream segment were generated and exported. These coordinates were employed to compute lengths of stream arcs used in the routing and smoothing routines discussed next.

2.3 Routing and Interpolating Stages Assigned to Stream Arcs

The stream entries to the model form cascading networks of tributaries from lower to higher order streams. A single network of stream arcs determined by the GIS procedures described above is called a segment. It is important that the model input properly direct water flow in the segment so that higher stages represent upstream locations relative to lower stages. The stages assigned to stream arcs through the above GIS procedures occasionally had to be reinterpolated within ArcInfo to ensure that downstream segment order was maintained. In particular, the DEM assignments in many flat-lying areas were not sufficiently precise to ensure downstream order of stages.

An algorithm was devised to smooth the initial assignment of stages along a segment. It included the following provisions when one arc in a segment or part of a segment violated downstream order:

- If a segment consisted of two arcs and the stage assigned the second was initially greater than the first, then the second was set equal to the first.
- If more than two arcs were in a segment and the slope of the initially assigned stages between any pair of arcs was upward in the downstream direction but less than or equal to 0.00001, then the second stage was set equal to the first.

- If multiple arcs were in a segment and over a set of three model cells and the slope of the initially assigned stages was downward but the elevation of the middle cell was either lower than the third cell or higher than the first cell, then the slope between the arcs in the first and third cells was calculated and the stage of the second arc was linearly interpolated on the basis of its position along the stream segment.

It also can happen that the violations within a segment involve more than one arc at a time so that the profile of stream stages takes the form of an undulating "wave." This is manifested as multiple places along a stream line where the upstream end has a lower stage than the downstream end. In such cases, the first arc upgradient and the first arc downgradient of the "wave" was identified, the slope over the distance of the segment was calculated, and the stages for arcs in between were assigned on the basis of linear interpolation along the stream segment. In the rare instance that the wave extended to the downgradient end of the segment, then stage assignments were based on an assumed gradient of 1E−5 ft/ft. Corrections to the stage-assigned stream arcs were common. For example, in the Lower Peninsula of Michigan (both nearfield and farfield), there are a total of 12,940 stream segments composed of 67,304 arcs. About 8.5 percent of the stages assigned these arcs were smoothed to preserve downstream order; the remaining arcs kept their initial DEM attributes. The corrected set of stages was then censored to include only those whose widths were above the selected threshold (that is, 8 ft). The qualified arcs were matched to the grid, then those associated with the highest-order streams present in a model cell were combined (weighted by conductance) to select the representative stage for the cell.

2.4 Calculation of Widths by Arbolate Sums

The conductance calculation for simulated streams in model cells is a function of the width assigned the stream arcs. In the absence of width information in the GAP databases, a regression equation was used to define a relation between a representative stream *length*, defined as the distance from the stream arc of interest to its originating headwater, and the *width* of the stream arc. This representative stream length is called the "Arbolate sum" following the method of Bartošová and others (2004). For this application, the length includes the length of the stream arc under consideration. Figure 2–1 shows the location of 152 streamgages in Michigan with a known relation between the Arbolate sum (upstream length) and steam width. Figure 2–2 shows the best-fit relation for these locations determined from regressing the stream width to the upstream distance.

The nonlinear best-fit equation is

$$y = 0.1193 * x^{0.5032} \quad [R^2 = 0.89]$$

where

y is width (feet), and
x is upstream length (meters).

The derived relation implies, for example, that a width of 8 ft corresponds to an upstream length of 2.65 mi. This relation was applied to calculate the width of all the stream arcs in the LMB model domain as a function of the Arbolate sum. For stream arcs representing headwaters, half the arc length was used to calculate width. For stream arcs downgradient from headwaters, half the arc length plus the entire distance of upgradient arcs was used.

It is useful to correlate the order of streams at streamgage locations with the distribution of widths recorded at the same locations (table 2–2).

Very few streams of order 1 display widths greater than 8 ft (3.7 percent), whereas the great majority of order 2 streams and virtually all order 3 streams are more than 8 ft wide. Cumulative distribution plots for observed stream widths for Wisconsin and Michigan show that 10 percent of stream locations are greater than 50 ft wide; the median width is 7.8 ft in Wisconsin and 8.9 ft in Michigan.

2.5 Selection Criteria for Streams and Water Bodies

One of the most important decisions in model construction is the choice of level at which the stream and water-body network delineated by the GIS databases is actually incorporated into the model as internal boundary conditions. Width and area thresholds for stream arcs and water-body polygons produce the percentage distributions listed in table 2–3 for inland nearfield cells in the LMB model.

It is clear from the first entry in table 2–3 that inclusion of all streams and water bodies mapped for the model nearfield would assign head-dependent boundary conditions to most water-table cells. Because the presence of a RIV boundary condition in a cell strongly limits head changes in response to pumping or recharge variations, incorporating all mappable surface-water features into the model would effectively fix the water-table elevation across the model through time.

The choice was made to censor stream arcs to at least 8 ft in width and water bodies to at least a 20-acre area. The 8-ft threshold limits qualifying streams mostly to order 2 and above, but it does allow order 1 streams to participate once they are sufficiently wide (equivalent to having upstream length greater than 2.65 mi). The thresholds selected imply that about 57 percent of nearfield water-table cells are constrained by head-dependent boundaries. The selection represents a rough compromise, one intended to represent a surface-water network in the model dense enough to prevent spurious simulated water-table mounding with reasonable input parameters, but not so dense that the water-table solution is almost everywhere constrained (see discussion in section 3, "Conceptual Model").

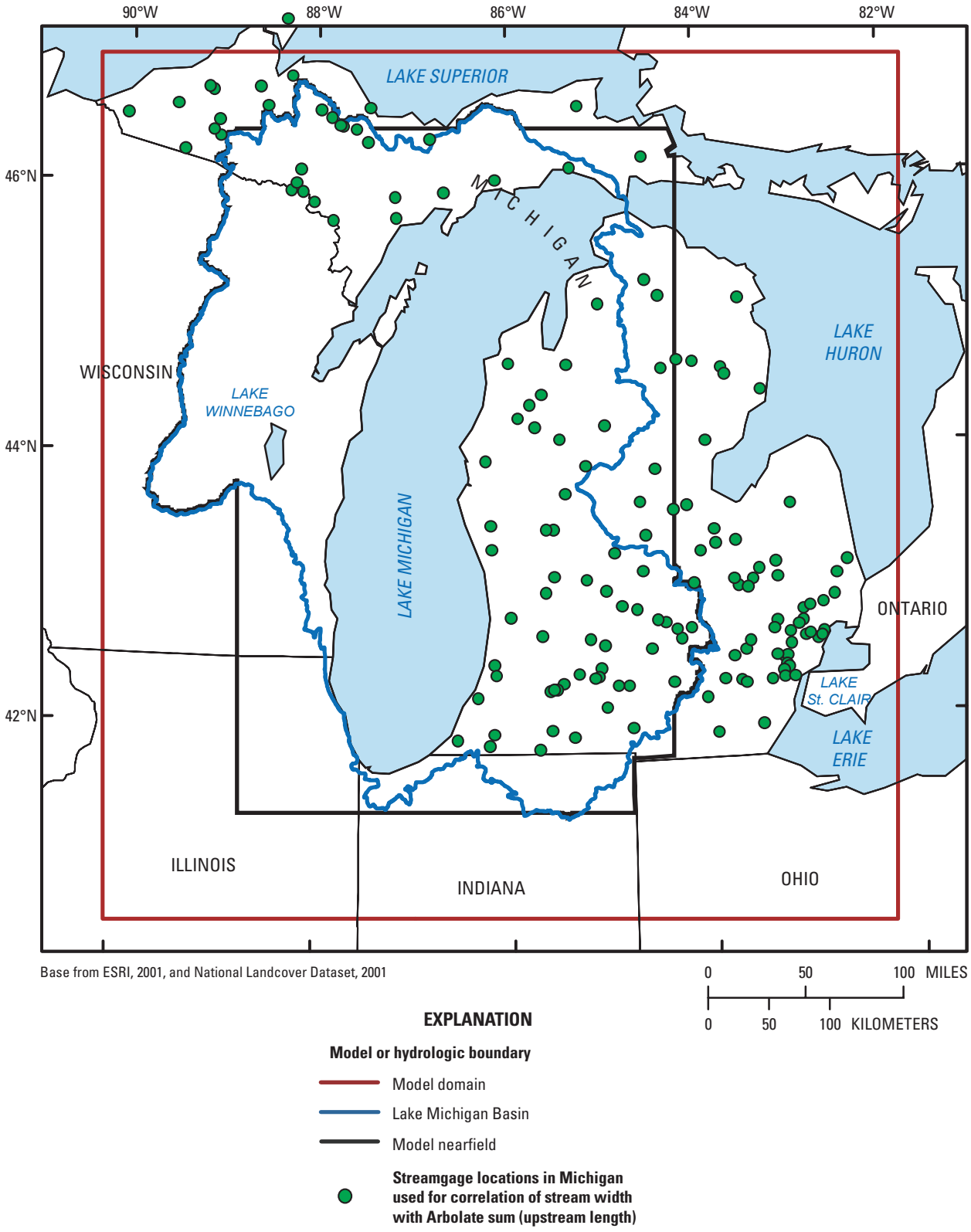

Figure 2–1. Location of USGS streamgages in Michigan used to determine relation between Arbolate sum (upstream distance) and stream width.

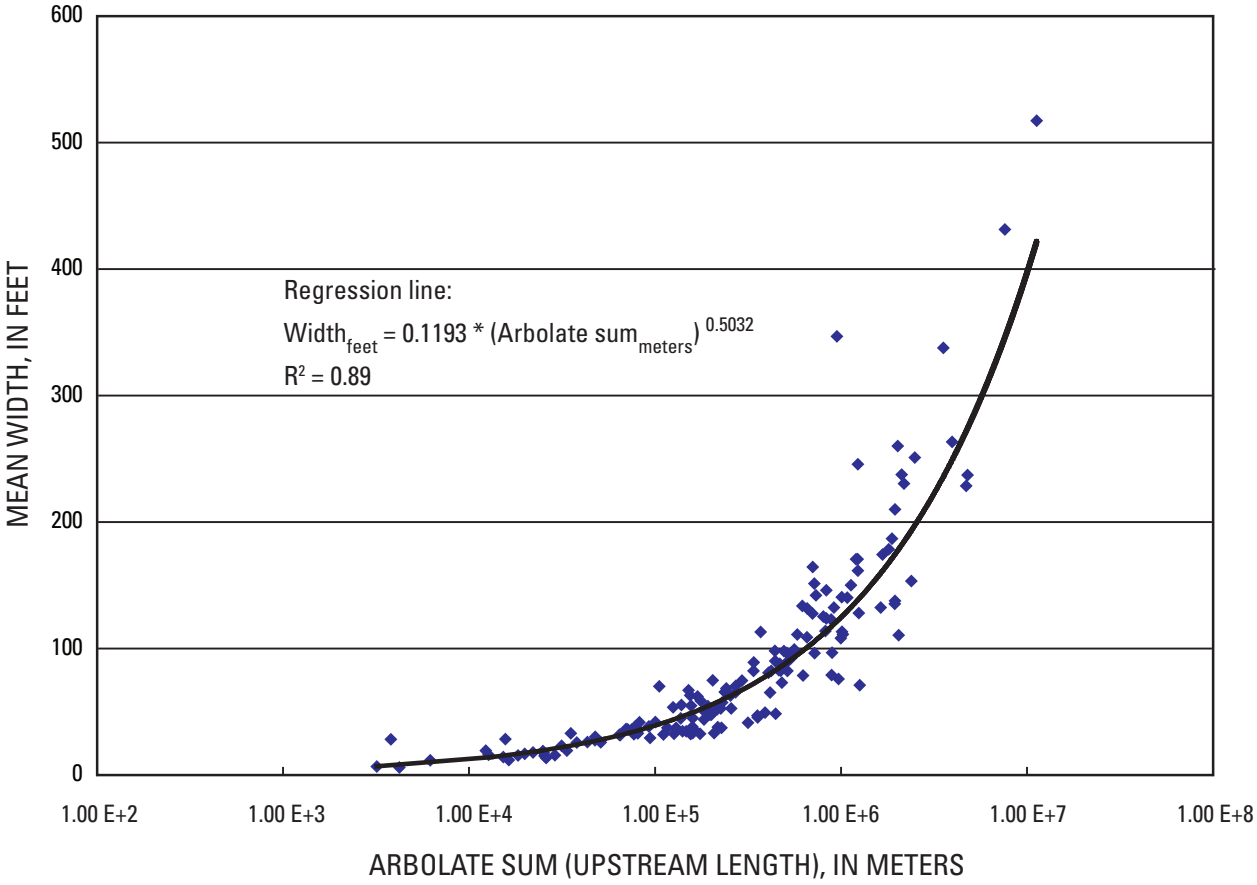

Figure 2–2. Relation between Arbolate sum (upstream distance) and observed stream width at USGS streamgages in Michigan.

Table 2–2. Relation between stream order and measured stream width at USGS streamgage locations in Michigan.

Order	Median width (feet)	Percentage of stream arcs greater than or equal to		
		5 feet	8 feet	10 feet
1	4.4	32.8	3.7	1.1
2	12.2	99.6	92.8	72.6
3	27.3	100.0	99.98	99.20

Table 2–3. Nearfield distribution of surface-water cells for different selection criteria.

Selection criteria	Distribution of features (percent)			
	Streams only in cell	Water bodies only in cell	Both in cell	Total
All streams included All water bodies included	39.0	16.3	26.5	81.8
Minimum stream width = 6 ft Minimum water-body area = 15 acres	33.7	16.7	14.4	64.8
Minimum stream width = 8 ft Minimum water-body area = 20 acres	27.5	18.5	11.1	57.1
Minimum stream width = 10 ft Minimum water-body area = 30 acres	24.5	18.2	8.5	51.2

2.6 Uncertainties and Limitations

The methodology described in this appendix identified many steps that involve approximations that can lead to error. For example, the assignment of DEMs to stream arcs probably entails a systematic bias insofar as the DEMs, distributed on 30-m centers, might often sample terrace rather than channel elevation and therefore yield stages that are too high in altitude. A comparison of DEM elevations to contours crossing streams in an area of southeastern Wisconsin near Milwaukee suggested that the average bias is on the order of 3 ft. Interpolation of DEM-derived stages to ensure downstream order also introduces some error, as does the assumption that stream stages are constant over the entire 141-year simulation history. Many broad assumptions are built into the calculation of the conductance terms for the RIV boundary conditions representing streams and water bodies, including the assignment of a single hydraulic conductivity value to stream sediments, a single value to lake sediment, and a single value to wetland sediments, as well as the assumption of a uniform thickness of 1 ft for all bed sediments. Restriction of the area over which lakes and wetlands interacts with the groundwater system to a 20-ft annular space along the perimeter is based on the common notion that most exchange occurs near the shoreline (McBride and Pfannkuch, 1975), but the precise behavior varies by location.

The practice of averaging stages to allow a single head-dependent boundary condition to substitute for multiple surface-water features inside a single cell is a simplification, the approximate nature of which depends on the number of features combined. For the nearfield inland cells that represent surface-water features (subject to the 8-ft width threshold for streams and 20-acre area threshold for water bodies), 48 percent contain 1 feature, 33 percent contain two features, 19 percent contain 3 features, and one cell contains 5 features. Thus, slightly over half the inland surface-water cells in the model are subject to the approximations that arise from stage averaging across features.

All inland surface-water cells are represented by RIV boundary conditions. The RIV cells serve to accept groundwater discharge (base flow) when the water-table elevation is higher than the stage assigned the surface-water feature. However, for the reverse case, when the surface-water stage is higher than the simulated water table in the cell, only RIV cells in the LMB model associated with *streams* can lose to the groundwater system. The input to the RIV cells for *lakes and wetlands* ensures that they can act only as drains, never as sources (because the variable RIVBOT in the RIV package is set equal to the stage, which automatically prohibits an outward gradient from the water body to the groundwater). The treatment of water bodies as drains was made to prevent one lake from simply routing water to an adjacent lake with a lower stage—an artifact of model construction that can distort the water budget for the model—whereas the ability of streams to lose water was maintained chiefly to allow surface water to act as a source of water to wells under stressed conditions. It is evident that this way of managing the inland boundary conditions does allow for the possibility that RIV cells representing streams will spuriously route water to other RIV cells or that lakes that actually should supply water to nearby wells are barred from doing so.

The censoring of the stream network to maintain the integrity of the water-table solution without distorting too greatly the estimates of hydraulic conductivity and recharge is an inevitable outcome of the coarse 5,000-ft grid spacing. As part of the work supporting the LMB model, a series of sensitivity simulations was done to examine the effect of the *density of the surface-water network with cell size held constant* on simulated results for different sets of hydraulic conductivity, recharge, and conductance values in RIV cells.

The schematic models, constructed to test the influence of surface-water density on simulated water levels, contain cells 5,000 ft on a side. Moreover, the surface-water pattern in the schematic models is based on an area of the LMB model centered on the Grand River watershed in the Lower Peninsula of Michigan (see fig. 29 in the main report text), encompassing a domain 47 mi on a side (50 rows by 50 columns). The western boundary of the model is associated with Lake Michigan (constant head = 577.5 ft), which acts as the regional discharge location. The K and recharge patterns used to conduct the sensitivity analyses are not necessarily representative of the Grand River watershed but, instead, express a range of conditions. In one schematic model, the inputs are typical of areas dominated by clayey till or lacustrine sequences: the K_h in the upper unconsolidated layers and the recharge to the water table are set to 2 ft/d and 4 in/yr, respectively. In a second schematic model, the inputs are typical of areas with loamy till and outwash: the shallow K_h and recharge are set to 20 ft/d and 8 in/yr, respectively. The K_v of the glacial sediments is varied between 0.1 and 0.01 ft/d, and the hydraulic conductivity of the beds of surface-water features is varied between 0.2, 2, and 20 ft/d for both schematic models. For both models, the surface-water density is varied between a low (30 percent), middle (48 percent), and high (86 percent) proportion of the inland water-table cells. The sensitivity analysis is intended to

a) show how the assumed stream network density, bed K, and other inputs such as recharge rate affect the overall water table configuration—that is, how they change the degree of *regional (intercell) mounding between stream reaches, and*

b) show how the assumed density, bed K, and other inputs affect the head difference between the water table and the surface-water feature within a head-dependent cell—that is, how it changes the degree of *local (intracell) mounding*.

The results of the sensitivity testing are as follows:

1. The choice of surface-water density for a fixed bed *K* *strongly influences the regional water-table gradient and the degree of mounding between surface-water features* but has only small influence on the gradient between the water table and surface water within a cell. The greatest contrast in the degree of mounding is between a sparse network on the one hand and either the middle- or high-density networks on the other. The sparse network commonly yielded water-table mounds 50 ft higher than the denser networks, which "stapled" the head to a larger number of known surface-water features.
2. The choice of *K* for the streambed or lakebed for a given surface-water density pattern strongly influences the intracell gradient between the water table and surface-water stage but has only small influence on the regional water-table trend. On average and at individual cells, the local mounding is consistently 10 times greater when the bed *K* is 10 times lower. The influence of the bed *K* on the regional water-table trend is only strong when its value is at the minimum value of 0.2 ft/d.
3. Mounding of the water table is roughly proportional, all other inputs held constant, to recharge rate.
4. On average, the local mounding of the water table between surface-water features simulated by the regional model is similar for the two K_h values assigned the shallow unconsolidated deposits. However, there are many cells where the degree of mounding is quite sensitive to the shallow K_h.
5. On average, the local mounding is quite insensitive to the value of shallow K_v.

The implications of these findings are as follows:

1. A sparse stream network that represents only major rivers will produce much more mounding between surface water than a dense network that also includes lower-order streams, and the mounding in the sparse case is likely to be inaccurate because existing discharge zones are neglected.
2. Calibration to head targets inside head-dependent cells is likely to be insensitive to the K_h and K_v assigned the glacial deposits of the cell. For this reason, targets inside RIV cells were excluded from the LMB model calibration process.
3. Calibration to head targets in head-dependent cells is likely to be sensitive to cell recharge and the conductance of the surface-water feature.

It is expected that *local intracell* mounding in head-dependent boundary cells is insensitive to the *K* of the shallow, unconsolidated sediments. MODFLOW, a discretized finite-difference code, solves for head primarily as a function of flow between cells, not in terms of flow within cells or from a cell to an internal boundary condition. Calibration to the *regional intercell* water table gradient is sensitive to K_h and (perhaps to a lesser extent) K_v of shallow sediments, whereas it is insensitive to surface-water bed conductance (that is, the *K* assigned the bed of the surface-water feature). In a regional model, the value of the bed *K* can be used as a blunt way to approximate local mounding that is in accord with expected water-table gradients toward streams or lakes. Stream density is only one issue that arises from the grid discretization. Because a finite-difference model like MODFLOW locates all stresses at the center of the model cell, it is clear that the larger the cell sizes, the less accurately will the model reproduce stream geometries and well locations. It is also clear that the interaction between nearby stresses, such as multiple streams or a stream and a pumping well, is compromised by large cell sizes when, from the standpoint of the finite-difference solution, they are forced to the same nodal point. These problems with coarse model grids are well understood. Less obvious are the errors in modeled streamflows that may result from an inaccurate representation of the *leakage between model layers* in the presence of surface-water features inserted as boundary conditions in large grid cells.

To understand this issue it is necessary to consider the "leakage factor" λ (m) (Hantush and Jacob, 1954; Verruijt, 1970), also referred to as the "characteristic leakage length" (Haitjema and others, 2001; Bakker and Strack, 2003). For a two-layer aquifer system, the characteristic leakage length is defined as

$$\lambda = \sqrt{\frac{T_u T_l c}{T_u + T_l}}$$

where T_u and T_l (meters squared per day) are the transmissivities of the upper and lower layer, respectively and *c* (days) is the vertical resistance (thickness divided by K_v) of a separating confining unit or the aquifer material itself.

The characteristic leakage length determines whether the vertical leakage to or from streams or wells is concentrated locally or is distributed ("smeared out") over a larger area. For example, it can be shown that the leakage induced by a stream nearly vanishes beyond a distance of 3λ from the stream boundary (Hunt and others, 2003). Thus, for small λ-values, the leakage is concentrated near the stream, whereas for large λ-values, it occurs over a much larger area. Haitjema and others (2001) found that in order to obtain an acceptable representation of the leakage distribution in finite-difference models, such as MODFLOW-2000 or SEAWAT-2000, the cell size should be less than λ, preferably as low as 0.1λ. When the model cell size is larger than this threshold value, inaccurate leakage distributions may result in inaccurate simulation of heads and streamflows.[3]

To better understand the degree of uncertainty in the LMB model arising from the characteristic leakage length associated with the model grid, sensitivity analyses were done for variable cell size with stream density held constant. The simulations were done along a vertical section 10,000 ft in length that incorporates transmissivity and resistance values (c) typical of the glacial terrain in southeastern Wisconsin. The analytical setup was a two-layer system consisting of saturated glacial material (on average about 115 ft thick) over dolomite (50 ft thick). Assuming that K_h =5 ft/d and K_v =0.01 ft/d in both units (reasonable values for till and dolomite), the transmissivity values are 575 and 250 ft²/d, and the resistance value for the vertical thickness between cell centers is 8,250 days. The resulting leakage length, λ, is about 1,000 ft. The experimental model was bounded at the upgradient end by a fully penetrating general-head boundary condition, which acted as the source of water to both layers, and at the downgradient end by a general head boundary in the glacial layer alone, which represented a partially penetrating outlet. At a distance 2,500 ft from the downgradient end, a RIV cell with fixed conductance and stage was inserted to represent a stream in layer 1. The variable column widths applied to the section graduate from 5,000 to 5 ft in nine steps. For the 5,000-ft spacing, the downgradient cell contained both the outlet and the stream.

Three fluxes were recorded for each simulation: the upward flow from layer 2 to layer 1, the discharge to the outlet boundary, and the discharge to the stream in the RIV cell. It was found that all three terms *stabilize* at a cell width between 1,000 or 500 ft. At the 5,000 ft-spacing, the upward flow is about 1.5 times higher, flow to the outlet is about 3.0 times higher, and discharge to the stream is about 0.70 times lower than the stabilized flow. In other words, an accurate simulation is not obtained until the cell size is less than λ. The implication is that in many areas of the LMB model domain (especially where the transmissivity of near-surface material is relatively small, such as in clay-till terrains), the regional model can produce appreciable leakage errors—even in those cases where the model cell size allows an accurate representation of the stream-network geometry. This analysis highlights possible limitations of the regional model when confronted with local management issues involving, for example, the interaction of wells with nearby headwater streams.

References

Bakker, Mark, and Strack, O.D.L., 2003, Analytic elements for multi-aquifer flow: Journal of Hydrology, no. 271, p. 119–129.

Bartošová, Alena; McConkey, Sally; Lin, Yu-Feng; and Walker, Douglas, 2004, Using NHD to estimate stream geometry characteristics for MODFLOW, *in* Geographic Information Systems and Water Resources III, American Water Resources Association Spring Specialty Conference, Nashville, Tenn., May 17–19, 2004: 7 p.

Brenden, T.O., Clark, R.D., Jr., Cooper, A.R., Seelbach, P.W., Wang, L., Aichele, S.S., Bissell, E.G., and Stewart, J.S., 2006, A GIS Framework for collecting, managing, and analyzing multi-scale landscape variables across large regions for river conservation and management, *in* Hughes, R.M., Wang, L., and Seelbach, P.W., eds., Influence of landscapes on stream habitats and biological assemblages: Bethesda, Md., American Fisheries Society Special Publication 48, p. 49–74.

Environmental Systems Research Institute, 2003, ArcInfo, version 8.3: Redlands, Calif.

Haitjema, Henk; Kelson, Vic; and de Lange, Wim, 2001, Selecting MODFLOW cells sizes for accurate flow fields: Ground Water, v. 39, no. 6, p. 931–938.

Hantush, M.S., and Jacob, C.E., 1954, Plane potential flow of groundwater with linear leakage: Transactions of the American Geophysical Union, v. 35, p. 917–936.

[3] For multilayer systems, the situation is more complicated, with different λ-values controlling the leakage exchange between the different layers (Bakker and Strack, 2003). In such cases, the cell size can be based on the largest λ-value in the system.

Hunt, R.J., Haitjema, H.M., Krohelski, J.T., and Feinstein, D.T., 2003, Simulating ground water-lake interactions—Approaches, analyses, and insights: Ground Water, v. 41, no. 2, p. 227–237.

MATLAB Central, 2009, Strahler stream order: Accessed September 22, 2009, at *http://www.mathworks.com/matlabcentral/fileexchange/22952*.

McBride, M.S., and Pfannkuch, H.O., 1975, The distribution of seepage within lakebeds: U.S. Geological Survey Journal of Research, v. 3, no. 5, p. 505–512.

Strahler, A.N., 1952, Hypsometric (area-altitude) analysis of erosional topology: Geological Society of America Bulletin v. 63, no. 11, p. 1117–1142.

U.S. Geological Survey, 2009, National Hydrography Dataset: U.S. Geological Survey database, accessed June 2005 at *http://nhd.ugs.gov/index.html*.

U.S. Geological Survey, Great Lakes Science Center, 2004, Riverine aquatic gap analysis: Accessed December 2008 at *http://www.glsc.usgs.gov/main.php?content=research_GAP_riverine&title=Aquatic%20GAP0&menu=research_NCE_GAP*.

Verruijt, A.,1970, Theory of groundwater flow: London, Macmillan, 200 p.

Appendix 3. Power Law for Horizontal Hydraulic Conductivity of QRNR Deposits

Power law: $$Kh_{initial} = [Kh_{expected} \times \mathbf{Base}^{(x/e)}] / \mathbf{Base}$$

where

x is percentage of coarse material in model cell and
e is expected coarse percentage for glacial category.

Subject to condition: If calculated $Kh_{initial}$ is greater than $Kh_{maximum}$, then it is reset to $Kh_{maximum}$.

Note: $Kh_{minimum}$ corresponds to a cell with coarse percentage equal to zero.
$Kh_{initial}$ refers to K values input to a model cell before calibration.
$Kv_{initial}$ is set in all QRNR cells to 0.05 × the value of $Kh_{initial}$.

Table 3–1. Inputs to power law for assigning horizontal hydraulic conductivity of QRNR deposits in model layers 1, 2, and 3.

Glacial category	Base	Expected coarse percentage	$Kh_{expected}$ (feet per day)	$Kh_{minimum}$ (feet per day)	$Kh_{maximum}$ (feet per day)
Clayey till	5	20%	1.0	0.2	10
Loamy till/organic	5	40%	5.0	1.0	50
Sandy till	5	50%	10.0	2.0	50
Fine stratified	5	10%	2.0	.4	20
Medium/coarse stratified	5	60%	100.0	20.0	292
Unknown	5	10%	2.0	1.0	20

Appendix 4. Initial Bedrock Hydraulic Conductivity

This appendix has two sections:

- An account of the sources used to quantify bedrock hydraulic conductivity.
- A description of the initial horizontal (K_h) and vertical (K_v) hydraulic conductivity input.

4.1 Sources of Block Assignments

Michigan

In Michigan, a primary source of hydraulic-conductivity estimates is the Michigan Department of Environmental Quality (MDEQ) aquifer-test archive (Michigan Department of Environmental Quality, 2005). This archive is a compilation of all aquifer tests submitted to the MDEQ as part of the permit process for new municipal water supplies, as well as tests submitted as part of wellhead-protection-area delineations. A second aquifer-test archive is associated with records on file at the Michigan Geological Survey (MGS) and compiled as part of the USGS Michigan RASA (Regional Aquifer Systems Analysis) studies in the 1980s and 1990s. The transmissivities generated by aquifer tests were converted into *K* estimates by correlating the well with an aquifer unit based on county reports or on a state geologic map (Milstein, 1987) and by assigning an aquifer thickness based on the RASA studies of the Michigan Basin (Westjohn and Weaver, 1998). In all, 212 aquifer tests were utilized to assign blocks of hydraulic conductivity to the model.

The Michigan database for water-well driller logs (available online at Michigan Center for Geographic Information, 2009) contains digital information for more than 400,000 well records. In cases where location and lithologic information can be verified, it allows computation of specific capacity (well discharge divided by drawdown), which in turn can be used to estimate transmissivity by means of a truncated, semi-log version of the Theis non-equilibrim formula (Freeze and Cherry, 1979). The calculations depend on a storage coefficient, which is assumed to equal 0.0004. The equation relating specific capacity to transmissivity is nonlinear (transmissivity appears on both sides of the equation); therefore, it is solved iteratively (Michigan Department of Environmental Quality, 2006). As in the case of aquifer tests, the transmissivities derived from specific-capacity calculations are converted to hydraulic conductivity on the basis of an appropriate aquifer thickness. Transmissivity estimates derived from specific capacity are considered less reliable than those from the aquifer-test results and are used to estimate block *K* values only when the latter are unavailable. In all, 1,089 specific-capacity calculations were utilized to assign blocks of hydraulic conductivity to the model.

Cooperative projects between the MGS and USGS contain descriptions of the hydrogeologic framework of individual counties and often also contain estimates of the hydraulic properties of aquifer material. Reports for the Michigan counties of Baraga (Doonan and Byerlay, 1973), Chippewa (Vanlier and Deutsch, 1958a), Delta (Sinclair, 1960), Gogebic (Doonan and Hendrickson, 1968), Iron (Doonan and Hendrickson, 1967), Mackinac (Vanlier and Deutsch, 1958b), Marquette (Doonan and VanAlstine, 1982), Ontonagon (Doonan and Hendrickson, 1969), and Schoolcraft (Sinclair, 1959), as well as the Keweenaw Peninsula (Doonan and others, 1970), furnish *K* estimates for the SLDV, SNNP, PCFR, and deeper C-O units (including the Precambrian Jacobsville Sandstone).

Aquifer-test results yield transmissivity and, given stratigraphic thickness, hydraulic-conductivity estimates for the major aquifers in the Lower Peninsula: the sandstones of the Grand River and Saginaw Formations in the PENN aquifer system and the Marshall Sandstone in the MSHL aquifer system. Estimates for Silurian and Devonian aquifers are derived partly from county reports and partly from specific-capacity calculations on data from wells in the southeastern part of the state, in the northern rim of the Lower Peninsula, and in the Upper Peninsula. Results from a few pumping tests in the SLDV aquifer system also are available for the northernmost counties of the Lower Peninsula. In the Upper Peninsula, wells drawing from the Sinnipee and Prairie du Chien-Franconia aquifers in the C-O aquifer system provide *K* estimates by means of specific-capacity calculations. Hydraulic conductivities for the Munising aquifer in the Upper Peninsula of Michigan (correlative with Ironton and Galesville, Eau Claire, and Mount Simon Sandstones) and for the Precambrian Jacobsville aquifer are derived from aquifer tests, specific-capacity calculations, and county reports.

Block values for vertical hydraulic conductivity assigned to aquifers are generally estimated by means of an assumed vertical anisotropy. No test data for *K* are available for the Jurassic, Michigan, and Maquoketa confining units in Michigan, but K_v estimates for some of these confining units, as well as K_h values for aquifers in areas devoid of tests, are available through the RASA modeling study of the northern Midwest (Mandle and Kontis, 1992). A study by Thornton and Wilson (2007) was used to characterize blocks of vertical hydraulic conductivity for the evaporites in the Salina Group within the SLDV aquifer system. The study indicates very low K_v where the evaporites are thickest in the center of the Michigan Basin. The rim of the Salina Group consists mostly of shale and dolomite, so these areas constitute a separate block.

Wisconsin

Results of many aquifer tests in Wisconsin involving pumping with observation wells provide transmissivity estimates for the entire C-O aquifer system that can be used, once divided by the stratigraphic thickness of the in model cells, to calculate an average hydraulic conductivity across multiple units. Aquifer-test data are supplemented by packer-test results, which provide estimates for specific hydrostratigraphic units. Pumping-test and packer-test analyses are available for the northeastern Wisconsin subregion and adjacent farfield (Drescher, 1953; LeRoux, 1957; Newport, 1962; Knowles, 1964; Olcott, 1966; Foth & Van Dyke, 1982; Krohelski, 1986; Young, 1992; Batten and Bradbury, 1996) and for the southeastern Wisconsin region and adjacent farfield (Foley and others, 1953; LeRoux, 1963; Nicholas and others, 1987; Young, 1992; Carlson and Feinstein, 1998).

Hydraulic conductivities based on specific-capacity calculations were compiled by aquifer unit for parts of southeastern Wisconsin by Eaton and others (1999). The database of *K* derived from specific-capacity calculations was extended to other parts of Wisconsin within the model domain by utilizing discharge and drawdown information contained in water-well driller logs compiled in support of the LMB model (Arihood, 2009). As in the case of the Michigan dataset, specific-capacity calculations were converted to transmissivity and ultimately to hydraulic-conductivity estimates via model-layer thickness by using a truncated semi-log version of the Theis non-equilibrium formula where transmissivity appears on both sides of the equation and is solved iteratively (Prudic, 1991; Arihood, 2009).

The specific-capacity calculations have proved particularly useful for assigning blocks of horizontal hydraulic conductivity to different depth intervals of the SLDV aquifer system in Wisconsin. Calculations were also used to supplement aquifer tests and generate K_h values for aquifers in the C-O aquifer system. In each case, the hydraulic-conductivity estimate based on specific-capacity calculations was assigned to the lowermost aquifer or model layer penetrated by the well (as inferred from the land surface at the well location), the well depth, and the tops and bottoms of model layers. Care was taken to use only wells that appear to penetrate at least 10 ft of the assigned unit or layer. Values derived from specific-capacity calculations are available for 4,099 cell locations in the SLDV unit, 1,909 in the SNNP aquifer, 1,341 in the STPT aquifer, 2,805 in the PCFR aquifer, 1,107 in the IRGA aquifer, and 1,055 in the MTSM aquifer.

Review of published models provided another source for quantifying both K_h and K_v. Hydraulic-conductivity zonations for single units and groups of units are available for the C-O aquifer system in the northeastern Wisconsin subregion and adjacent farfield (Krohelski, 1986; Emmons, 1987; Feinstein and Anderson, 1987; Weaver and Bahr, 1990; Mandle and Kontis, 1992; Conlon, 1998; Cherkauer and Carlson, 2003) and in the area of the farfield model domain around Madison, Wis. (Krohelski and others, 2000). Some of these models also include distributions of hydraulic conductivity for SLDV rocks that form the bedrock surface. For southeastern Wisconsin, the mapping of hydraulic conductivity by bedrock unit corresponds to the calibrated input of a recently constructed model for the area centered on Waukesha and Milwaukee, Wis. (Feinstein, Eaton, and others, 2005; Feinstein, Hart, and others, 2005).

Additional sources of data are slug tests and laboratory tests of *K* mostly for Silurian rocks (Nauta, 1987; Craig, 1989; Webb, 1989; Mueller, 1992; Cherkauer and Carlson, 2003; Dunning and others, 2004). These studies help to distinguish the value of K_h in the shallow and presumably weathered part of the SLDV aquifer system from the permeability deeper in the unit.

To facilitate assignment of hydraulic conductivity, the available aquifer-test results, specific-capacity calculations, and model estimates were organized into six sections for the Wisconsin part of the model domain. The area between the Silurian subcrop (see fig. 20*H* in the main report text) and Lake Michigan was divided into three sections, the first in the southeastern Wisconsin subregion and the second and third covering the eastern part of the northeastern Wisconsin subregion. Adjacent to these sections, the area west of the Silurian subcrop also was divided into three sections that extend from the Silurian subcrop to the farfield western edge of the model, roughly coincident with the Wisconsin River. Within the six sections, distinct hydraulic-conductivity blocks were assigned to areas where a particular bedrock unit subcrops below QRNR material as opposed to areas where it is beneath another bedrock unit. In the subcropping aquifer locations, K_h was assumed 50 percent higher than in the buried locations, owing to weathering and fracturing.

In general, the value of bedrock K_v was determined as a function of K_h. For most of the Wisconsin sections and units, the horizontal to vertical anisotropy ratio was assumed to be relatively low (typically between 100 and 500) in subcrop areas and higher (in the neighborhood of 1,000) elsewhere. The vertical hydraulic conductivity of the Maquoketa Formation, an important confining unit in the nearfield part of Wisconsin, was assigned K_v values based on previous investigations (Walton, 1960; Krohelski, 1986; Mandle and Kontis, 1992; Feinstein, Eaton, and others, 2005; Hart and others, 2006).

Indiana

The methods used to assign hydraulic conductivities and transmissivities to bedrock formations in northern Indiana involved specific-capacity calculations, packer tests, and field observations. The specific-capacity calculations are based on data (discharge, drawdown, and time pumped) from 2,711 water-well driller logs for bedrock formations. The packer tests were done at three sites in northwestern Indiana on Devonian and Silurian deposits as part of the USGS Midwestern Basins and Arches RASA study (Arihood, 1994). Field observations of fracture patterns were made during a field trip of several limestone quarries within Indiana and Ohio as part of the RASA study to help understand the relation of permeability to fracturing. The packer tests and observations on bedrock fracture patterns were used to extend the information gained from the specific-capacity calculations.

The field observations indicated that the majority of fracturing ended about 50 to 100 ft below the bedrock surface, whereas the packer tests indicated that most of the permeability ended within about the first 100 ft below the bedrock surface. In other words, the field observations hinted that the major permeability of the bedrock deposits was within the first 100 ft, and the packer tests confirmed that observation. The upper part of the Devonian and Mississippian deposits (model layer 9) in northern Indiana was also assumed to be fractured, enhancing the average hydraulic conductivity of the DVMS unit.

Specific-capacity calculations were converted to transmissivity and ultimately to hydraulic-conductivity estimates via model layer thickness by using the Theis non-equilibrium equation described previously for Michigan and Wisconsin. Block assignments represent median values over different areas and depth intervals.

A second source of hydraulic-conductivity information for Devonian and Silurian deposits composing the SLDV aquifer system is an additional RASA publication (Joseph and Eberts, 1994) that contains transmissivity data from reports and files from state agencies and municipalities. The median from this dataset is much larger than the median based chiefly on the specific-capacity data, but the number derived from this RASA study could be biased high because it relied on municipal production wells sited in areas of especially favorable transmissivity. The production-well results are taken to represent an upper limit to a reasonable range for SLDV transmissivity and hydraulic conductivity.

The vertical hydraulic conductivity of the Devonian and Silurian dolomites appears from field observations to be strongly influenced by the depth of the weathered fracture zone where these units subcrop. For this reason, the block K_v for the upper part of the SLDV aquifer system is higher than for the lower part, with the most pronounced difference being to the south where the SLDV system is overlain by the glacial overburden rather than by fine-grained Devonian and Mississippian deposits. The DVMS bedrock consists largely of black shale and a siltstone and shale combination. The median value of specific-capacity-derived horizontal hydraulic conductivity for these rocks is low and is assumed to mostly represent the contribution of shallow fracture zones.

Almost no information is available in northern Indiana for the C-O layers below the SLDV aquifer system (Arihood, 1994). The assignments of K_h and K_v to these deep units reflects values assumed for northern Illinois and blocks used in the RASA model for the northern Midwest (Mandle and Kontis, 1992).

Illinois

The assignment of bedrock hydraulic conductivities to the LMB model in the northeastern Illinois subregion closely reflects the zonation adopted in a recently completed regional model for the area (Meyer and others, 2009). That study, in turn, relied on previous investigations (Mandle and Kontis, 1992; Bair and Roadcap, 1992; Feinstein, Eaton, and others, 2005), default tables of horizontal hydraulic conductivity by rock type (Freeze and Cherry, 1979), and local expertise. Vertical anisotropy of the bedrock ranges from 20 in the St. Peter aquifer to 5,000 in the Eau Claire confining unit.

Ohio

The part of northwestern Ohio that is within the model domain falls entirely in the farfield. Transmissivity estimates are available in this area for the DSVL aquifer system (Joseph and Eberts, 1994; Sheets, 1999). In general, however, the bedrock units are assigned K values according to input values used in the northern Midwest RASA model (Mandle and Kontis, 1992) or based on rock type.

4.2 Block Values by Layer

The sources for hydraulic-conductivity assignments provide initial block estimates for K_h and K_v. In a number of cases, the block values were adjusted to minimize step changes across state lines or to simplify patterns. Some blocks reflect the average transmissivity derived from aquifer tests, but because the thickness of the unit changes across model cells, they are represented by gradational K values in the model. Because no source information is available under Lake Michigan, bedrock layers under the lake are assigned values that reflect surrounding blocks. In areas where a unit is absent (and the layer assigned a nominal thickness less than 1 ft), the resulting "pinched" cells assume K values from the first overlying bedrock or QRNR cell in the same row/column location that has a thickness equal to or greater than 1 ft.

The description of the *initial* block K_h and K_v assignments to bedrock units is organized by model layer. Each layer is referenced to a map in the main report text showing the geometry and extent of the unit to which it belongs. The extent of the K_v blocks within a layer do not necessarily coincide with those of the K_h blocks; the decoupling of K_h and K_v block assignments allows for maximum flexibility in reflecting available estimates from previous investigations. The distribution of K_h and K_v *blocks* are shown for selected units in appendix 6, with accompanying maps showing the distribution of K_h and K_v *values* after calibration.

Layer=**4**, Unit=**JURA**, Type=**Confining unit**, Aquifer system=**PENN**

The extent of this unit is patchy and limited to the center of the Lower Peninsula of Michigan (fig. 20*B* in the main report text). The unit is treated as a homogeneous block. The initial K_h is assumed equal to 0.5 ft/d, and the initial K_v is assumed equal to 5.0 E−4 ft/d.

Layer=**5**, Unit=**PEN1**, Type=**Aquifer**, Aquifer system=**PENN**

The rocks in this layer cover about one-quarter of the center of the Lower Peninsula of Michigan (fig. 20*C* in the main report text). On the basis of previous investigations, initial K_h is assigned block values of 10 ft/d to the north and 6 ft/d to the south with a small block of 20 ft/d near Lansing, Mich. Initial K_v is assumed to be homogeneous and is assigned a single value of 0.01 ft/d.

Layer=**6**, Unit=**PEN2**, Type=**Aquifer/Confining unit**, Aquifer system=**PENN**

The rocks in this layer are found under about one-quarter of the center of the Lower Peninsula of Michigan (fig. 20*D* in the main report text) and are quite heterogeneous owing to the presence of sandstone (Parma), limestone (Bayport), and shale (Saginaw). On the basis of previous investigations of transmissivity, initial K_h is assigned gradational block values ranging from about 3 to 6 ft/d, with lower values on the order of 0.5 ft/d at the fringes. On the basis of previous investigations, gradational values of initial K_v range from 3.0 E−4 to 3.0 E−3 ft/d, with values as high as 7.0 E−2 ft/d along the fringes of the unit in the farfield.

Layer=**7**, Unit=**MICH**, Type=**Confining unit**, Aquifer system=**MSHL**

This unit extends over about one-third of the center of the Lower Peninsula of Michigan (fig. 20*E* in the main report text). The unit is treated as a homogeneous block. The initial K_h is assumed equal to 0.1 ft/d, and the initial K_v is assumed equal to 1.0 E−4 ft/d.

Layer=**8**, Unit=**MSHL**, Type=**Aquifer**, Aquifer system=**MSHL**

This unit is present under almost one-half of the Lower Peninsula of Michigan (fig. 20*F* in the main report text). On the basis of previous investigations, it is assigned three initial K_h block values equal to 5, 15, and 20 ft/d from north to south and three initial K_v block values equal to 5.2 E−3, 1.56, and 2.08 ft/d from north to south.

Layer=**9**, Unit=**DVMS**, Type=**Confining unit**, Aquifer system=**SLDV**

The shales that make up this unit intersect roughly half the model domain (fig. 20*G* in the main report text). Where the unit is present under the Lower Peninsula of Michigan, Lake Michigan, northwestern Ohio, and isolated areas in the farfield of northeastern Illinois, the initial K_h value is assumed to be 0.1 ft/d; but under northern Indiana where the shales subcrop under the glacial material, previous investigations suggest a value of 1 ft/d. The initial K_v value is assumed to be 5.0 E−6 ft/d under the Lower Peninsula of Michigan, Lake Michigan, northwestern Ohio, and northern Indiana, but a value of 2.0 E−6 ft/d is assigned in the farfield of northeastern Illinois on the basis of previous modeling.

Layer=**10**, Unit=**upper SLDV**, Type=**Aquifer**, Aquifer system=**SLDV**

This layer is part of the SLDV unit, which dips from its subcrop along the Wisconsin/Kankakee Arches into the Michigan Basin (fig. 20*H* in the main report text). In the western and southern areas where it is the uppermost bedrock layer, previous investigations indicate that assignment of multiple initial K_h values is appropriate. In northeastern Illinois there are two blocks: K_h is equal to 5 ft/d except in the western part of the nearfield and adjacent part of the farfield, where it is raised to 9 ft/d to reflect more active weathering. For the nearfield of southeastern Wisconsin, K_h is set to 5 ft/d everywhere except for a highly fractured belt of Devonian rock near Milwaukee, where it raised to 30 ft/d. For northwestern Wisconsin, field tests show that, on average, K_h decreases from a block 6.48 ft/d in the nearfield midlatitudes to a block of 2 ft/d farther to the north. The thin rim of SLDV rock in the Upper Peninsula of Michigan is assigned blocks ranging from 0.5 to 2.0 ft/d. The subcrop area in the farfield margin of northern Indiana is assigned an initial K_h block of 4.6 ft/d on the basis of previous modeling. Elsewhere under Lake Michigan, the Lower Peninsula of Michigan, the nearfield of northern Indiana, and northwestern Ohio, the initial K_h is assumed to be 5 ft/d except in subcrop areas in the farfield southeast of the Lower Peninsula, where previous investigations suggest a value of 10 ft/d. The initial assignments of K_v for this layer are simpler than for K_h. A value of 1.0 E−2 ft/d is assumed where the layer is present under Wisconsin and for adjacent parts of northeastern Illinois except under the fractured block near Milwaukee, where it is set to about 1.0 E−2 ft/d. A value of 3.0 E−3 ft/d is assumed under Lake Michigan and for most of the Lower Peninsula of Michigan, the farfield of northeastern Illinois, northern Indiana, and northwestern Ohio. However, where the layer subcrops under glacial material in the Upper Peninsula, northern Lower Peninsula, and southeastern Lower Peninsula of Michigan as well as under parts of northern Indiana and northwestern Ohio, it is assumed to be weathered and is assigned initial K_v blocks in the neighborhood of 1.0 E−2 or 1.0 E−1 ft/d.

Layer=**11**, Unit=**middle SLDV**, Type=**Aquifer/Confining unit**, Aquifer system=**SLDV**

This layer consists of Silurian rocks (fig. 20*H*). It contains thick and poorly permeability evaporite deposits over much of the Lower Peninsula of Michigan, which are grouped into a single block with an initial K_h set to 0.01 ft/d. Another block with K_h set to 0.5 ft/d is assumed to be present under Lake Michigan, northern Indiana, northwestern Ohio, and the Upper Peninsula of Michigan. On the basis of previous investigations, blocks between 0.5 and 2.5 ft/d are assigned to eastern Wisconsin and northeastern Illinois except along its western margin where, although overlain by 50 ft of bedrock, it is still assumed to be shallow enough to be affected by weathering; therefore, its K_h is set as high as 4 ft/d. As for K_v, an initial value of 1 E−7 ft/d is assigned in the area of the Lower Peninsula of Michigan where the evaporites are most thick and a value of 1 E−4 ft/d in a surrounding area where the poor-permeability deposits are more patchy. Under Lake Michigan, northern Indiana, northwestern Ohio, and most of eastern Wisconsin and northeastern Illinois, the assumed value is 1.0 E−3 ft/d. It is raised to around 1.0 E−2 ft/d in thin blocks where the rocks are close to the bedrock surface in Wisconsin and Illinois, as well as the restricted areas where the layer is unpinched in the Upper Peninsula of Michigan along the Lake Michigan shoreline.

Layer=**12**, Unit=**lower SLDV**, Type=**Aquifer/Confining unit**, Aquifer system=**SLDV**

For this lowestmost part of the SLDV unit (fig. 20*H*), where field-test results largely are unavailable, the block assignments are simple. The initial K_h is assumed to be everywhere equal to 0.5 ft/d except for the unpinched areas just west of Lake Michigan, where the value is raised to 2.5 ft/d. The initial K_v is assumed everywhere equal to 1.0 E−3 ft/d.

Layer=**13**, Unit=**MAQU**, Type=**Confining unit**, Aquifer system=**C-O**

This unit extends updip from the Michigan Basin partway along the Wisconsin/Kankakee Arches and subcrops a small distance west of the subcrop of Silurian rocks (fig. 20*I* in the main report text). Dolomite horizons in the Maquoketa afford it limited ability to transmit water horizontally; its relatively thick shale horizons limit vertical flow. The entire unit is represented by a single K_h block with an assumed initial value of 0.1 ft/d except in fringe areas in Wisconsin, where the overlying SLDV unit is missing. There, the value is raised to 0.5 ft/d. The block pattern is somewhat more refined for K_v. On the basis of previous investigations, an initial value of 6.7 E−6 ft/d is assigned to a block extending under Lake Michigan, the Lower Peninsula of Michigan, Indiana, and Ohio, and also under the Upper Peninsula of Michigan, except in a small fringe area that is part of a subcrop block set to 1.0 E−3 ft/d. For northeastern Illinois, one block is assigned an initial value of 6.7 E−6 ft/d to represent unweathered Maquoketa, and a second block is assigned a value of 1.3 E−5 ft/d to represent areas farther to the west where the shale beds are assumed to have undergone some weathering. A third block is reserved for thin bands in fringe areas, where the unit subcrops under glacial material and is assigned an initial value of 1.0 E−3 ft/d. A similar pattern is adopted for southeastern Wisconsin, where areas assumed to be unweathered are assigned 6.7 E−6 ft/d, weathered areas are assigned 2.0 E−5 ft/d, and fringe subcropping areas are assigned 1.0 E−3 ft/d. Finally, for northeastern Wisconsin, previous investigations suggest a zonation limited to two K_v blocks, one with an initial value equal to 2.0 E−5 ft/d and one for the thin subcropping bands set to 3.0 E−3 ft/d.

Layer=**14**, Unit=**SNNP**, Type=**Aquifer/Confining unit**, Aquifer system=**C-O**

This unit extends further up the Wisconsin/Kankakee Arches then does either the SLDV or MAQU (fig. 20*J* in the main report text). A block where initial K_h is assumed to be 0.05 ft/d covers the Lower Peninsula of Michigan, northern Indiana, northwestern Ohio, the area below Lake Michigan, and most of the nearfield of northeastern Illinois, southeastern Wisconsin and the Upper Peninsula of Michigan. Previous investigations indicate that a higher value of 0.5 ft/d is appropriate for the nearfield of northwestern Wisconsin. In the western, mostly farfield parts of northeastern Illinois, Wisconsin, and the Upper Peninsula of Michigan, where the SNNP is not covered by the Maquoketa and the unit serves as a shallow aquifer, previous investigations suggest that the initial K_h be distributed among blocks with values between 0.1 and 5 ft/d. The initial K_v for the SNNP is almost everywhere set to 6.25 E−4 ft/d. Previous investigations indicate that a somewhat lower value be assigned in part of the Upper Peninsula of Michigan and a somewhat higher value in parts of southeastern Wisconsin.

Layer=**15**, Unit=**STPT**, Type=**Aquifer**, Aquifer system=**C-O**

This important aquifer is present across most of the model domain but absent in the north and parts of the northwest and southwest (fig. 20*K* in the main report text). Previous investigations converge on a K_h value of 2.0 ft/d initially assigned a block extending below Lake Michigan, the Lower Peninsula of Michigan, northern Indiana, and northwestern Ohio. The block assignments are more variable for northwestern Wisconsin, southeastern Wisconsin, and northeastern Illinois, owing to multiple sources for hydraulic-conductivity estimates, but initial K_h values are all close to 2.0 ft/d except in mostly farfield areas to the west, where the unit is not covered by the Maquoketa and possibly subcrops—there, the initial values are as high as 9.0 ft/d. The distribution of K_v follows a block configuration dictated in large measure by assumed vertical anisotropy. A large K_v block with an assumed initial value of 5.0 E−3 ft/d is input under Lake Michigan, the Lower Peninsula of Michigan, northern Indiana, and northwestern Ohio. On the basis of previous investigations, block values under northeastern Illinois are set to 5.0 E−4 ft/d in the nearfield and 7.5 E−2 ft/d farther west in the farfield, where the unit is closer to the bedrock surface. In a disrupted area associated with the Sandwich fault (fig. 8*B*), a block with initial K_v value equal to 4.0 E−1 is included. On the basis of previous investigations, nearfield blocks under southeastern Wisconsin are assigned initial values equal to 4.0 E−2, 4.0 E−3, and 4.0 E−4 ft/d; farfield blocks take values of 6.0 E−2 and 6.0 E−1 ft/d. For northeastern Wisconsin where the unit is overlain by the Maquoketa unit, an initial block value of 5.0 E−3 is assigned; but in the western nearfield and in the farfield, values of 4.0 E−2 and 5.0 E−1 ft/d are input to K_v blocks.

Layer=**16**, Unit=**PCFR**, Type=**Aquifer/Confining unit**, Aquifer system=**C-O**

The variable lithologies in this unit (dolomite, sandstone, siltstone) are present across the entire domain except in parts of the northwest (fig. 20*L* in the main report text). It is assumed that lower K_h is, on average, present under Lake Michigan, the Lower Peninsula of Michigan, northern Indiana, and northwestern Ohio (initial value equal to 0.5 ft/d), but field test results indicate that higher values should be assigned in the Upper Peninsula of Michigan, Wisconsin, and northeastern Illinois (blocks of 1.0 to 3.0 ft/d) and that the highest values should be assigned in the farfield areas of Wisconsin where the unit is near the bedrock surface (blocks with initial K_h values as high as 7.5 ft/d). The initial K_v block assignments, dictated in large measure by assumed vertical anisotropy ratios, are as follows: 1.0 E−4 under Lake Michigan, the Lower Peninsula

of Michigan, northern Indiana and northwestern Ohio; mostly around 1.0 E−4 ft/d in northeastern Illinois except for the farfield near the Wisconsin State line, where a block of 5.0 E−2 is input; 4.0 E−4 ft/d for the nearfield of southeastern Wisconsin and 5.0 E−2 ft/d for the farfield; 1.0 E−3 ft/d in northwestern Wisconsin for areas where the Maquoketa is present as a confining bed, but blocks of 1.0 E−2 ft/d and 3.0 E−1 ft/d are input farther to the west (both nearfield and farfield); 1.0 E−4 ft/d in the Upper Peninsula of Michigan near Lake Michigan but increased to around 2.0 E−2 ft/d to the northwest.

Layer=**17**, Unit=**IRGA**, Type=**Aquifer**, Aquifer system=**C-O**

This aquifer, which extends over all but the northwestern part of the model domain (fig. 20*M* in the main report text) is assigned hydraulic conductivities that are as high or higher than for other C-O units. Previous investigations suggest the following initial block assignments for K_h: around 2.0 ft/d to the farfield of the eastern Lower Peninsula of Michigan, to the Upper Peninsula of Michigan, under the northern part of Lake Michigan, in the northern Lower Peninsula of Michigan, and in northwestern Ohio; 6.0 ft/d under the southern part of Lake Michigan and northern Indiana; 5.3 ft/d under the nearfield of northeastern Illinois and most of its farfield except southern parts, where it is set to 3.0 ft/d; a range of values equal to 1.5, 6.0, and 8.4 ft/d for the nearfield of southeastern Wisconsin but 6.0 ft/d in all the farfield; 1.5 ft/d in northwestern Wisconsin where the unit is under the Maquoketa, but 7.0 ft/d farther to the west; and between 1.5 and 3.0 ft/d for most of the Upper Peninsula of Michigan except for a block immediately west of Green Bay, where the initial K_h value is set to 9.0 ft/d. The distribution of K_v follows a block configuration dictated in large measure by assumed vertical anisotropy ratios. Values are set to 1.0 E−2 ft/d under Lake Michigan, the Lower Peninsula of Michigan, northern Indiana, and northwestern Ohio. They are also set to 1.0 E−2 ft/d in the nearfield of northwestern Illinois and to the south in the farfield; but in the western farfield, blocks with initial values of 6.0 E−2 and 1.0 E−1 ft/d are assigned. Initial K_v values for blocks under southeastern Wisconsin are 1.0 E−2 and 4.0 E−2 ft/d in the nearfield and 6.0 E−2 ft/d in the farfield. A value of 1.0 E−2 ft/d is assigned for northwestern Wisconsin where the Maquoketa is present, but blocks of 2.0 E−2, 7.0 E−2, and 7.0 E−1 ft/d are input farther to the west. In the Upper Peninsula of Michigan, initial K_v block values range between 2.0 E−2 and about 1.0 E−2 ft/d.

Layer=**18**, Unit=**EACL**, Type=**Aquifer/Confining unit**, Aquifer system=**C-O**

Like the other C-O layers, this unit is present over most of the domain (fig. 20*N* in the main report text), but sources of hydraulic-conductivity estimates allow more detail west of Lake Michigan than east of it. West of the lake, stratigraphic evidence suggests that its hydraulic conductivity decreases from the north (where it is predominantly sandstone) to the south (where it is increasingly fine grained). A block with initial K_h set to 0.5 ft/d is input under Lake Michigan, the Lower Peninsula of Michigan, northern Indiana, and northwestern Ohio, as well as the southern part of northeastern Illinois. Higher K_h values on the order of 1.0 ft/d are set under the northern part of northeastern Illinois and southeastern Wisconsin, with values in the neighborhood of 2.0 ft/d assigned to blocks under northeastern Wisconsin and the Upper Peninsula of Michigan. On the basis of available data, one high K_h block equal to 9 ft/d is assigned for the Upper Peninsula immediately west of the Green Bay arm of Lake Michigan. The presence of fine-grained silt and shale beds in some parts of the Eau Claire justifies the input of lower vertical hydraulic conductivities (and higher vertical anisotropy ratios) than those assigned to other C-O aquifer units. Under Lake Michigan, the Lower Peninsula of Michigan, northern Indiana, and northwestern Ohio, an initial block K_v value of 1.0 E−5 is assumed. Under northeastern Illinois, the values trend higher from the southeast to northeast, from 1.0 E−5 to 4.0 E−5 ft/d, with an additional block set equal to 6.0 E−4 ft/d near the Wisconsin State line. For southeastern Wisconsin, blocks are set with initial K_v of 4.0 E−5, 4.0 E−4, and 6.0 E−4 ft/d. For much of northwestern Wisconsin, the initial value is raised to 5.0 E−3 ft/d to reflect the change to predominantly sandstone lithology to the north. A relatively low initial K_v value of 1.0 E−5 ft/d is assigned to a block in the Upper Peninsula that is close to Lake Michigan, but farther to the northwest relatively high initial values of 3.0 E−2 and 1.0 E−1 ft/d are input.

Layer=**19**, Unit=**upper MTSM**, Type=**Aquifer**, Aquifer system=**C-O**

This unit is present across almost all the model domain (fig. 20*O* in the main report text). On the basis of lithostratigraphic trends, its hydraulic conductivity is assumed to increase from south to north as well as increase to the west where the unit is shallow and sometimes forms the bedrock surface. For the upper 300 ft of the Mount Simon corresponding to layer 19, a K_h block with initial value 1.0 ft/d is set for the southern part of the Lower Peninsula of Michigan, northern Indiana, and northwestern Ohio. A value of 3.0 ft/d is assumed for the block under Lake Michigan and the central and northern part of the Lower Peninsula. West of Lake Michigan, there are multiple zones linked to available sources of estimates. To the south in northeastern Illinois, a low K_h value of 0.4 ft/d is assigned. More to the north in the nearfield of southeastern Wisconsin, northeastern Wisconsin, and the Upper Peninsula of Michigan, block values range between 1.0 and 3.0 ft/d. To the west in the farfield of southeastern Wisconsin and also in the Upper Peninsula immediately west of the Green Bay arm of Lake Michigan, block values as high as 8.5 ft/d are assigned. The block configuration of initial K_v is as follows: under Lake Michigan, the Lower Peninsula of Michigan, northern Indiana, and northwestern Ohio, it is set to 3.0 E−3 ft/d; under most of northeastern Illinois, it is also set to 3.0 E−3 ft/d except in part of the farfield to the west, where a higher value of 8.5 E−2 ft/d reflects shallower and presumably more weathered conditions; under southeastern Wisconsin, previous investigations suggest block K_v values

of 4.0 E−4, 4.0 E−3, and 4.0 E−2 ft/d, but to the west in the farfield the value rises to 8.5 E−2 ft/d; under northwestern Wisconsin, the value is set to 3.0 E−3 where the Maquoketa confining unit is present, but blocks with initial K_v values of 1.0 E−2, 5.0 E−2, and 1.0 E−1 ft/d are input to the west, with a maximum value of 5.0 E−1 ft/d assigned to some areas where the Mount Simon forms the bedrock surface; and finally, under the Upper Peninsula of Michigan, a value of 3.0 E−3 ft/d is assumed near Lake Michigan, but toward the northwest higher blocks of about 3.0 E−2 and 1.0 E−1 ft/d are input.

Layer=**20**, Unit=**lower MTSM**, Type=**Aquifer/Confining unit**, Aquifer system=**C-O**

This layer represents the thickness of the MTSM unit at depths of more than 300 ft below the unit surface. Well logs west of Lake Michigan suggest that fine-grained beds become more common at these depths, although sandstone horizons are still plentiful. For this reason, the block assignments for the initial horizontal hydraulic conductivity are assumed to be identical to those assigned for layer 19, but the vertical hydraulic conductivity distribution is different. Where cells are unpinched under Lake Michigan, the Lower Peninsula of Michigan, northern Indiana, northwestern Ohio, and the Upper Peninsula of Michigan, K_v is set to 3.0 E−4 ft/d, an order of magnitude lower than for layer 19. Under the nearfield of northeastern Illinois and in farfield areas to the south of the nearfield, the initial value is also 3.0 E−4 ft/d. However, the K_v in the western part of the farfield in northeastern Illinois is assumed to be 3.0 E−3 ft/d to reflect the possibility of weathering, with the value increasing to 5.0 E−3 ft/d near the Wisconsin State line. Under most of the nearfield of southeastern Wisconsin, previous investigations suggest that initial block K_v values grade from 1.0 E−4 to 3.0 E−4 ft/d, whereas under the western nearfield and under the farfield, a block of 1.0 E−2 ft/d is set. For northwestern Wisconsin where the layer is unpinched and confined by the Maquoketa unit, the block value is assumed to be 5.0 E−3 ft/d; but to the west, initial K_v values of 2.0 E−2 and 5.0 E−2 ft/d are assigned. A block equal to 2.0 E−1 ft/d is reserved for areas where the Mount Simon constitutes the bedrock surface.

References

Arihood, L.D., 1994, Hydrogeology and paths of flow in the carbonate bedrock aquifer, northwestern Indiana: Water Resources Bulletin, v. 30, no. 2, p. 205–218.

Arihood, L.D., 2009, Processing, analysis, and general evaluation of well-driller logs for estimating hydrogeologic parameters of the glacial sediments in a ground-water flow model of the Lake Michigan Basin: U.S. Geological Survey Scientific Investigations Report 2008–5184, 26 p.

Bair E.S., and Roadcap, G.S., 1992, Comparison of flow models used to delineate capture zones of wells—Leaky-confined fractured carbonate aquifers: Ground Water, v. 30, no. 2, p. 199−211.

Batten, W.G., and Bradbury, K.R., 1996, Regional groundwater flow system between the Wolf and Fox Rivers near Green Bay, Wisconsin: Wisconsin Geological and Natural History Survey Information Circular 75, 28 p.

Carlson, D.A., and Feinstein, D.T., 1998, Preliminary model design and literature review for the sandstone aquifer system in southeastern Wisconsin: Unpublished letter report submitted by the USGS to the Wisconsin Department of Natural Resources, 38 p. plus tables and figures.

Cherkauer, D., and Carlson, D., 2003, Development and calibration of a ground water flow model of Fond du Lac County, Wisconsin: Unpublished.

Conlon, T.D., 1998, Hydrogeology and simulation of groundwater flow in the sandstone aquifer, Northeastern Wisconsin: U.S. Geological Survey Water-Resources Investigations Report 97–4096, 60 p.

Craig, K.D., 1989, Determination of ground-water discharge into Green Bay and Lake Michigan Door Peninsula, Wisconsin: University of Wisconsin-Milwaukee, unpublished M.S. thesis, 162 p.

Doonan, C.J., and Byerlay, J.R., 1973, Ground water and geology of Baraga County, Michigan: Michigan Geological Survey Water Investigation 11, 26 p.

Doonan, C.J., and Hendrickson, G.E., 1967, Ground water in Iron County, Michigan: Michigan Geological Survey Water Investigation 7, 61 p.

Doonan, C.J., and Hendrickson, G.E., 1968, Ground water in Gogebic County, Michigan: Michigan Geological Survey Water Investigation 8, 22 p.

Doonan, C.J., and Hendrickson, G.E., 1969, Ground water in Ontonagon County, Michigan: Michigan Geological Survey Water Investigation 9, 29 p.

Doonan, C.J., Hendrickson, G.E., and Byerlay, J.R., 1970, Ground water and geology of Keweenaw Peninsula, Michigan: Michigan Geological Survey Water Investigation 10, 41 p.

Doonan, C.J., and VanAlstine, J.L., 1982, Ground water and geology of Marquette County, Michigan: U.S. Geological Survey Open-File Report 82–501, 46 p.

Drescher, W.J., 1953, Ground-water conditions in artesian aquifers in Brown County, Wisconsin: U.S. Geological Survey Water-Supply Paper 1190, 49 p.

Dunning, C.P., Feinstein, D.T., Hunt, R.J., and Krohelski, J.T., 2004, Simulation of ground-water flow, surface-water flow, and a deep sewer tunnel system in the Menonminee Valley, Milwaukee, Wisconsin: U.S. Geological Survey Scientific Investigations Report 2004–5031, 40 p.

Eaton, T.T., Bradbury, K.R., and Evans, T.J.,1999, Characterization of the hydrostratigraphy of the deep sandstone aquifer in southeastern Wisconsin—Final report to the Wisconsin Deptartment of Natural Resources: Wisconsin Geological and Natural History Survey Open-File Report 1999–02, 30 p.

Emmons, P.J., 1987, An evaluation of the bedrock aquifer system in northeastern Wisconsin: U.S. Geological Survey Water-Resources Investigations Report 85–4199, 48 p.

Feinstein, D.T., and Anderson, M.P., 1987, Recharge to and pontial for contamination of an aquifer system in northeastern Wisconsin: Madison, University of Wisconsin Water Resources Center Technical Report 87–01, 112 p.

Feinstein, D.T., Eaton, T.T., Hart, D.J., Krohelski, J.T., and Bradbury, K.R., 2005. Regional aquifer model for southeastern Wisconsin, Report 1—Data collection, conceptual model development, numerical model construction, and model calibration: Administrative report to the Southeastern Wisconsin Regional Planning Commission, 81 p.

Feinstein, D.T., Hart, D.J., Krohelski, J.T., Eaton, T.T., and Bradbury, K.R., 2005. Regional aquifer model for southeastern Wisconsin; Report 2—Model results and interpretation: Southeastern Wisconsin Regional Planning Commission, Technical Report 41b, 63 p.

Foley, F.C., Walton, W.C., and Drescher, W.J., 1953, Groundwater conditions in the Milwaukee-Waukesha Area, Wisconsin: U.S. Geological Survey Water-Supply Paper 1229, 96 p.

Foth & Van Dyke, 1982, Joint water supply study, Marinette and Menominee report on test well #3: Green Bay, Wis., unpublished report,, 28 p.

Freeze, R.A., and Cherry, J.A., 1979, Groundwater: Englewood Cliffs, N.J., Prentice-Hall, 604 p.

Hart, D.J., Bradbury, K.R., and Feinstein, D.T., 2006, The vertical hydraulic conductivity of an aquitard at two spatial scales: Ground Water, v. 44, no 2, p. 201–211.

Joseph, R.L., and Eberts, S.M., 1994, Selected data on characteristics of glacial-deposit and carbonate-rock aquifers, Midwestern Basins and Arches region: U.S. Geological Survey Open-File Report 93–627, 43 p.

Knowles, D.B., 1964, Ground-water conditions in the Green Bay area, Wisconsin, 1950–60: U.S. Geological Survey Water-Supply Paper 1669–J, 37 p.

Krohelski, J.T., 1986, Hydrogeology and ground-water use and quality, Brown County, Wisconsin: Wisconsin Geological and Natural History Survey Information Circular 57, 42 p.

Krohelski, J.T., Bradbury, K.R., Hunt, R.J., and Swanson, S.K., 2000, Numerical simulation of groundwater flow in Dane County, Wisconsin: Wisconsin Geological and Natural History Survey Bulletin 98, 31 p.

LeRoux, E.F., 1957, Geology and ground-water resources of Outagamie County, Wisconsin: U.S. Geological Survey Water-Supply Paper 1421, 57 p.

LeRoux, E.F., 1963, Geology and ground-water resources of Rock County, Wisconsin: U.S. Geological Survey Water-Supply Paper 1619–X, 50 p.

Mandle, R.J., and Kontis, A.L., 1992, Simulation of regional ground-water flow in the Cambrian-Ordovician aquifer system in the northern Midwest, United States: U.S. Geological Survey Professional Paper 1405–C, 97 p.

Meyer, S.C., Lin, Y.-F., Roadcap, G.S., and Walker, D.D., 2009, Kane County water resources investigations—Simulation of groundwater flow in Kane County and northeastern Illinois: Illinois State Water Survey Contract Report 2009–07, 425 p.

Michigan Department of Environmental Quality, 2005, Groundwater Mapping Project: Accessed January 20, 2009, at *http://gwmap.rsgis.msu.edu/*.

Michigan Center for Geographic Information, 2009, Michigan Geographic Data Library—Drinking water wells geographic theme: Accessed January 22, 2009, at *http://www.mcgi.state.mi.us/mgdl/?rel=thext&action=thmname&cid=2&cat=Drinking+Water+Wells.*

Michigan Department of Environmental Quality, 2006, State of Michigan, Public Act 148, Groundwater Inventory and Map (GWIM) Project, Technical report: 257 p., accessed February 3, 2008, at *http://gwmap.rsgis.msu.edu/Technical_Report.pdf.*

Milstein, R.L., 1987, Bedrock geology of southern Michigan: Michigan Geological Survey, map sheet, scale 1:500,000.

Mueller, S.D., 1992, Three-dimensional digital simulation of the ground-water contribution to Lake Michigan from the Silurian aquifer of southeastern Wisconsin: University of Wisconsin-Milaukee, unpublished M.S. thesis, 231 p.

Nauta, R., 1987, A three-dimensional groundwater flow model of the Silurian dolomite aquifer of Door County, Wisconsin: University of Wisconsin-Madison, unpublished M.S. thesis, 105 p.

Newport, T.G., 1962, Geology and ground-water resources of Fond du Lac County, Wisconsin: U.S. Geological Survey Water-Supply Paper 1604, 52 p.

Nicholas, J.R., Sherrill, M.G., and Young, H.L., 1987, Hydrogeology of the Cambrian-Ordovician aquifer system at a test well in northeastern Illinois: U.S. Geological Survey Water-Resources Investigations/Open-File Report 84–4165, 30 p.

Olcott, P.G., 1966, Geology and ground-water resources of Winnebago County, Wisconsin: U.S. Geological Survey Water-Supply Paper 1814, 61 p.

Prudic, D.E., 1991, Estimates of hydraulic conductivity from aquifer-test analysis and specific-capacity data, Gulf Coast Regional Aquifer Systems, south-central United States: U.S. Geological Survey Water-Resources Investigations Report 90–4121, 38 p.

Sheets, R.A., 1999, Background hydrogeologic data, water quality, and aquifer characteristics, western Allen County, Ohio: U.S. Geological Survey Water-Resources Investigations Report 99–4146, 23 p.

Sinclair, W.C., 1959, Reconnaissance of the ground-water resources of Schoolcraft County, Michigan: Michigan Geological Survey Progress Report 22, 84 p.

Sinclair, W.C., 1960, Reconnaissance of the ground-water resources of Delta County, Michigan: Michigan Geological Survey Progress Report 24, 93 p.

Thornton, M.M., and Wilson, A.M., 2007, Topography-driven flow versus buoyancy-driven flow in the U.S. midcontinent—Implications for the residence time of brines: Geofluids, v. 7, no. 1, p. 69–78.

Vanlier, K.E., and Deutsch, Morris, 1958a, Reconnaissance of the ground-water resources of Chippewa County, Michigan: Michigan Geological Survey Progress Report 17, 56 p.

Vanlier, K.E., and Deutsch, Morris, 1958b, Reconnaissance of the ground-water resources of Mackinac County, Michigan: Michigan Geological Survey Progress Report 19, 82 p.

Walton, W.C., 1960, Leaky artesian aquifer conditions in Illinois: Illinois State Water Survey Report of Investigation 39, 27 p.

Weaver, T.R., and Bahr, J.M., 1990, Groundwater geochemistry and radionuclide activity in the Cambrian-Ordovician aquifer of Dodge and Fond du Lac Counties, Wisconsin: Madison, Wis., University of Wisconsin Water Resources Center Technical Report 90–01, 67 p.

Webb, E.K., 1989, Estimating groundwater discharge to Lake Michigan using a three-dimensional groundwater flow model, along a portion of the shoreline from Door County to Port Washington, Wisconsin: University of Wisconsin-Madison, unpublished M.S. thesis, 227 p.

Westjohn, D.B., and Weaver, T.L., 1998, Hydrogeologic framework of the Michigan Basin regional aquifer system, central Lower Peninsula of Michigan: U.S. Geological Survey Professional Paper 1418, 47 p.

Young, H.L., 1992, Summary of ground-water hydrology of the Cambrian-Ordovician aquifer system in the northern Midwest, United States: U.S. Geological Survey Professional Paper 1405–A, 55 p.

Appendix 5. Calibration Parameters

This appendix contains two tables. The first, table 5–1, lists the 38 multiplier parameters that are fixed at a value of 1 during the calibration process, so the initial values of the input represented by these parameters do not change. The second, table 5–2, lists the 165 multiplier parameters (plus 178 pilot points) that are subject to estimation during the calibration process.

Both tables list

- the aquifer system corresponding to each parameter,
- the model layer(s) corresponding to each parameter,
- the number of input values in the zone represented by the parameter,

Table 5–1. Parameters with fixed values.

[Kh, horizontal hydraulic conductivity; Kv, vertical hydraulic conductivity; --, not applicable; gradational, number of nearfield values implies values are interpolated across cells]

Parameter name	Number	Aquifer system	Layer	Number of nearfield values	Fixed value(s) or geometric mean of fixed values	Unit
Kh_Lake_Michigan_bed_sediments	1	QRNR	1,2,3	4	0.1–1.0	Feet per day
Kh_JURA_zone1	2	PENN	4	1	0.50	Feet per day
Kv_PEN1_zone1	3	PENN	5	1	1.00 E−01	Feet per day
Kh_MICH_zone1	4	MSHL	7	1	0.10	Feet per day
Kv_MSHL_zone1	5	MSHL	8	1	5.20 E−02	Feet per day
Kv_MSHL_zone2	6	MSHL	8	1	1.56 E−01	Feet per day
Kv_MSHL_zone3	7	MSHL	8	1	2.08 E−01	Feet per day
Kh_DVMS_zone1	8	SLDV	9	1	0.0002	Feet per day
Kh_DVMS_zone2	9	SLDV	9	1	0.10	Feet per day
Kh_DVMS_zone3	10	SLDV	9	1	0.10	Feet per day
Kh_DVMS_zone4	11	SLDV	9	1	0.30	Feet per day
Kh_DVMS_zone5	12	SLDV	9	1	0.50	Feet per day
Kh_DVMS_zone6	13	SLDV	9	1	1.00	Feet per day
Kv_SLDV_layer10_zone1	14	SLDV	10	2	3.01 E−03	Feet per day
Kv_SLDV_layer10_zone2	15	SLDV	10	3	1.01 E−02	Feet per day
Kv_SLDV_layer10_zone3	16	SLDV	10	1	1.67 E−02	Feet per day
Kv_SLDV_layer10_zone4	17	SLDV	10	1	1.00 E−01	Feet per day
Kv_SLDV_layer10_zone5	18	SLDV	10	2	1.52 E−01	Feet per day

- the initial value(s) or the geometric mean of multiple initial values in the zone, and
- the dimensional units of the input.

For the estimated parameters, table 5–2 also lists

- the sensitivity group to which the parameter belongs,
- a flag indicating if the parameter is included for analysis in appendix 6,
- the upper and lower bounds imposed on the parameter during inversion,
- the parameter multiplier resulting from calibration of the confined model SLMB-C (color coded to indicate if bounds hit or if multiplier is less than 0.5 or greater than 2.0),
- the parameter multiplier resulting from calibration of the unconfined model SLMB-U (also color coded), and
- comments for selected parameters.

Table 5–1. Parameters with fixed values.—Continued

[Kh, horizontal hydraulic conductivity; Kv, vertical hydraulic conductivity; --, not applicable; gradational, number of nearfield values implies values are interpolated across cells]

Parameter name	Number	Aquifer system	Layer	Number of nearfield values	Fixed value(s) or geometric mean of fixed values	Unit
Kh_MAQU_zone1	19	C-O	13	1	0.10	Feet per day
Kh_MAQU_zone2	20	C-O	13	1	0.50	Feet per day
Kv_STPT_zone1	21	C-O	15	1	4.00 E−04	Feet per day
Kv_STPT_zone2	22	C-O	15	5	4.94 E−03	Feet per day
Kv_STPT_zone3	23	C-O	15	3	4.32 E−02	Feet per day
Kv_STPT_zone4	24	C-O	15	0	--	--
Kv_STPT_zone5	25	C-O	15	3	4.69 E−01	Feet per day
Kv_STPT_zone6	26	C-O	15	1	6.00 E−01	Feet per day
Kv_IRGA_zone1	27	C-O	17	3	1.04 E−02	Feet per day
Kv_IRGA_zone2	28	C-O	17	2	3.12 E−02	Feet per day
Kv_IRGA_zone3	29	C-O	17	3	7.56 E−02	Feet per day
Kv_IRGA_zone4	30	C-O	17	1	2.00 E−01	Feet per day
Kv_IRGA_zone5	31	C-O	17	1	7.00 E−01	Feet per day
Kv_MTSM_layer19_zone1	32	C-O	19	1	4.00 E−04	Feet per day
Kv_MTSM_layer19_zone2	33	C-O	19	Gradational	3.14 E−03	Feet per day
Kv_MTSM_layer19_zone3	34	C-O	19	Gradational	9.85 E−03	Feet per day
Kv_MTSM_layer19_zone4	35	C-O	19	2	2.38 E−02	Feet per day
Kv_MTSM_layer19_zone5	36	C-O	19	2	4.90 E−02	Feet per day
Kv_MTSM_layer19_zone6	37	C-O	19	3	8.97 E−02	Feet per day
Kv_MTSM_layer19_zone7	38	C-O	19	1	5.00 E−01	Feet per day

Table 5–2. Parameters estimated in calibration process.

[--, not applicable; Kh, horizontal hydraulic conductivity; Kv, vertical hydraulic conductivity; gradational, number of nearfield values implies values are interpolated across cells; ft, feet; ft/d, feet per day; ft^2/d, feet squared per day]

Parameter name	Number	Aquifer system	Layer(s)	Parameter group for sensitivity analysis	Figure and table in appendix 6	Number of nearfield values	Initial value(s) or geometric mean of mulitple initial values
Recharge_1991–2005	1	--	Highest active	Recharge_ 1990-2005		Cell by cell	--
Kh_clayey_till	2	QRNR	1,2,3	Kh_QRNR	x	Cell by cell	1.04
Kh_loamy_till_and_organic_ deposits	3	QRNR	1,2,3	Kh_QRNR	x	Cell by cell	4.12
Kh_sandy_till	4	QRNR	1,2,3	Kh_QRNR	x	Cell by cell	12.43
Kh_fine-stratified_deposits	5	QRNR	1,2,3	Kh_QRNR	x	Cell by cell	4.54
Kh_medium_and_coarse stratified	6	QRNR	1,2,3	Kh_QRNR	x	Cell by cell	70.79
Kh_unknown_QRNR_deposits	7	QRNR	1,2,3	Kh_QRNR	x	Cell by cell	5.69
Kv/Kh_clayey_till	8	QRNR	1,2,3	Kv/Kh_ QRNR	x	1	0.05
Kh/Kv_loamy_till_and_organic_ deposits	9	QRNR	1,2,3	Kv/Kh_ QRNR	x	1	0.05
Kh/Kv_sandy_till	10	QRNR	1,2,3	Kv/Kh_ QRNR	x	1	0.05
Kh/Kv_fine_stratified_deposits	11	QRNR	1,2,3	Kv/Kh_ QRNR	x	1	0.05
Kh/Kv_medium_and_coarse stratified	12	QRNR	1,2,3	Kv/Kh_ QRNR	x	1	0.05
Kh/Kv_unknown_QRNR_deposits	13	QRNR	1,2,3	Kv/Kh_ QRNR	x	1	0.05
Kv_Lake_Michigan_bed_ sediments	14	QRNR	1	Kv/Kh_ QRNR	x	4	0.1–0.001
Kh_PEN1_zone1	15	PENN	5	Kh_PENN-MSHL	x	1	6.00
Kh_PEN1_zone2	16	PENN	5	Kh_PENN-MSHL	x	1	10.00
Kh_PEN1_zone3	17	PENN	5	Kh_PENN-MSHL	x	1	20.00
Kh_PEN2_zone1	18	PENN	6	Kh_PENN-MSHL		Gradational	0.31
Kh_PEN2_zone2	19	PENN	6	Kh_PENN-MSHL		Gradational	0.57
Kh_PEN2_zone3	20	PENN	6	Kh_PENN-MSHL		Gradational	0.86
Kh_PEN2_zone4	21	PENN	6	Kh_PENN-MSHL		Gradational	1.30

Table 5–2. Parameters estimated in calibration process.—Continued

[--, not applicable; Kh, horizontal hydraulic conductivity; Kv, vertical hydraulic conductivity; gradational, number of nearfield values implies values are interpolated across cells; ft, feet; ft/d, feet per day; ft²/d, feet squared per day]

Parameter name	Unit	Bounds imposed on multiplier of initial values	Confined calibration multiplier (SLMB-C)	Unconfined calibration multiplier (SLMB-U)	Comments: for multipliers, red indicates at bound; blue indicates less than 0.5× or greater than 2.0×
Recharge_1990-2005	--	--	1.048	1.060	Recharge multiplier applied to all stress periods.
Kh_clayey_till	ft/d	0.5×–5.0×	5.00	5.00	
Kh_loamy_till_and_organic_deposits	ft/d	0.27×–2.7×	2.70	2.70	
Kh_sandy_till	ft/d	0.163×–1.63×	1.63	1.63	
Kh_fine-stratified_deposits	ft/d	0.3×–3.0×	2.09	2.73	
Kh_medium_and_coarse stratified	ft/d	--	2.04	1.51	
Kh_unknown_QRNR_deposits	ft/d	--	0.85	0.74	
Kh/Kv_clayey_till	--	--	0.18	0.34	Kv derived from Kh and anisotropy factor.
Kh/KV_loamy_till_and_organic_deposits	--	--	0.51	0.31	Kv derived from Kh and anisotropy factor.
Kh/Kv_sandy_till	--	--	0.64	0.65	Kv derived from Kh and anisotropy factor.
Kh/Kv_fine_stratified_deposits	--	--	0.65	0.55	Kv derived from Kh and anisotropy factor.
Kh/Kv_medium_and_coarse stratified	--	--	0.54	0.58	Kv derived from Kh and anisotropy factor
Kh/Kv_unknown_QRNR_deposits	--	--	1.56	1.62	Kv derived from Kh and anisotropy factor.
Kv_Lake_Michigan_bed_sediments	--	--	1.08	1.24	Three coastal Kv zones and one interior Kv zone.
Kh_PEN1_zone1	ft/d	0.1×–10×	0.97	0.83	
Kh_PEN1_zone2	ft/d	0.1×–10×	1.25	1.54	
Kh_PEN1_zone3	ft/d	0.1×–10×	1.38	1.30	
Kh_PEN2_zone1	ft/d	0.1×–10×	1.51	1.20	Gradational values depend on transmissivity zones divided by unit thickness.
Kh_PEN2_zone2	ft/d	0.1×–10×	1.92	2.61	
Kh_PEN2_zone3	ft/d	0.1×–10×	1.26	2.09	
Kh_PEN2_zone4	ft/d	0.1×–10×	1.33	0.81	

Table 5–2. Parameters estimated in calibration process.—Continued

[--, not applicable; Kh, horizontal hydraulic conductivity; Kv, vertical hydraulic conductivity; gradational, number of nearfield values implies values are interpolated across cells; ft, feet; ft/d, feet per day; ft^2/d, feet squared per day]

Parameter name	Number	Aquifer system	Layer(s)	Parameter group for sensitivity analysis	Figure and table in appendix 6	Number of nearfield values	Initial value(s) or geometric mean of mulitple initial values
Kh_PEN2_zone5	22	PENN	6	Kh_PENN-MSHL		Gradational	2.01
Kh_PEN2_zone6	23	PENN	6	Kh_PENN-MSHL		Gradational	3.12
Kh_PEN2_zone7	24	PENN	6	Kh_PENN-MSHL		Gradational	4.59
Kh_PEN2_zone8	25	PENN	6	Kh_PENN-MSHL		Gradational	5.80
Kh_MSHL_zone1	32	MSHL	8	Kh_PENN-MSHL	x	1	5.00
Kh_MSHL_zone2	33	MSHL	8	Kh_PENN-MSHL	x	1	15.00
Kh_MSHL_zone3	34	MSHL	8	Kh_PENN-MSHL	x	1	20.00
Kv_JURA_zone1	26	PENN	4	Kv_PENN-MSHL		1	5.00E−04
Kv_PEN2_zone1	27	PENN	6	Kv_PENN-MSHL	x	Gradational	4.40E−04
Kv_PEN2_zone2	28	PENN	6	Kv_PENN-MSHL	x	Gradational	8.54E−04
Kv_PEN2_zone3	29	PENN	6	Kv_PENN-MSHL	x	Gradational	1.54E−03
Kv_PEN2_zone4	30	PENN	6	Kv_PENN-MSHL	x	Gradational	2.62E−03
Kv_PEN2_zone5	31	PENN	6	Kv_PENN-MSHL	x	1	7.00E−02
Kv_MICH_zone1	35	MSHL	7	Kv_PENN-MSHL	x	1	1.00E−04
Kh_SLDV_layer10_zone1	36	SLDV	10	Kh_SLDV	x	1	0.54
Kh_SLDV_layer10_zone2	37	SLDV	10	Kh_SLDV	x	1	2.00
Kh_SLDV_layer10_zone3	38	SLDV	10	Kh_SLDV	x	1	5.00
Kh_SLDV_layer10_zone4	39	SLDV	10	Kh_SLDV	x	1	9.09
Kh_SLDV_layer10_zone5	40	SLDV	10	Kh_SLDV	--	0	--
Kh_SLDV_layer10_zone6	41	SLDV	10	Kh_SLDV	x	1	5.00
Kh_SLDV_layer10_zone7	42	SLDV	10	Kh_SLDV	x	1	6.48
Kh_SLDV_layer10_zone8	43	SLDV	10	Kh_SLDV	x	1	4.60
Kh_SLDV_layer10_zone9	44	SLDV	10	Kh_SLDV	x	1	30.22
Kh_SLDV_layer11_zone1	45	SLDV	11	Kh_SLDV		1	0.01

Table 5–2. Parameters estimated in calibration process.—Continued

[--, not applicable; Kh, horizontal hydraulic conductivity; Kv, vertical hydraulic conductivity; gradational, number of nearfield values implies values are interpolated across cells; ft, feet; ft/d, feet per day; ft²/d, feet squared per day]

Parameter name	Unit	Bounds imposed on multiplier of initial values	Confined calibration multiplier (SLMB-C)	Unconfined calibration multiplier (SLMB-U)	Comments: for multipliers, red indicates at bound; blue indicates less than 0.5× or greater than 2.0×
Kh_PEN2_zone5	ft/d	0.1×–10×	0.83	0.77	
Kh_PEN2_zone6	ft/d	0.1×–10×	1.09	0.81	
Kh_PEN2_zone7	ft/d	0.1×–10×	1.55	1.07	
Kh_PEN2_zone8	ft/d	0.1×–10×	1.02	0.74	
Kh_MSHL_zone1	ft/d	0.1×–10×	0.85	0.79	
Kh_MSHL_zone2	ft/d	0.1×–10×	2.57	1.80	
Kh_MSHL_zone3	ft/d	0.1×–10×	1.38	1.44	
Kv_JURA_zone1	ft/d	0.1×–10×	1.25	1.32	
Kv_PEN2_zone1	ft/d	0.1×–10×	0.99	0.61	Gradational values depend on relative thickness of Saginaw Formation (shale).
Kv_PEN2_zone2	ft/d	0.1×–10×	1.80	2.37	
Kv_PEN2_zone3	ft/d	0.1×–10×	1.14	0.99	
Kv_PEN2_zone4	ft/d	0.1×–10×	1.57	1.41	
Kv_PEN2_zone5	ft/d	0.1×–10×	0.77	1.06	
Kv_MICH_zone1	ft/d	0.1×–10×	1.20	0.72	
Kh_SLDV_layer10_zone1	ft/d	0.1×–10×	1.13	1.21	
Kh_SLDV_layer10_zone2	ft/d	0.1×–2×	2.00	2.00	
Kh_SLDV_layer10_zone3	ft/d	0.1×–10×	2.60	1.88	
Kh_SLDV_layer10_zone4	ft/d	0.1×–10×	0.98	0.71	
Kh_SLDV_layer10_zone5	--	--	--	--	
Kh_SLDV_layer10_zone6	ft/d	0.1×–2×	1.09	1.22	
Kh_SLDV_layer10_zone7	ft/d	0.1×–2×	1.47	1.56	
Kh_SLDV_layer10_zone8	ft/d	0.1×–10×	0.88	0.60	
Kh_SLDV_layer10_zone9	ft/d	0.1×–10×	0.94	0.67	
Kh_SLDV_layer11_zone1	ft/d	0.1×–10×	1.10	0.89	

Table 5–2. Parameters estimated in calibration process.—Continued

[--, not applicable; Kh, horizontal hydraulic conductivity; Kv, vertical hydraulic conductivity; gradational, number of nearfield values implies values are interpolated across cells; ft, feet; ft/d, feet per day; ft^2/d, feet squared per day]

Parameter name	Number	Aquifer system	Layer(s)	Parameter group for sensitivity analysis	Figure and table in appendix 6	Number of nearfield values	Initial value(s) or geometric mean of mulitple initial values
Kh_SLDV_layer11_zone2	46	SLDV	11	Kh_SLDV		2	0.50
Kh_SLDV_layer11_zone3	47	SLDV	11	Kh_SLDV		1	0.80
Kh_SLDV_layer11_zone4	48	SLDV	11	Kh_SLDV		1	1.00
Kh_SLDV_layer11_zone5	49	SLDV	11	Kh_SLDV		1	1.67
Kh_SLDV_layer11_zone6	50	SLDV	11	Kh_SLDV		2	2.53
Kh_SLDV_layer11_zone7	51	SLDV	11	Kh_SLDV		1	4.00
Kh_SLDV_layer12_zone1	52	SLDV	12	Kh_SLDV		1	0.50
Kh_SLDV_layer12_zone2	53	SLDV	12	Kh_SLDV		1	0.80
Kh_SLDV_layer12_zone3	54	SLDV	12	Kh_SLDV		1	1.00
Kh_SLDV_layer12_zone4	55	SLDV	12	Kh_SLDV		1	1.67
Kh_SLDV_layer12_zone5	56	SLDV	12	Kh_SLDV		1	2.50
Kv_DVMS_zone1	57	SLDV	9	Kv_SLDV	x	1	2.20E−06
Kv_DVMS_zone2	58	SLDV	9	Kv_SLDV	x	1	5.00E−06
Kv_DVMS_zone3	59	SLDV	9	Kv_SLDV	--	0	--
Kv_SLDV_layer11_zone1	60	SLDV	11	Kv_SLDV	x	1	1.00E−07
Kv_SLDV_layer11_zone2	61	SLDV	11	Kv_SLDV	x	1	1.00E−04
Kv_SLDV_layer11_zone3	62	SLDV	11	Kv_SLDV	x	1	1.00E−03
Kv_SLDV_layer11_zone4	63	SLDV	11	Kv_SLDV	x	3	8.36E−03
Kv_SLDV_layer11_zone5	64	SLDV	11	Kv_SLDV	x	1	1.67E−02
Kv_SLDV_layer12_zone1	65	SLDV	12	Kv_SLDV		1	1.00E−03
Kv_SLDV_layer12_zone1	66	SLDV	12	Kv_SLDV		1	8.00E−03
Kv_SLDV_layer12_zone1	67	SLDV	12	Kv_SLDV		1	1.67E−02
Kh_SNNP_zone1	68	C-O	14	Kh_C-O		8	0.05
Kh_SNNP_zone2	69	C-O	14	Kh_C-O		Gradational	0.16
Kh_SNNP_zone3	70	C-O	14	Kh_C-O		Gradational	0.27
Kh_SNNP_zone4	71	C-O	14	Kh_C-O		3	0.60
Kh_SNNP_zone5	72	C-O	14	Kh_C-O		Gradational	2.20

Table 5–2. Parameters estimated in calibration process.—Continued

[--, not applicable; Kh, horizontal hydraulic conductivity; Kv, vertical hydraulic conductivity; gradational, number of nearfield values implies values are interpolated across cells; ft, feet; ft/d, feet per day; ft²/d, feet squared per day]

Parameter name	Unit	Bounds imposed on multiplier of initial values	Confined calibration multiplier (SLMB-C)	Unconfined calibration multiplier (SLMB-U)	Comments: for multipliers, red indicates at bound; blue indicates less than 0.5× or greater than 2.0×
Kh_SLDV_layer11_zone2	ft/d	0.1×–2×	0.74	0.91	
Kh_SLDV_layer11_zone3	ft/d	0.1×–10×	1.47	1.53	
Kh_SLDV_layer11_zone4	ft/d	0.1×–2×	1.28	0.82	
Kh_SLDV_layer11_zone5	ft/d	0.1×–10×	2.05	1.63	
Kh_SLDV_layer11_zone6	ft/d	0.1×–2×	1.41	1.36	
Kh_SLDV_layer11_zone7	ft/d	0.1×–10×	0.90	1.23	
Kh_SLDV_layer12_zone1	ft/d	0.1×–10×	0.95	1.47	
Kh_SLDV_layer12_zone2	ft/d	0.1×–10×	1.64	2.22	
Kh_SLDV_layer12_zone3	ft/d	0.1×–2×	1.32	1.71	
Kh_SLDV_layer12_zone4	ft/d	0.1×–10×	0.87	1.05	
Kh_SLDV_layer12_zone5	ft/d	0.1×–2×	0.92	0.91	
Kv_DVMS_zone1	ft/d	0.1×–10×	1.37	1.11	
Kv_DVMS_zone2	ft/d	0.1×–10×	0.86	0.98	
Kv_DVMS_zone3	--	--	--	--	
Kv_SLDV_layer11_zone1	ft/d	0.1×–10×	1.14	0.82	
Kv_SLDV_layer11_zone2	ft/d	0.1×–10×	1.44	1.46	
Kv_SLDV_layer11_zone3	ft/d	0.1×–10×	2.83	5.20	
Kv_SLDV_layer11_zone4	ft/d	0.1×–10×	1.46	0.97	
Kv_SLDV_layer11_zone5	ft/d	0.1×–10×	1.12	1.64	
Kv_SLDV_layer12_zone1	ft/d	0.1×–10×	1.38	1.15	
Kv_SLDV_layer12_zone1	ft/d	0.1×–10×	1.17	1.07	
Kv_SLDV_layer12_zone1	ft/d	0.1×–10×	1.14	1.40	
Kh_SNNP_zone1	ft/d	0.1×–10×	0.85	0.51	
Kh_SNNP_zone2	ft/d	0.1×–10×	1.24	1.18	Gradational values correspond to weathered areas.
Kh_SNNP_zone3	ft/d	0.1×–10×	0.96	0.45	Gradational values correspond to weathered areas.
Kh_SNNP_zone4	ft/d	0.1×–10×	2.08	2.02	
Kh_SNNP_zone5	ft/d	0.1×–10×	1.51	1.61	Gradational values correspond to weathered areas.

Table 5–2. Parameters estimated in calibration process.—Continued

[--, not applicable; Kh, horizontal hydraulic conductivity; Kv, vertical hydraulic conductivity; gradational, number of nearfield values implies values are interpolated across cells; ft, feet; ft/d, feet per day; ft^2/d, feet squared per day]

Parameter name	Number	Aquifer system	Layer(s)	Parameter group for sensitivity analysis	Figure and table in appendix 6	Number of nearfield values	Initial value(s) or geometric mean of mulitple initial values
Kh_SNNP_zone6	73	C-O	14	Kh_C-O		4	5.46
Kh_STPT_zone1	74	C-O	15	Kh_C-O	x	5	1.62
Kh_STPT_zone2	75	C-O	15	Kh_C-O	x	3	1.55
Kh_STPT_zone3	76	C-O	15	Kh_C-O	x	5	1.98
Kh_STPT_zone4	77	C-O	15	Kh_C-O	x	3	1.44
Kh_STPT_zone5	78	C-O	15	Kh_C-O	x	4	6.72
Kh_PCFR_zone1	79	C-O	16	Kh_C-O		1	0.24
Kh_PCFR_zone2	80	C-O	16	Kh_C-O		3	0.50
Kh_PCFR_zone3	81	C-O	16	Kh_C-O		4	1.48
Kh_PCFR_zone4	82	C-O	16	Kh_C-O		10	1.46
Kh_PCFR_zone5	83	C-O	16	Kh_C-O		Gradational	2.15
Kh_PCFR_zone6	84	C-O	16	Kh_C-O		Gradational	2.99
Kh_PCFR_zone7	85	C-O	16	Kh_C-O		3	4.53
Kh_PCFR_zone8	86	C-O	16	Kh_C-O		1	7.50
Kh_IRGA_zone1	87	C-O	17	Kh_C-O	x	5	1.52
Kh_IRGA_zone2	88	C-O	17	Kh_C-O	x	6	4.62
Kh_IRGA_zone3	89	C-O	17	Kh_C-O	x	3	2.58
Kh_IRGA_zone4	90	C-O	17	Kh_C-O	x	2	5.44
Kh_IRGA_zone5	91	C-O	17	Kh_C-O	x	7	3.98
Kh_IRGA_zone6	92	C-O	17	Kh_C-O	x	7	3.14
Kh_EACL_zone1	93	C-O	18	Kh_C-O		3	0.51
Kh_EACL_zone2	94	C-O	18	Kh_C-O		3	1.08
Kh_EACL_zone3	95	C-O	18	Kh_C-O		3	2.38
Kh_EACL_zone4	96	C-O	18	Kh_C-O		1	1.50
Kh_EACL_zone5	97	C-O	18	Kh_C-O		1	8.92
Kh_MTSM_layer19_zone1	98	C-O	19	Kh_C-O	x	1	0.43
Kh_MTSM_layer19_zone2	99	C-O	19	Kh_C-O	x	3	1.03
Kh_MTSM_layer19_zone3	100	C-O	19	Kh_C-O	x	Gradational	1.97
Kh_MTSM_layer19_zone4	101	C-O	19	Kh_C-O	x	5	3.02

Table 5–2. Parameters estimated in calibration process.—Continued

[--, not applicable; Kh, horizontal hydraulic conductivity; Kv, vertical hydraulic conductivity; gradational, number of nearfield values implies values are interpolated across cells; ft, feet; ft/d, feet per day; ft²/d, feet squared per day]

Parameter name	Unit	Bounds imposed on multiplier of initial values	Confined calibration multiplier (SLMB-C)	Unconfined calibration multiplier (SLMB-U)	Comments: for multipliers, red indicates at bound; blue indicates less than 0.5× or greater than 2.0×
Kh_SNNP_zone6	ft/d	0.1×–10×	0.73	0.47	
Kh_STPT_zone1	ft/d	0.1×–10×	0.32	0.26	
Kh_STPT_zone2	ft/d	0.1×–10×	2.34	2.59	
Kh_STPT_zone3	ft/d	0.1×–10×	0.24	0.28	
Kh_STPT_zone4	ft/d	0.1×–10×	3.43	3.69	
Kh_STPT_zone5	ft/d	0.1×–10×	1.56	2.25	
Kh_PCFR_zone1	ft/d	0.1×–10×	1.68	1.74	
Kh_PCFR_zone2	ft/d	0.1×–10×	0.10	0.10	
Kh_PCFR_zone3	ft/d	0.1×–10×	0.17	0.15	
Kh_PCFR_zone4	ft/d	0.1×–10×	1.18	1.44	
Kh_PCFR_zone5	ft/d	0.1×–10×	1.36	1.47	Gradational values correspond to weathered areas.
Kh_PCFR_zone6	ft/d	0.1×–10×	0.10	0.10	Gradational values correspond to weathered areas.
Kh_PCFR_zone7	ft/d	0.1×–10×	1.81	0.65	
Kh_PCFR_zone8	ft/d	0.1×–10×	0.97	0.65	
Kh_IRGA_zone1	ft/d	0.1×–10×	1.08	1.78	
Kh_IRGA_zone2	ft/d	0.1×–10×	4.38	4.71	
Kh_IRGA_zone3	ft/d	0.1×–10×	0.31	0.38	
Kh_IRGA_zone4	ft/d	0.1×–10×	0.87	0.92	
Kh_IRGA_zone5	ft/d	0.1×–10×	0.50	0.69	
Kh_IRGA_zone6	ft/d	0.1×–10×	0.86	0.91	
Kh_EACL_zone1	ft/d	0.1×–10×	2.01	2.14	
Kh_EACL_zone2	ft/d	0.1×–10×	0.95	0.85	
Kh_EACL_zone3	ft/d	0.1×–10×	0.86	0.78	
Kh_EACL_zone4	ft/d	0.1×–10×	1.15	0.76	
Kh_EACL_zone5	ft/d	0.1×–10×	0.77	0.92	
Kh_MTSM_layer19_zone1	ft/d	0.1×–10×	6.90	8.98	
Kh_MTSM_layer19_zone2	ft/d	0.1×–10×	1.32	0.90	
Kh_MTSM_layer19_zone3	ft/d	0.1×–10×	1.50	1.43	Gradational values correspond to weathered areas.
Kh_MTSM_layer19_zone4	ft/d	0.1×–10×	1.52	2.32	

Table 5–2. Parameters estimated in calibration process.—Continued

[--, not applicable; Kh, horizontal hydraulic conductivity; Kv, vertical hydraulic conductivity; gradational, number of nearfield values implies values are interpolated across cells; ft, feet; ft/d, feet per day; ft²/d, feet squared per day]

Parameter name	Number	Aquifer system	Layer(s)	Parameter group for sensitivity analysis	Figure and table in appendix 6	Number of nearfield values	Initial value(s) or geometric mean of mulitple initial values
Kh_MTSM_layer19_zone5	102	C-O	19	Kh_C-O	x	2	2.43
Kh_MTSM_layer19_zone6	103	C-O	19	Kh_C-O	x	3	1.52
Kh_MTSM_layer19_zone7	104	C-O	19	Kh_C-O	x	1	1.40
Kh_MTSM_layer19_zone8	105	C-O	19	Kh_C-O	x	2	6.95
Kh_MTSM_layer20_zone1	106	C-O	20	Kh_C-O		1	0.23
Kh_MTSM_layer20_zone2	107	C-O	20	Kh_C-O		1	0.43
Kh_MTSM_layer20_zone3	108	C-O	20	Kh_C-O		Gradational	1.12
Kh_MTSM_layer20_zone4	109	C-O	20	Kh_C-O		Gradational	1.46
Kh_MTSM_layer20_zone5	110	C-O	20	Kh_C-O		2	2.06
Kh_MTSM_layer20_zone6	111	C-O	20	Kh_C-O		3	2.36
Kh_MTSM_layer20_zone7	112	C-O	20	Kh_C-O		4	1.48
Kh_MTSM_layer20_zone8	113	C-O	20	Kh_C-O		Gradational	1.95
Kv_MAQU_zone1	114	C-O	13	Kv_MAQU-zone	x	1	6.70E−06
Kv_MAQU_zone2 replaced by pilot points				--	--	--	--
Kv_MAQU_zone3 replaced by pilot points				--	--	--	--
Kv_MAQU_zone4	115	C-O	13	Kv_MAQU-zone	x	2	1.31E−05
Kv_MAQU_zone5	116	C-O	13	Kv_MAQU-zone	x	3	5.07E−04
Kv_MAQU_zone6	117	C-O	13	Kv_MAQU-zone	x	4	9.08E−04
Kv_MAQU_zone7	118	C-O	13	Kv_MAQU-zone	x	2	1.42E−03
Kv_SNNP_zone1	119	C-O	14	Kv_C-O		1	6.25E−04
Kv_SNNP_zone2	120	C-O	14	Kv_C-O		1	1.50E−03
Kv_SNNP_zone3	121	C-O	14	Kv_C-O		1	7.82E−04
Kv_SNNP_zone4	122	C-O	14	Kv_C-O		1	6.25E−04
Kv_SNNP_zone5	123	C-O	14	Kv_C-O		1	2.43E−04
Kv_SNNP_zone6	124	C-O	14	Kv_C-O		1	6.25E−04
Kv_SNNP_zone7	125	C-O	14	Kv_C-O		1	6.25E−04

Table 5–2. Parameters estimated in calibration process.—Continued

[--, not applicable; Kh, horizontal hydraulic conductivity; Kv, vertical hydraulic conductivity; gradational, number of nearfield values implies values are interpolated across cells; ft, feet; ft/d, feet per day; ft²/d, feet squared per day]

Parameter name	Unit	Bounds imposed on multiplier of initial values	Confined calibration multiplier (SLMB-C)	Unconfined calibration multiplier (SLMB-U)	Comments: for multipliers, red indicates at bound; blue indicates less than 0.5× or greater than 2.0×
Kh_MTSM_layer19_zone5	ft/d	0.1×–10×	0.10	0.10	
Kh_MTSM_layer19_zone6	ft/d	0.1×–10×	0.10	0.10	
Kh_MTSM_layer19_zone7	ft/d	0.1×–10×	0.92	0.93	
Kh_MTSM_layer19_zone8	ft/d	0.1×–10×	1.08	0.86	
Kh_MTSM_layer20_zone1	ft/d	0.1×–10×	1.05	0.99	
Kh_MTSM_layer20_zone2	ft/d	0.1×–10×	3.25	4.25	
Kh_MTSM_layer20_zone3	ft/d	0.1×–10×	1.82	1.54	Gradational values correspond to weathered areas.
Kh_MTSM_layer20_zone4	ft/d	0.1×–10×	2.21	2.17	Gradational values correspond to weathered areas.
Kh_MTSM_layer20_zone5	ft/d	0.1×–10×	1.64	1.76	
Kh_MTSM_layer20_zone6	ft/d	0.1×–10×	1.16	0.93	
Kh_MTSM_layer20_zone7	ft/d	0.1×–10×	0.83	0.75	
Kh_MTSM_layer20_zone8	ft/d	0.1×–10×	0.25	0.22	Gradational values correspond to weathered areas.
Kv_MAQU_zone1		0.3×–10×	0.30	0.30	
Kv_MAQU_zone2 replaced by pilot points		--	--	--	
Kv_MAQU_zone3 replaced by pilot points		--	--	--	
Kv_MAQU_zone4	ft/d	0.1×–10×	0.87	0.86	
Kv_MAQU_zone5	ft/d	0.1×–10×	2.80	3.38	
Kv_MAQU_zone6	ft/d	0.1×–10×	1.11	0.81	
Kv_MAQU_zone7	ft/d	0.1×–10×	1.74	0.78	
Kv_SNNP_zone1	ft/d	0.1×–10×	2.80	2.69	
Kv_SNNP_zone2	ft/d	0.1×–10×	0.96	1.08	
Kv_SNNP_zone3	ft/d	0.1×–10×	1.52	2.02	
Kv_SNNP_zone4	ft/d	0.1×–10×	2.51	2.05	
Kv_SNNP_zone5	ft/d	0.1×–10×	0.89	1.25	
Kv_SNNP_zone6	ft/d	0.1×–10×	0.16	0.15	
Kv_SNNP_zone7	ft/d	0.1×–10×	0.27	0.28	

Table 5–2. Parameters estimated in calibration process.—Continued

[--, not applicable; Kh, horizontal hydraulic conductivity; Kv, vertical hydraulic conductivity; gradational, number of nearfield values implies values are interpolated across cells; ft, feet; ft/d, feet per day; ft²/d, feet squared per day]

Parameter name	Number	Aquifer system	Layer(s)	Parameter group for sensitivity analysis	Figure and table in appendix 6	Number of nearfield values	Initial value(s) or geometric mean of mulitple initial values
Kv_PCFR_zone1	126	C-O	16	Kv_C-O		Gradational	1.01 E−04
Kv_PCFR_zone2	127	C-O	16	Kv_C-O		2	4.07 E−04
Kv_PCFR_zone3	128	C-O	16	Kv_C-O		1	1.00 E−03
Kv_PCFR_zone4	129	C-O	16	Kv_C-O		3	8.54 E−03
Kv_PCFR_zone5	130	C-O	16	Kv_C-O		3	2.12 E−02
Kv_PCFR_zone6	131	C-O	16	Kv_C-O		2	9.81 E−02
Kv_PCFR_zone7	132	C-O	16	Kv_C-O		2	2.99 E−01
Kv_PCFR_zone8	133	C-O	16	Kv_C-O		1	5.00 E−01
Kv_EACL_zone1	134	C-O	18	Kv_C-O	x	1	1.00 E−05
Kv_EACL_zone2	135	C-O	18	Kv_C-O	x	1	4.00 E−05
Kv_EACL_zone3	136	C-O	18	Kv_C-O	x	2	4.07 E−04
Kv_EACL_zone4	137	C-O	18	Kv_C-O	x	1	6.00 E−04
Kv_EACL_zone5	138	C-O	18	Kv_C-O	x	3	4.91 E−03
Kv_EACL_zone6	139	C-O	18	Kv_C-O	x	2	2.38 E−02
Kv_EACL_zone7	140	C-O	18	Kv_C-O	x	1	8.92 E−02
Kv_MTSM_layer20_zone1	141	C-O	20	Kv_C-O		Gradational	1.59 E−04
Kv_MTSM_layer20_zone2	142	C-O	20	Kv_C-O		Gradational	3.01 E−04
Kv_MTSM_layer20_zone3	143	C-O	20	Kv_C-O		1	2.34 E−03
Kv_MTSM_layer20_zone4	144	C-O	20	Kv_C-O		2	5.29 E−03
Kv_MTSM_layer20_zone5	145	C-O	20	Kv_C-O		2	2.03 E−02
Kv_MTSM_layer20_zone6	146	C-O	20	Kv_C-O		2	5.22 E−02
Kv_MTSM_layer20_zone7	147	C-O	20	Kv_C-O		1	2.00 E−01
Kv_MTSM_layer20_zone8	148	C-O	20	Kv_C-O		1	5.00 E−01
RIV_conductance_clayey_till	149	QRNR	1,2,3	RIV_COND		Cell by cell	--
RIV_conductance_loamy_till_organic_deposits	150	QRNR	1,2,3	RIV_COND		Cell by cell	--
RIV_conductance_sandy_till	151	QRNR	1,2,3	RIV_COND		Cell by cell	--
RIV_conductance_fine_stratified_deposits	152	QRNR	1,2,3	RIV_COND		Cell by cell	--
RIV_conductance_medium_and_coarse_stratified	153	QRNR	1,2,3	RIV_COND		Cell by cell	--

Table 5–2. Parameters estimated in calibration process.—Continued

[--, not applicable; Kh, horizontal hydraulic conductivity; Kv, vertical hydraulic conductivity; gradational, number of nearfield values implies values are interpolated across cells; ft, feet; ft/d, feet per day; ft²/d, feet squared per day]

Parameter name	Unit	Bounds imposed on multiplier of initial values	Confined calibration multiplier (SLMB-C)	Unconfined calibration multiplier (SLMB-U)	Comments: for multipliers, red indicates at bound; blue indicates less than 0.5× or greater than 2.0×
Kv_PCFR_zone1	ft/d	0.1×–10×	2.07	2.20	
Kv_PCFR_zone2	ft/d	0.1×–10×	0.16	0.20	
Kv_PCFR_zone3	ft/d	0.1×–10×	3.86	5.58	
Kv_PCFR_zone4	ft/d	0.1×–10×	2.23	2.40	
Kv_PCFR_zone5	ft/d	0.1×–10×	1.23	1.67	
Kv_PCFR_zone6	ft/d	0.1×–10×	1.20	1.57	
Kv_PCFR_zone7	ft/d	0.1×–10×	1.63	1.46	
Kv_PCFR_zone8	ft/d	0.1×–10×	1.39	1.45	
Kv_EACL_zone1	ft/d	0.1×–10×	0.11	0.10	
Kv_EACL_zone2	ft/d	0.1×–10×	3.45	2.15	
Kv_EACL_zone3	ft/d	0.1×–10×	0.54	0.66	
Kv_EACL_zone4	ft/d	0.1×–10×	0.94	0.67	
Kv_EACL_zone5	ft/d	0.1×–10×	0.87	0.76	
Kv_EACL_zone6	ft/d	0.1×–10×	1.52	1.11	
Kv_EACL_zone7	ft/d	0.1×–10×	1.48	2.14	
Kv_MTSM_layer20_zone1	ft/d	0.1×–10×	1.84	2.39	
Kv_MTSM_layer20_zone2	ft/d	0.1×–10×	2.17	1.16	
Kv_MTSM_layer20_zone3	ft/d	0.1×–10×	1.90	1.60	
Kv_MTSM_layer20_zone4	ft/d	0.1×–10×	1.53	1.63	
Kv_MTSM_layer20_zone5	ft/d	0.1×–10×	1.33	1.42	
Kv_MTSM_layer20_zone6	ft/d	0.1×–10×	1.14	1.19	
Kv_MTSM_layer20_zone7	ft/d	0.1×–10×	0.88	0.76	
Kv_MTSM_layer20_zone8	ft/d	0.1×–10×	1.20	0.49	
RIV_conductance_clayey_till	ft²/d	--	1.52	2.08	Initial cell-by-cell conductances estimated as function of sediment Kv, area of surface water.
RIV_conductance_loamy_till_organic_deposits	ft²/d	--	1.38	2.15	
RIV_conductance_sandy_till	ft²/d	--	0.96	0.83	Features, bed thickness, and type of feature.
RIV_conductance_fine_stratified_deposits	ft²/d	--	1.96	1.79	
RIV_conductance_medium_and_coarse_stratified	ft²/d	--	0.96	1.25	

Table 5–2. Parameters estimated in calibration process.—Continued

[--, not applicable; Kh, horizontal hydraulic conductivity; Kv, vertical hydraulic conductivity; gradational, number of nearfield values implies values are interpolated across cells; ft, feet; ft/d, feet per day; ft^2/d, feet squared per day]

Parameter name	Number	Aquifer system	Layer(s)	Parameter group for sensitivity analysis	Figure and table in appendix 6	Number of nearfield values	Initial value(s) or geometric mean of mulitple initial values
RIV_conductance_unknown_QRNR	154	QRNR	1,2,3	RIV_COND		Cell by cell	--
RIV_conductance_bedrock	155	PENN, MSHL, SLDV, C-O	5–20	RIV_COND		Cell by cell	--
Ss_QRNR	156	QRNR	1,2,3	Ss_QRNR_PENN_MSHL_SLDV		1	5.70 E−06
Ss_JURA_PEN1_PEN2	157	PENN	4,5,6	Ss_QRNR_PENN_MSHL_SLDV		1	2.60 E−07
Ss_MICH_MSHL	158	MSHL	7,8,9	Ss_QRNR_PENN_MSHL_SLDV		1	2.60 E−07
Ss_DVMS_SLDV	159	SLDV	10,11,12	Ss_QRNR_PENN_MSHL_SLDV		1	2.60 E−07
Ss_C-O	160	C-O	13–20	Ss_C-O		1	2.60 E−07

Table 5–2. Parameters estimated in calibration process.—Continued

[--, not applicable; Kh, horizontal hydraulic conductivity; Kv, vertical hydraulic conductivity; gradational, number of nearfield values implies values are interpolated across cells; ft, feet; ft/d, feet per day; ft^2/d, feet squared per day]

Parameter name	Unit	Bounds imposed on multiplier of initial values	Confined calibration multiplier (SLMB-C)	Unconfined calibration multiplier (SLMB-U)	Comments: for multipliers, red indicates at bound; blue indicates less than 0.5× or greater than 2.0×
RIV_conductance_ unknown_QRNR	ft^2/d	--	1.50	2.30	
RIV_conductance_bedrock	ft^2/d	--	1.27	0.95	
Ss_QRNR	ft^{-1}	0.67×–2×	1.099	0.964	
Ss_JURA_PEN1_PEN2	ft^{-1}	--	1.187	1.105	
Ss_MICH_MSHL	ft^{-1}	--	1.690	1.515	
Ss_DVMS_SLDV	ft^{-1}	--	1.060	1.006	
Ss_C-O	ft^{-1}	--	0.697	0.636	

Table 5–2. Parameters estimated in calibration process.—Continued

[--, not applicable; Kh, horizontal hydraulic conductivity; Kv, vertical hydraulic conductivity; gradational, number of nearfield values implies values are interpolated across cells; ft, feet; ft/d, feet per day; ft^2/d, feet squared per day]

Parameter name	Number	Aquifer system	Layer(s)	Parameter group for sensitivity analysis	Figure and table in appendix 6	Number of nearfield values	Initial value(s) or geometric mean of mulitple initial values
Sy_QRNR*	161	QRNR	1,2,3	Sy_QRNR-PENN-MSHL-SLDV		1	0.15
Sy_JURA_PEN1_PEN2*	162	PENN	4,5,6	Sy_QRNR-PENN-MSHL-SLDV		1	0.05
Sy_MICH_MSHL*	163	MSHL	7,8,9	Sy_QRNR-PENN-MSHL-SLDV		1	0.05
Sy_DVMS_SLDV*	164	SLDV	10,11,12	Sy_QRNR-PENN-MSHL-SLDV		1	0.005
Sy_C-O*	165	C-O	13–20	Sy_C-O		2	.005, .05
*Only for unconfined calibration							
Kv_MAQU_PILOT_POINTS	166–243	C-O	13	Kv_MAQU-pilot_points	x	Cell by cell	5.85 E−6, 2.0 E−5

Table 5–2. Parameters estimated in calibration process.—Continued

[--, not applicable; Kh, horizontal hydraulic conductivity; Kv, vertical hydraulic conductivity; gradational, number of nearfield values implies values are interpolated across cells; ft, feet; ft/d, feet per day; ft^2/d, feet squared per day]

Parameter name	Unit	Bounds imposed on multiplier of initial values	Confined calibration multiplier (SLMB-C)	Unconfined calibration multiplier (SLMB-U)	Comments: for multipliers, red indicates at bound; blue indicates less than 0.5× or greater than 2.0×
Sy_QRNR*	--	0.67×–2×	--	1.014	Unconsolidated units assigned initial Sy = 0.15
Sy_JURA_PEN1_PEN2*	--	--	--	1.392	Carbonate and shale dominated units assigned 0.005
Sy_MICH_MSHL*	--	--	--	1.611	Sandstone dominated units assigned 0.05
Sy_DVMS_SLDV*	--	--	--	0.988	
Sy_C-O*	--	--	--	0.889	
*Only for unconfined calibration					
Kv_MAQU_PILOT_POINTS	ft/d	0.1×–10×	--	--	Confined case:
					Geometric mean where unweathered = 6.30 E−6
					Geometric mean where weathered = 2.61 E−5
					Unconfined case:
					Geometric mean where unweathered = 6.36 E−6
					Geometric mean where weathered = 2.68 E−5

Appendix 6. Initial and Calibrated Input for Hydraulic-Conductivity Zones

In order to provide detailed documentation on the organization of the model input for the calibration process, as well as to display the calibrated results, this appendix contains tables and figures that show

- the spatial distribution of hydraulic-conductivity zones corresponding to calibration parameters,
- the initial input(s) by zone,
- the calibrated results by zone for the confined model, SLMB-C, and
- the spatial distribution of calibrated results for the confined model, SLMB-C

for

- the K_h of QRNR layers 1, 2 and 3;
- the K_h of layers corresponding to principal aquifers—PEN1 (layer 5), MSHL (layer 8), upper SLDV (layer 10), STPT (layer 15), IRGA (layer 17), and upper MTSM (layer 19);
- the K_v of QRNR layers 1, 2 and 3; and
- the K_v of layers corresponding to principal confining units—PEN2 (layer 6), MICH (layer 7), DVMS (layer 9), middle SLDV (layer 11), MAQU (layer 13), and EACL (layer 18).

The appendix is divided into subsections corresponding to the selected aquifers (6*A*–1 to 6*A*–9) and subsections corresponding to the selected confining units (6*B*–1 to 6*B*–9). Each subsection contains a figure showing the hydraulic-conductivity zonation, a table of initial input by zone, a table of calibrated input by zone, and a figure showing the spatial distribution of calibrated hydraulic-conductivity input values.

Table 6*A*–1. Horizontal hydraulic conductivity of QRNR-L1 (Upper Quaternary: aquifer or confining unit depending on location).
[Kh, horizontal hydraulic conductivity. Statistics limited to nearfield (including under Lake Michigan)]

Zone or statistic	Clayey till	Loamy till	Sandy till	Fine stratified	Medium-coarse stratified	Lake Michigan bed			
Initial Kh (feet per day)									
Zone	1	2	3	4	5	6	7	8	9
Number nearfield cells	10,260	20,874	167	4,051	23,727	217	6,102	420	18,210
Number nearfield values	Vary by cell	Vary by cell	Vary by cell	Vary by cell	Vary by cell	1	1	1	1
Ave_thickness (feet)	88	78	90	76	88	52	55	84	56
Median_Kh	1.00	3.64	11.76	2.73	69.30	.10	.30	1.00	.10
Geometric_mean_Kh	1.07	4.10	12.10	4.10	71.88	.10	.30	1.00	.10
Min_Kh	.20	1.00	3.45	.40	20.00	.10	.30	1.00	.10
Max_Kh	10.00	50.00	44.37	20.00	291.42	.10	.30	1.00	.10
Calibrated Kh (feet per day)									
Zone	1	2	3	4	5	6	7	8	9
PEST inversion multiplier	5	2.703	1.6304	2.086314	2.044649	1	1	1	1
Median_Kh	5.00	9.83	19.17	5.69	141.70	.10	.30	1.00	.10
Geometric_mean_Kh	5.35	11.08	19.73	8.55	146.97	.10	.30	1.00	.10
Min_Kh	1.00	2.70	5.62	.83	40.89	.10	.30	1.00	.10
Max_Kh	50.00	135.15	72.34	41.73	595.85	.10	.30	1.00	.10

Thickness units are feet, Kh units are feet per day. Statistics calculated only for nearfield cells where thickness is equal to at least 1 foot.

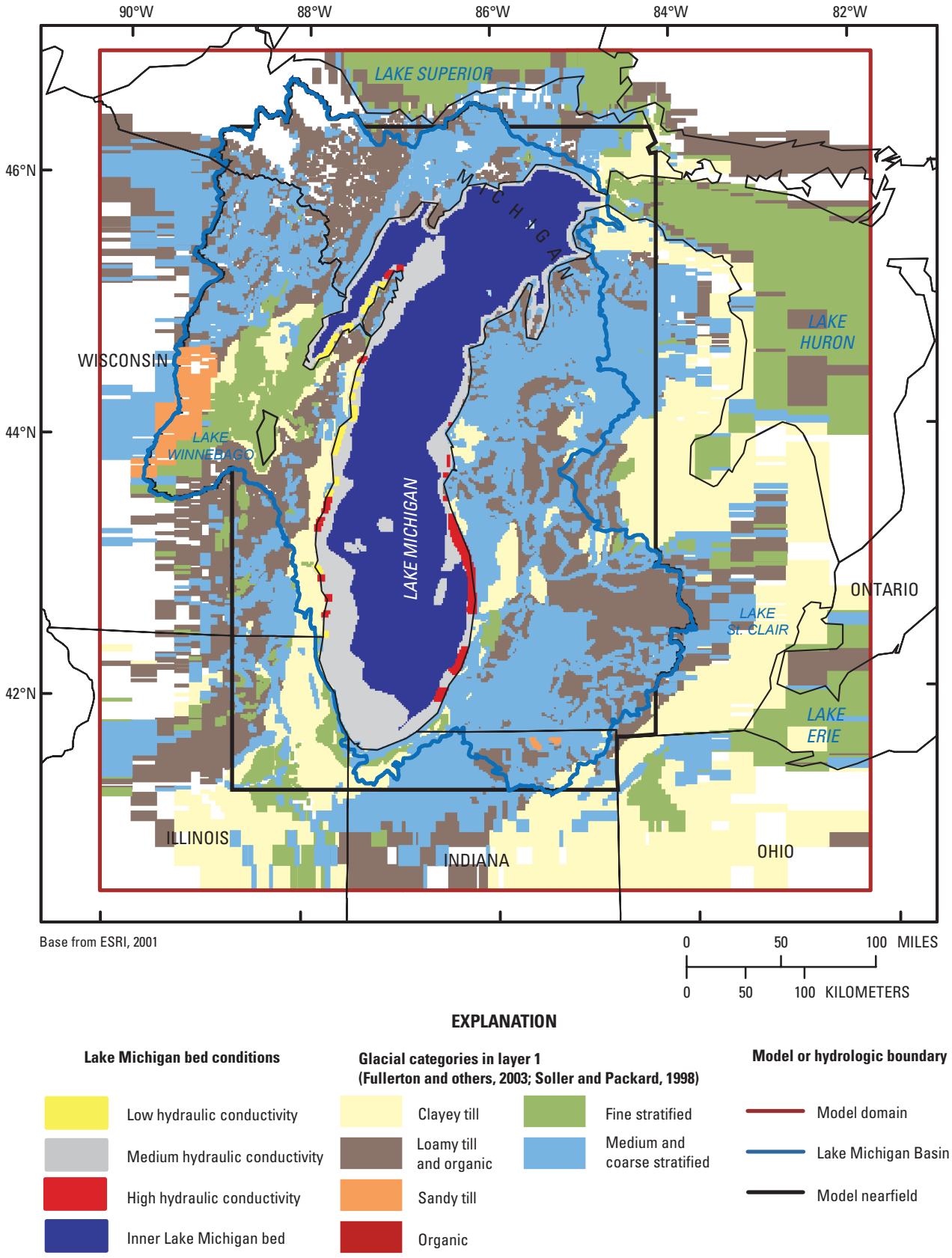

Figure 6*A*–1*A*. Horizontal hydraulic conductivity, upper QRNR including Lake Michigan lakebed: zonation.

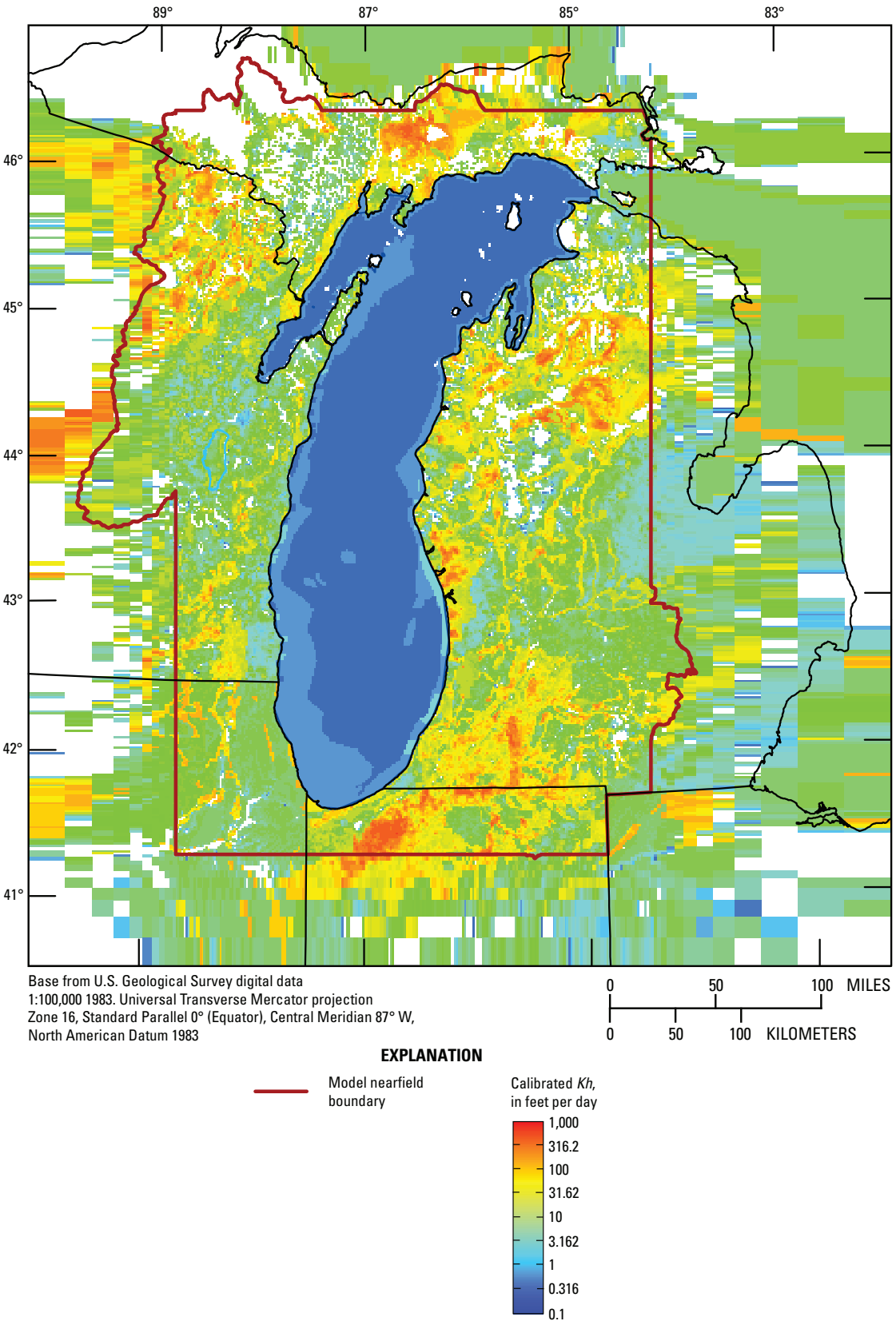

Figure 6*A*–1*B*. Horizontal hydraulic conductivity, upper QRNR including Lake Michigan lakebed: calibrated input.

Table 6*A*–2. Horizontal hydraulic conductivity of QRNR-L2 (middle Quaternary: aquifer or confining unit depending on location).

[Kh, horizontal hydraulic conductivity. Statistics limited to nearfield (including under Lake Michigan)]

Zone or statistic	Clayey till	Loamy till	Sandy till	Fine stratified	Medium-coarse stratified	Unknown
Initial Kh (feet per day)						
Zone	1	2	3	4	5	6
Number nearfield cells	2,379	1,612	58	1,529	2,381	29,993
Number nearfield values	Vary by cell	Vary by cell	Vary by cell	Vary by cell	Vary by cell	Vary by cell
Ave_thickness (ft)	58	65	42	56	55	149
Median_Kh	1.00	5.00	13.01	6.49	58.51	3.66
Geometric_mean_Kh	.92	4.29	13.41	5.62	60.40	5.05
Min_Kh	.10	1.01	3.03	.40	.10	.10
Max_Kh	10.00	42.69	35.00	20.00	284.09	200.00
Calibrated Kh (feet per day)						
Zone	1	2	3	4	5	6
PEST inversion multiplier	5	2.703	1.6304	2.086314	2.044649	0.8488675
Median_Kh	5.00	13.52	21.21	13.54	119.62	3.11
Geometric_mean_Kh	4.60	11.60	21.86	11.73	123.50	4.29
Min_Kh	.50	2.73	4.94	.83	.20	.08
Max_Kh	50.00	115.39	57.06	41.73	580.86	169.77

Thickness units are feet, Kh units are feet per day. Statistics calculated only for nearfield cells where thickness is equal to at least 1 foot.

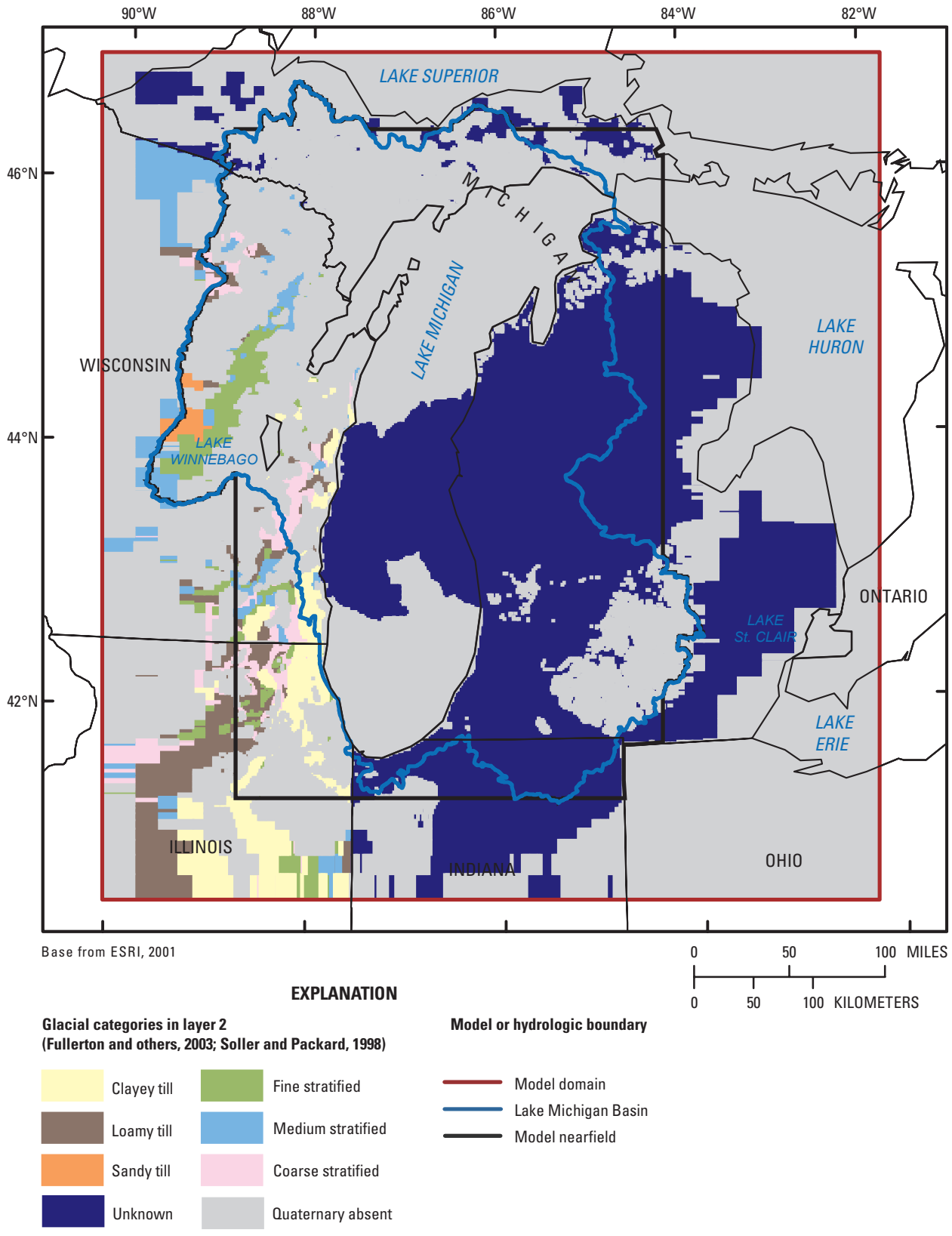

Figure 6*A*–2*A*. Horizontal hydraulic conductivity, middle QRNR: zonation.

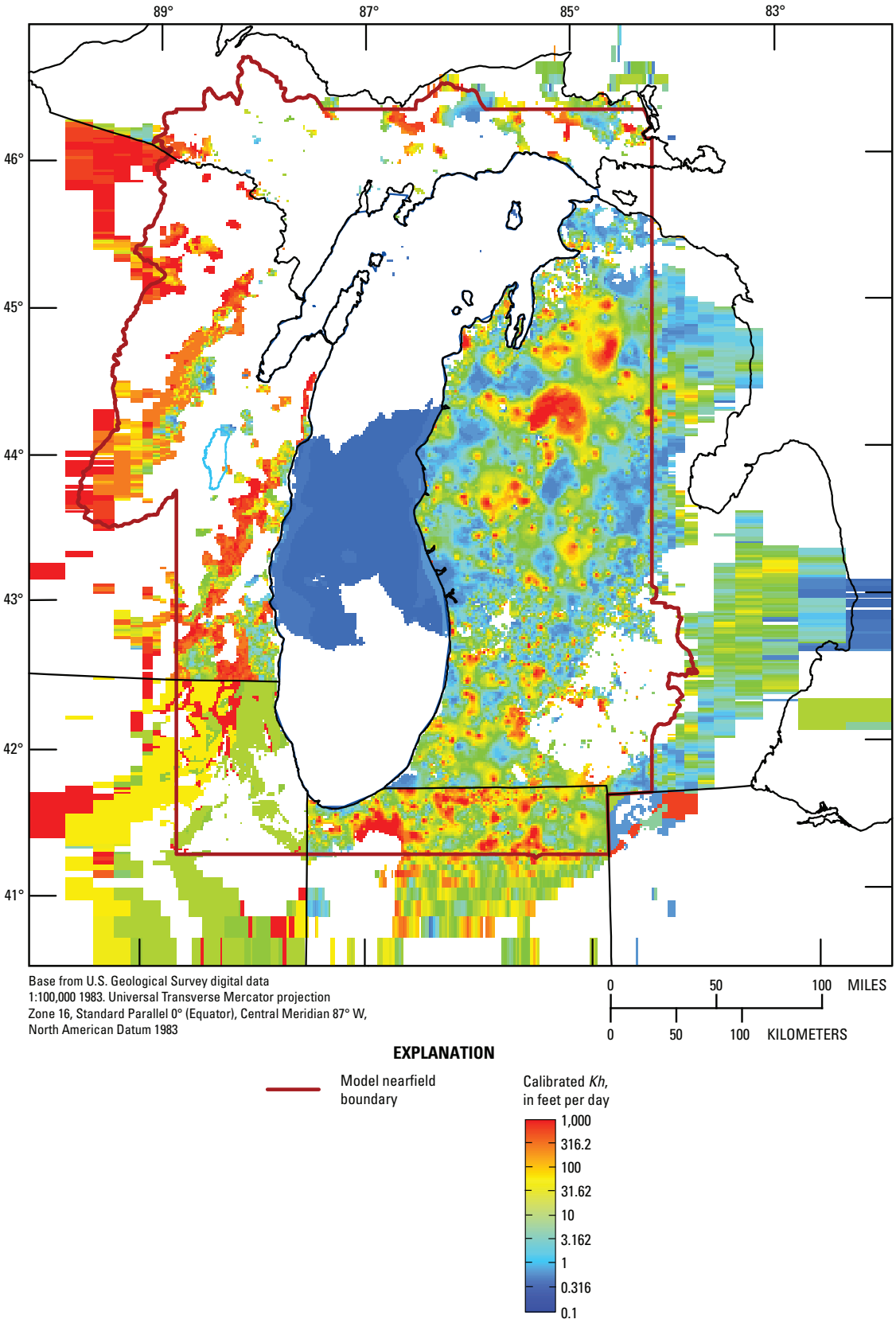

Figure 6*A*–2*B*. Horizontal hydraulic conductivity, middle QRNR: calibrated input.

Table 6*A*–3. Horizontal hydraulic conductivity of QRNR-L3 (Lower Quaternary: aquifer or confining unit depending on location).

[Kh, horizontal hydraulic conductivity. Statistics limited to nearfield (including under Lake Michigan)]

Zone or statistic	Clayey till	Loamy till	Sandy till	Fine stratified	Medium-coarse stratified	Unknown
Initial Kh (feet per day)						
Zone	1	2	3	4	5	6
Number nearfield cells	21	40	0	33	42	15,330
Number nearfield values	Vary by cell	Vary by cell		Vary by cell	Vary by cell	Vary by cell
Ave_thickness (feet)	16	43		23	23	199
Median_Kh	0.42	5.00		2.34	73.18	5.41
Geometric_mean_Kh	.46	5.61		4.49	69.07	7.19
Min_Kh	.23	2.48		1.69	26.68	.30
Max_Kh	1.00	13.51		20.00	179.34	20.00
Calibrated Kh (feet per day)						
Zone	1	2	3	4	5	6
PEST inversion multiplier	5	2.703		2.086314	2.044649	0.8488675
Median_Kh	2.12	13.52		4.89	149.64	4.60
Geometric_mean_Kh	2.30	15.16		9.37	141.22	6.10
Min_Kh	1.15	6.70		3.53	54.55	.25
Max_Kh	5.00	36.52		41.73	366.69	16.98

Thickness units are feet, Kh units are feet per day. Statistics calculated only for nearfield cells where thickness is equal to at least 1 foot.

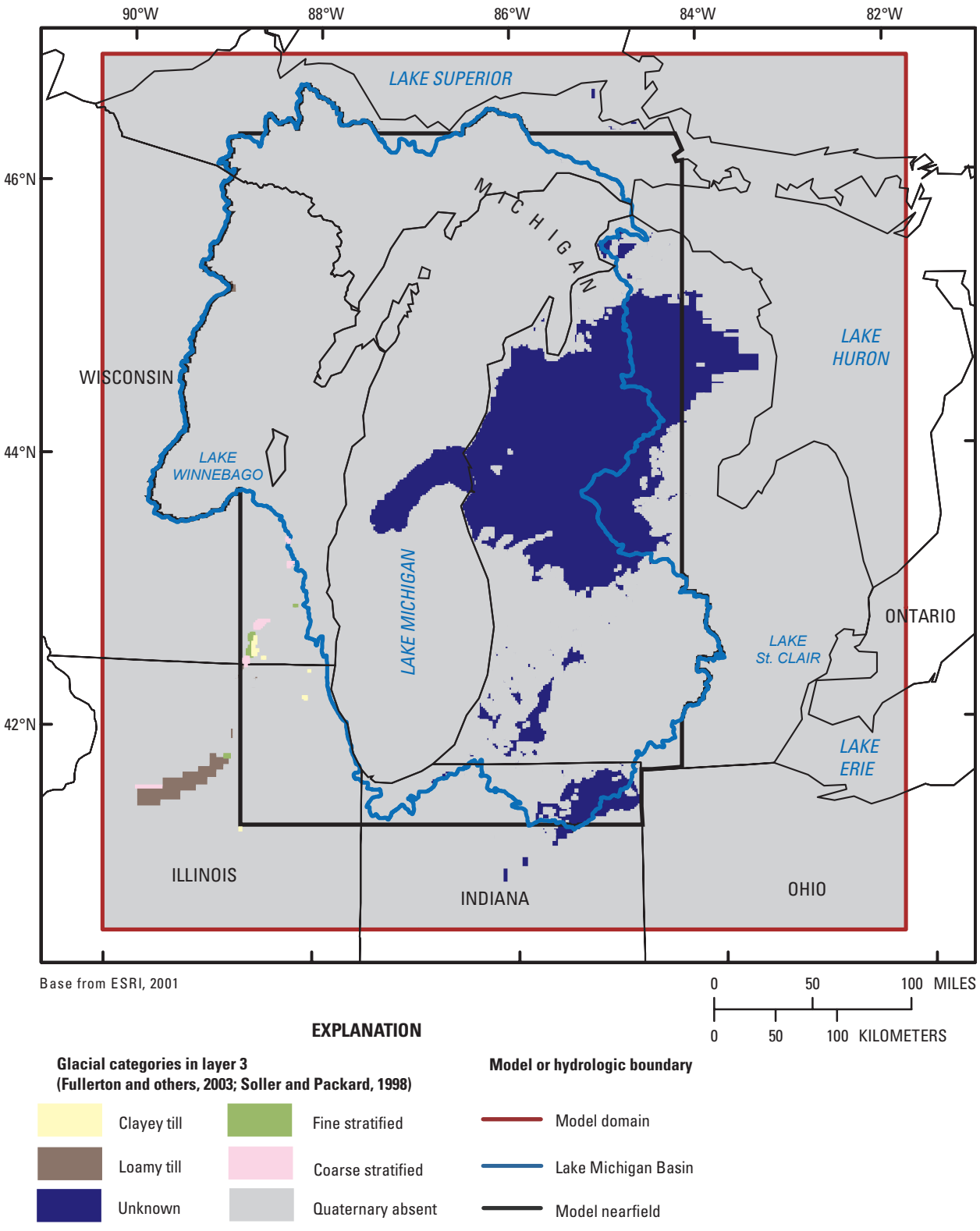

Figure 6*A*–3*A*. Horizontal hydraulic conductivity, lower QRNR: zonation.

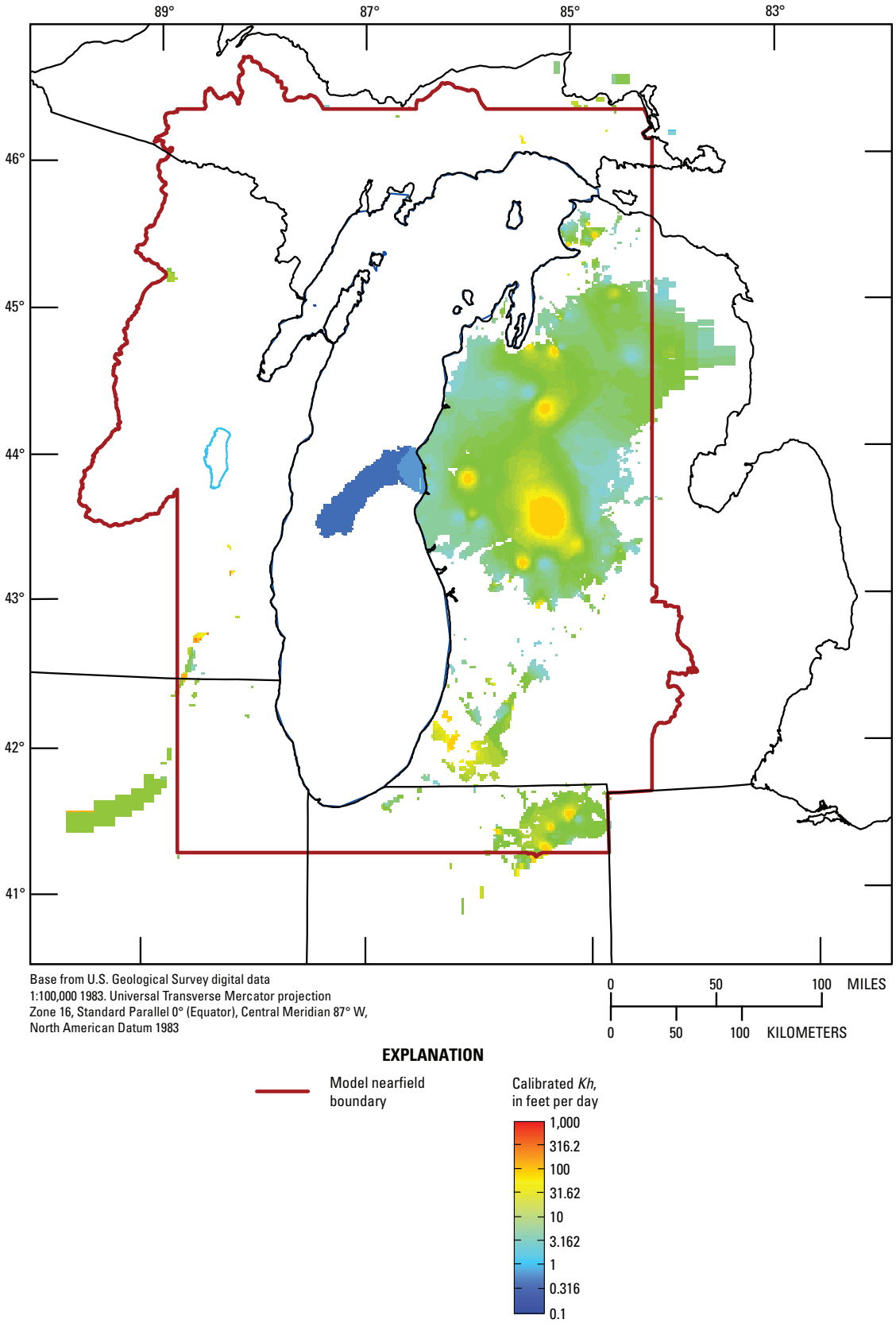

Figure 6*A*–3*B*. Horizontal hydraulic conductivity, lower QRNR: calibrated input.

Table 6*A*–4. Horizontal hydraulic conductivity of PEN1-L5 (Grand River-Saginaw sandstones: aquifer).

[Kh, horizontal hydraulic conductivity. Statistics limited to nearfield (including under Lake Michigan)]

Initial Kh (feet per day)			
Zone	1	2	3
Number nearfield cells	4,861	4,304	115
Number nearfield values	1	1	1
Ave_thickness (ft)	176	226	281
Median_Kh	6.00	10.00	20.00
Geometric_mean_Kh	6.00	10.00	20.00
Min_KhG	6.00	10.00	20.00
Max_Kh	6.00	10.00	20.00
Calibrated Kh (feet per day)			
Zone	1	2	3
PEST inversion multiplier	0.9706929	1.245297	1.379779
Median_Kh	5.82	12.45	27.60
Geometric_mean_Kh	5.82	12.45	27.60
Min_Kh	5.82	12.45	27.60
Max_Kh	5.82	12.45	27.60

Thickness units are feet, Kh units are feet per day. Statistics calculated only for nearfield cells where thickness is equal to at least 1 foot.

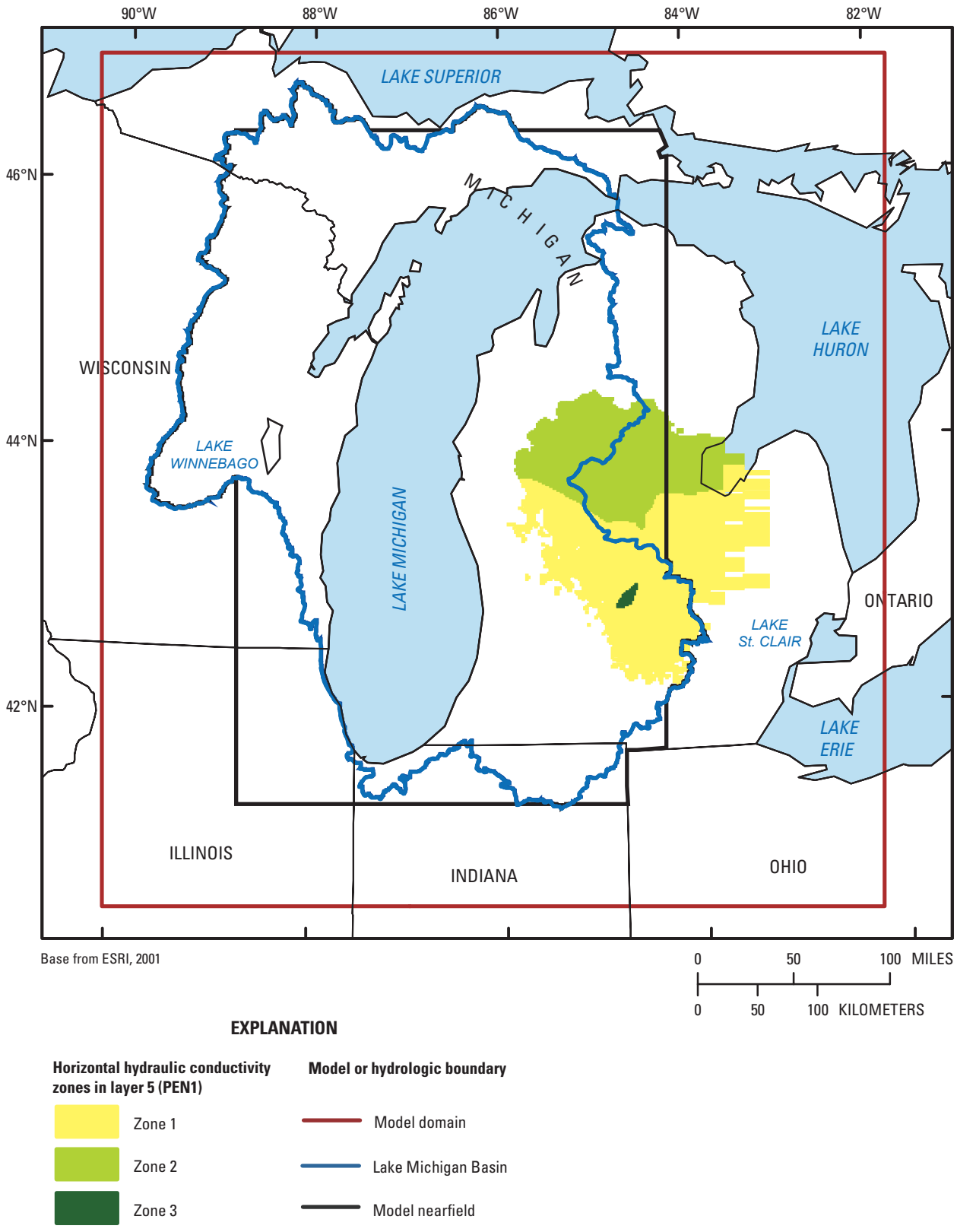

Figure 6*A*–4*A*. Horizontal hydraulic conductivity, PEN1: zonation.

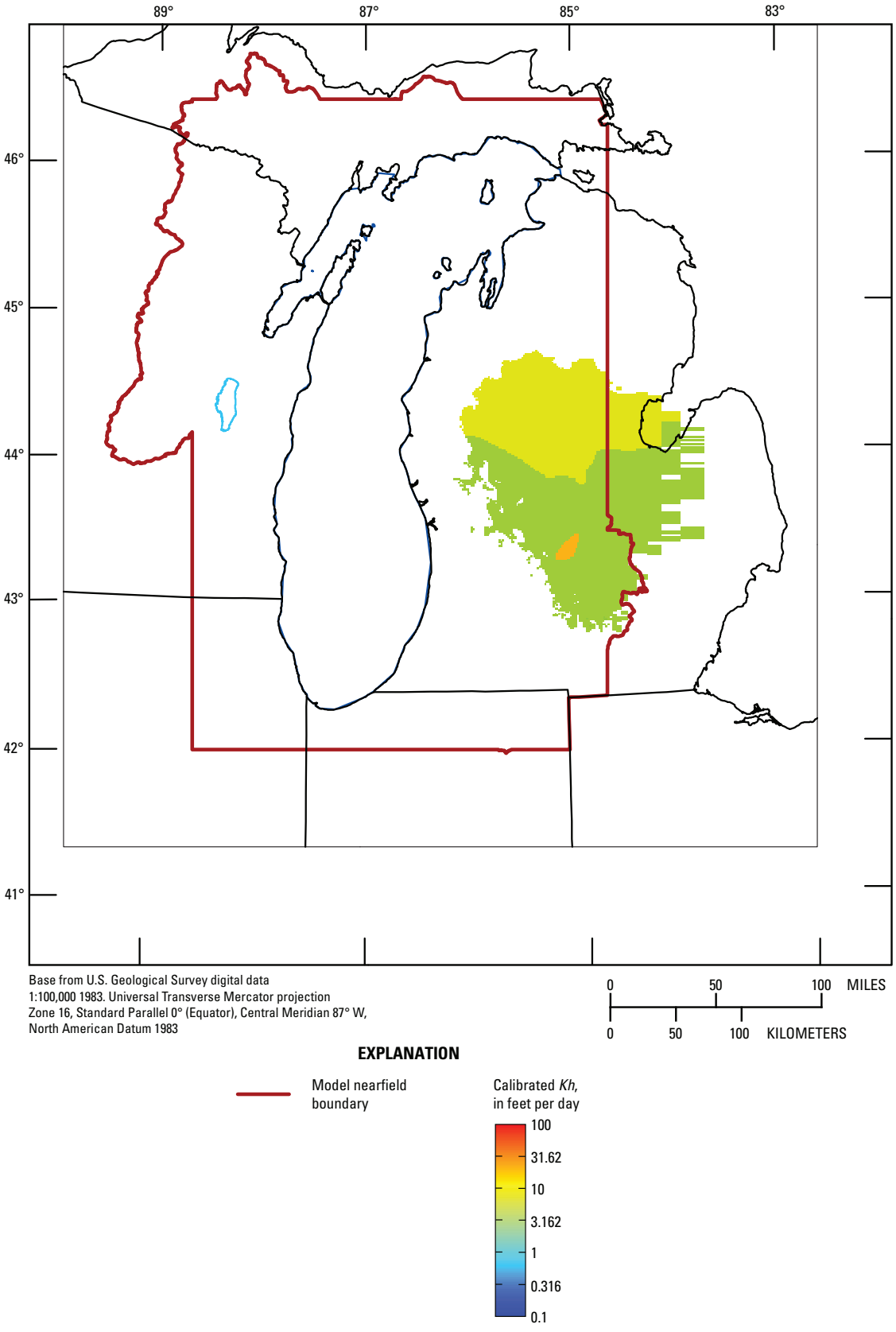

Figure 6*A*–4*B*. Horizontal hydraulic conductivity, PEN1: calibrated input.

Table 6*A*–5. Horizontal hydraulic conductivity of MSHL-L8 (Marshall sandstone: aquifer).

[Kh, horizontal hydraulic conductivity. Statistics limited to nearfield (including under Lake Michigan)]

Initial Kh (feet per day)			
Zone	1	2	3
Number nearfield cells	11,011	3,440	2,413
Number nearfield values	1	1	1
Ave_thickness (ft)	191	191	209
Median_Kh	5.00	15.00	20.00
Geometric_mean_Kh	5.00	15.00	20.00
Min_Kh	5.00	15.00	20.00
Max_Kh	5.00	15.00	20.00
Calibrated Kh (feet per day)			
Zone	1	2	3
PEST inversion multiplier	0.8471831	2.569927	1.380918
Median_Kh	4.24	38.55	27.62
Geometric_mean_Kh	4.24	38.55	27.62
Min_Kh	4.24	38.55	27.62
Max_Kh	4.24	38.55	27.62

Thickness units are feet, Kh units are feet per day. Statistics calculated only for nearfield cells where thickness is equal to at least 1 foot.

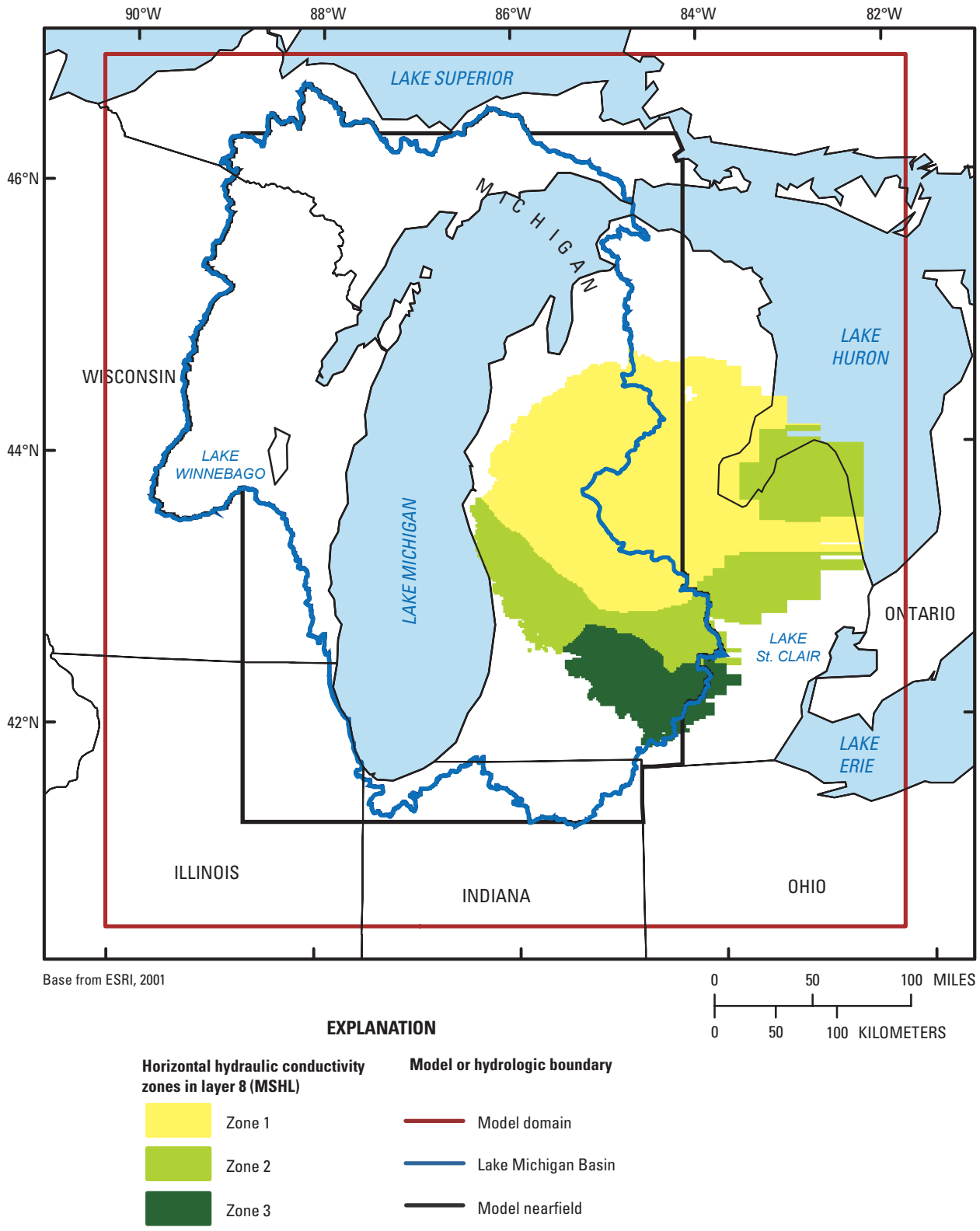

Figure 6*A*–5*A*. Horizontal hydraulic conductivity, MSHL: zonation.

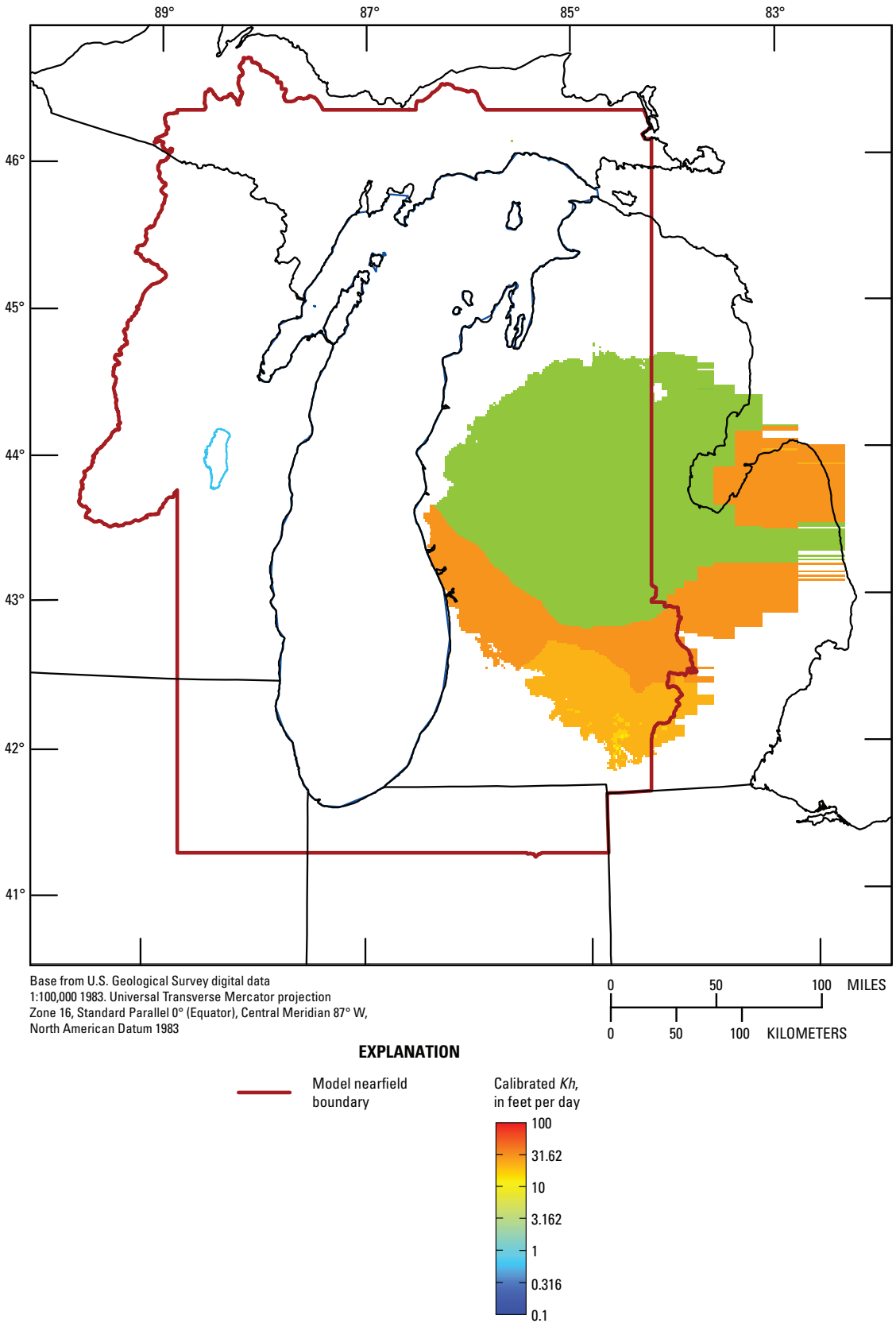

Figure 6*A*–5*B*. Horizontal hydraulic conductivity, MSHL: calibrated input.

Table 6*A*–6. Horizontal hydraulic conductivity of SLDV-L10 (upper Silurian-Devonian: aquifer).

[Kh, horizontal hydraulic conductivity; --, not applicable. Statistics limited to nearfield (including under Lake Michigan)]

Initial Kh (feet per day)									
Zone	1	2	3	4	5	6	7	8	9
Number nearfield cells	103	5,636	2,122	2,635	0	58,850	2,913	260	165
Number nearfield values	1	1	1	1	0; only farfield	1	1	1	1
Ave_thickness (feet)	50	56	970	8	--	656	52	51	50
Median_Kh	.54	2.00	5.00	9.09	--	5.00	6.48	4.60	30.22
Geometric_mean_Kh	.54	2.00	5.00	9.09	--	5.00	6.48	4.60	30.22
Min_Kh	.54	2.00	5.00	9.09	--	5.00	6.48	4.60	30.22
Max_Kh	.54	2.00	5.00	9.09	--	5.00	6.48	4.60	30.22
Calibrated Kh (feet per day)									
Zone	1	2	3	4	5	6	7	8	9
PEST inversion multiplier	1.129304	2	2.599394	0.9848144	1.21082	1.09004	1.465473	0.8763114	0.9395545
Median_Kh	.61	4.00	13.00	8.95	--	5.45	9.50	4.03	28.39
Geometric_mean_Kh	.61	4.00	13.00	8.95	--	5.45	9.50	4.03	28.39
Min_Kh	.61	4.00	13.00	8.95	--	5.45	9.50	4.03	28.39
Max_Kh	.61	4.00	13.00	8.95	--	5.45	9.50	4.03	28.39

Thickness units are feet, Kh units are feet per day. Statistics calculated only for nearfield cells where thickness is equal to at least 1 foot.

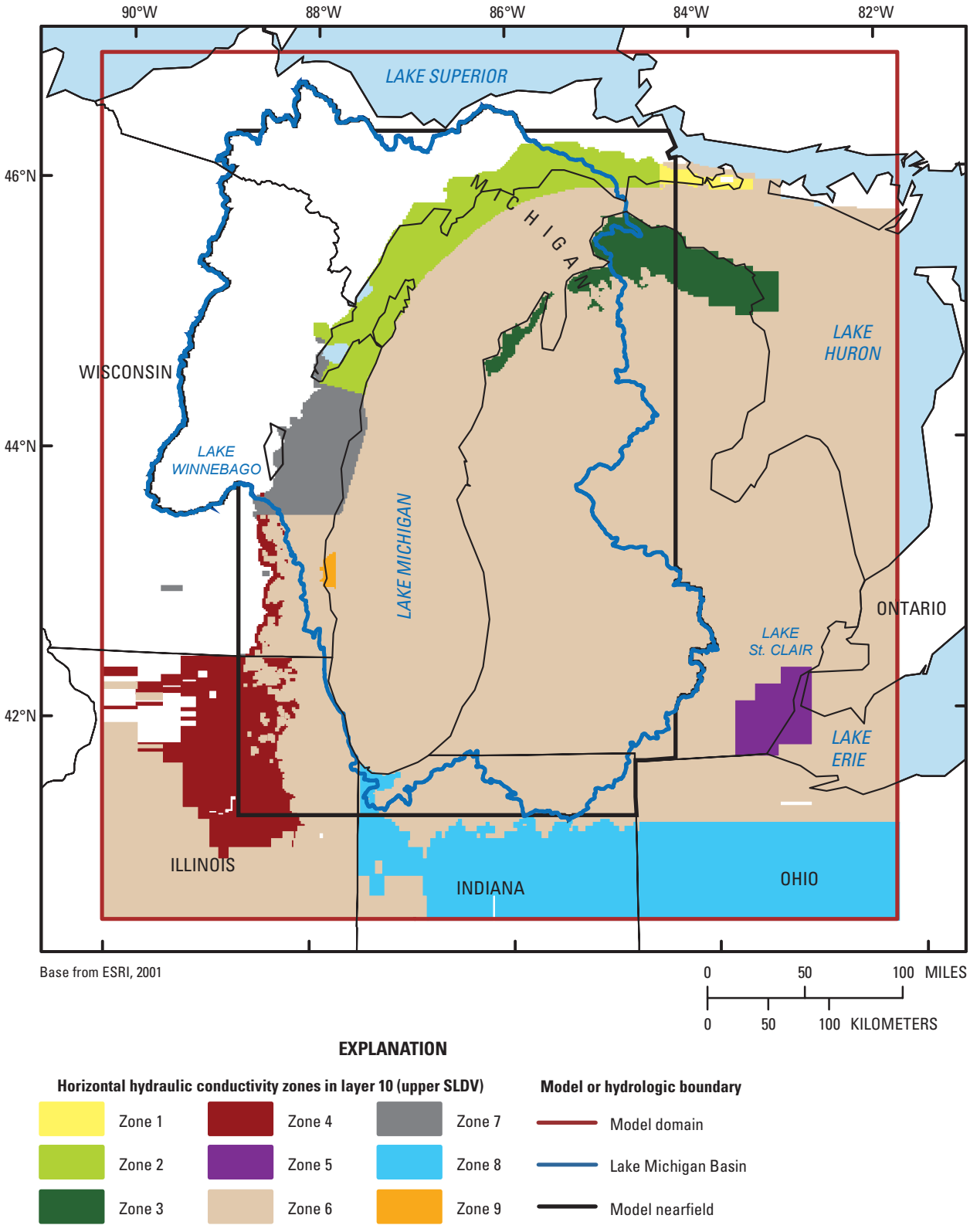

Figure 6*A*–6*A*. Horizontal hydraulic conductivity, upper SLDV: zonation.

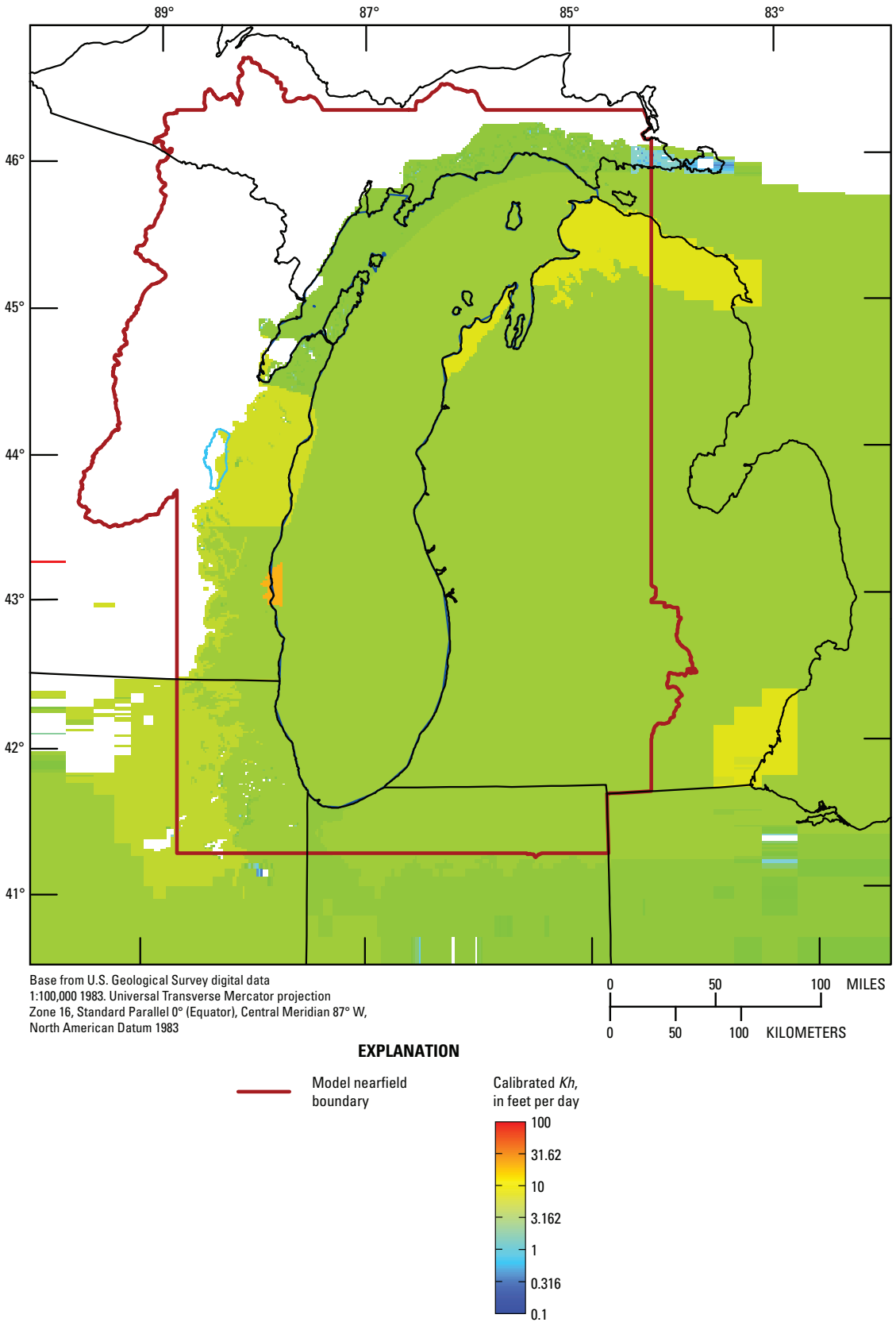

Figure 6*A*–6*B*. Horizontal hydraulic conductivity, upper SLDV: calibrated input.

Table 6*A*–7. Horizontal hydraulic conductivity of STPT-L15 (St. Peter sandstone: aquifer).

[Kh, horizontal hydraulic conductivity. Statistics limited to nearfield (including under Lake Michigan)]

Initial Kh (feet per day)					
Zone	1	2	3	4	5
Number nearfield cells	3,624	5,063	50,845	6,615	955
Number nearfield values	5	3	5	3	4
Ave_thickness (feet)	162	219	438	82	67
Median_Kh	1.50	1.50	2.00	1.50	7.50
Geometric_mean_Kh	1.62	1.55	1.98	1.44	6.72
Min_Kh	1.08	1.50	.50	1.20	2.00
Max_Kh	2.40	7.30	2.40	2.00	9.00
Calibrated Kh (feet per day)					
Zone	1	2	3	4	5
PEST inversion multiplier	0.3174998	2.33505	0.2382006	3.426454	1.561579
Median_Kh	.48	3.50	.48	5.14	11.71
Geometric_mean_Kh	.51	3.62	.47	4.93	10.49
Min_Kh	.34	3.50	.12	4.11	3.12
Max_Kh	.76	17.05	.57	6.85	14.05

Thickness units are feet; Kh units are feet perday. Statistics calculated only for nearfield cells where thickness is equal to at least 1 foot.

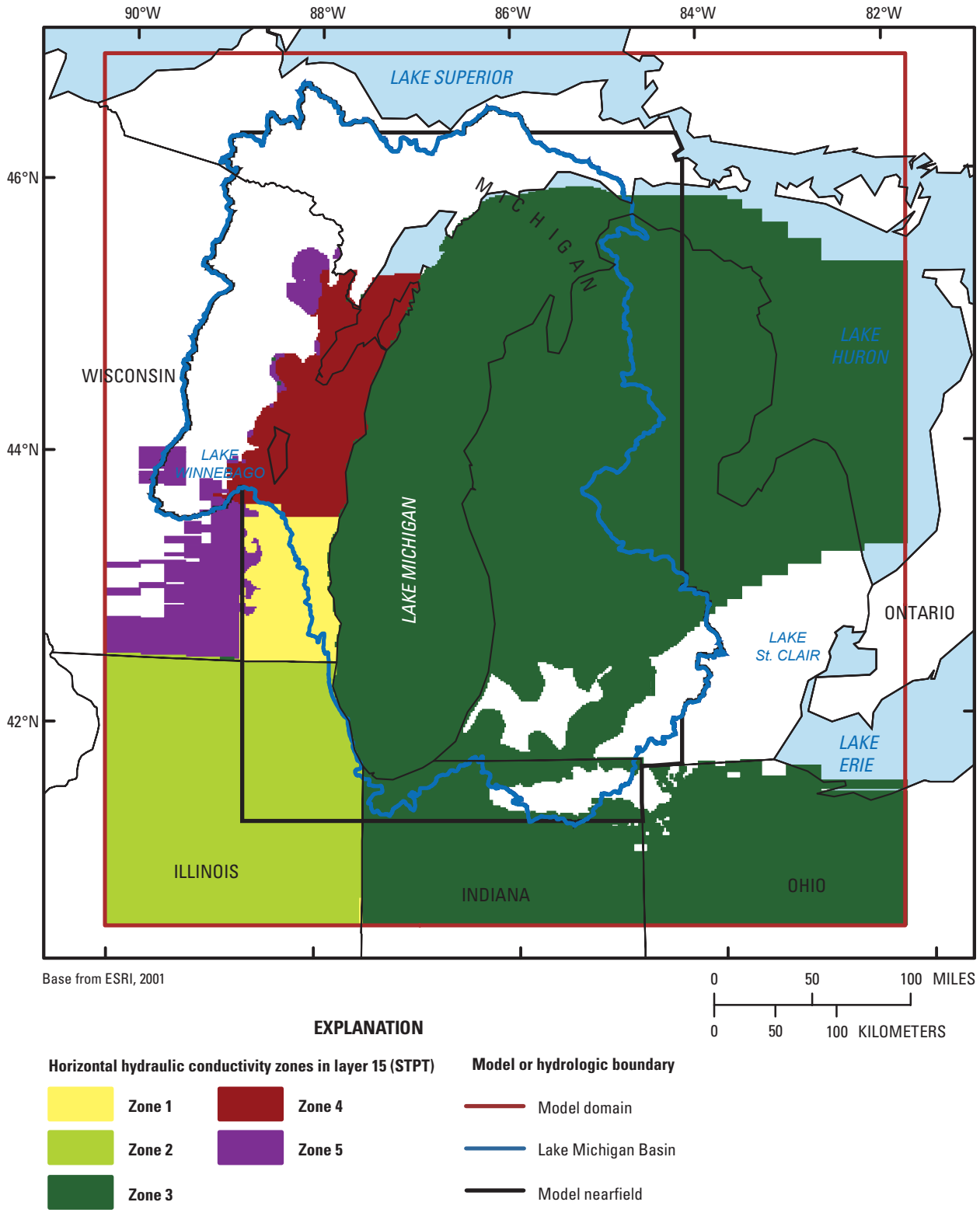

Figure 6*A*–7*A*. Horizontal hydraulic conductivity, STPT: zonation.

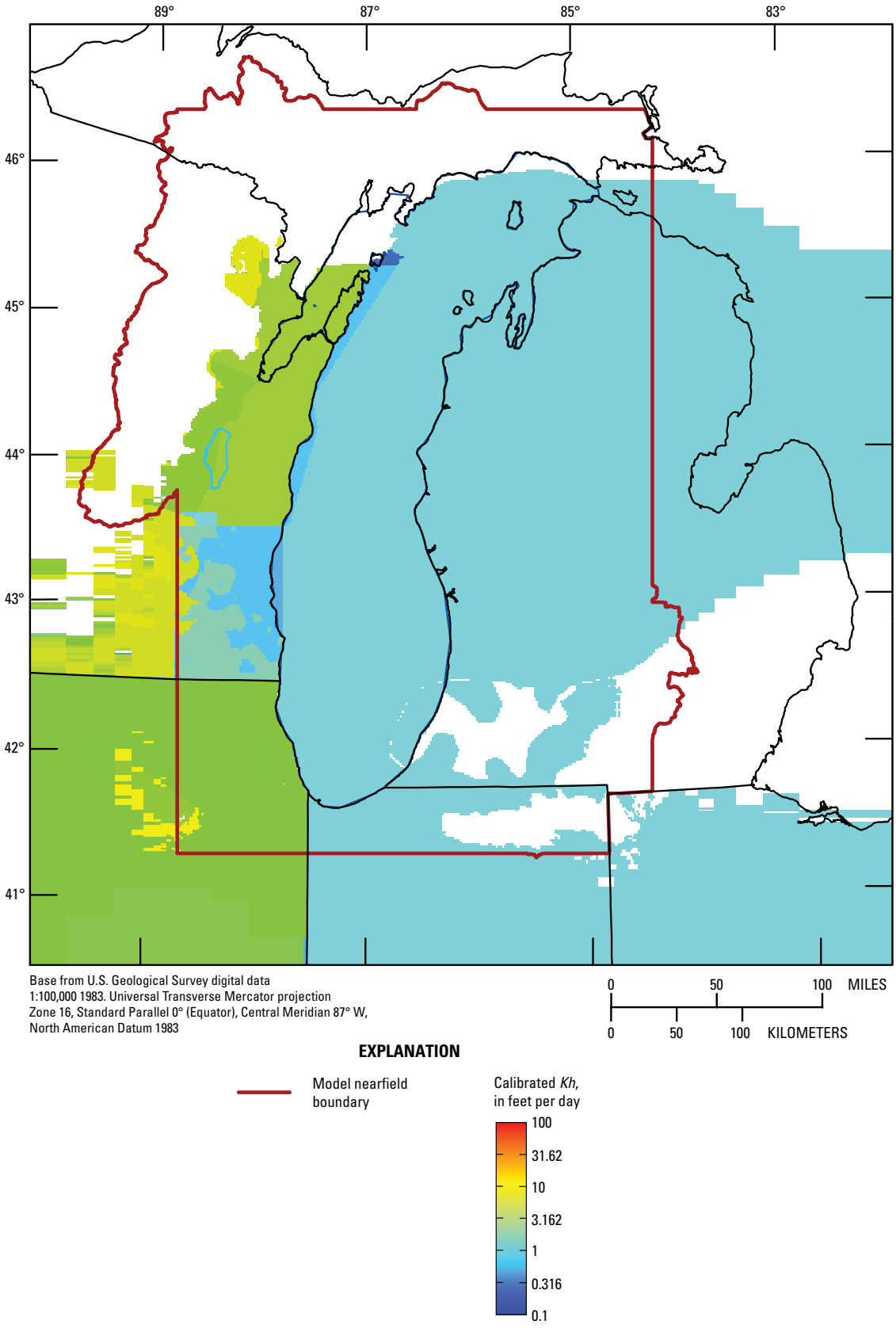

Figure 6*A*–7*B*. Horizontal hydraulic conductivity, STPT: calibrated input.

Table 6*A*–8. Horizontal hydraulic conductivity of IRGA-L17 (Ironton-Galesville sandstone: aquifer).

[Kh, horizontal hydraulic conductivity. Statistics limited to nearfield (including under Lake Michigan)]

Initial Kh (feet per day)						
Zone	1	2	3	4	5	6
Number nearfield cells	7,577	6,129	50,821	6,359	4,816	5,986
Number nearfield values	5	6	3	2	7	7
Ave_thickness (feet)	60	66	180	158	41	77
Median_Kh	1.50	6.00	1.79	5.30	7.00	2.76
Geometric_mean_Kh	1.52	4.62	2.58	5.44	3.98	3.14
Min_Kh	1.50	1.50	1.50	5.30	2.00	1.79
Max_Kh	8.92	8.40	6.00	6.00	10.50	8.92
Calibrated Kh (feet per day)						
Zone	1	2	3	4	5	6
PEST inversion multiplier	1.07861	4.383464	0.3107841	0.8680759	0.5019471	0.8589401
Median_Kh	1.62	26.30	.56	4.60	3.51	2.37
Geometric_mean_Kh	1.64	20.25	.80	4.72	2.00	2.70
Min_Kh	1.62	6.58	.47	4.60	1.00	1.54
Max_Kh	9.62	36.82	1.86	5.21	5.27	7.66

Thickness units are feet; Kh units are feet per day. Statistics calculated only for nearfield cells where thickness is equal to at least 1 foot.

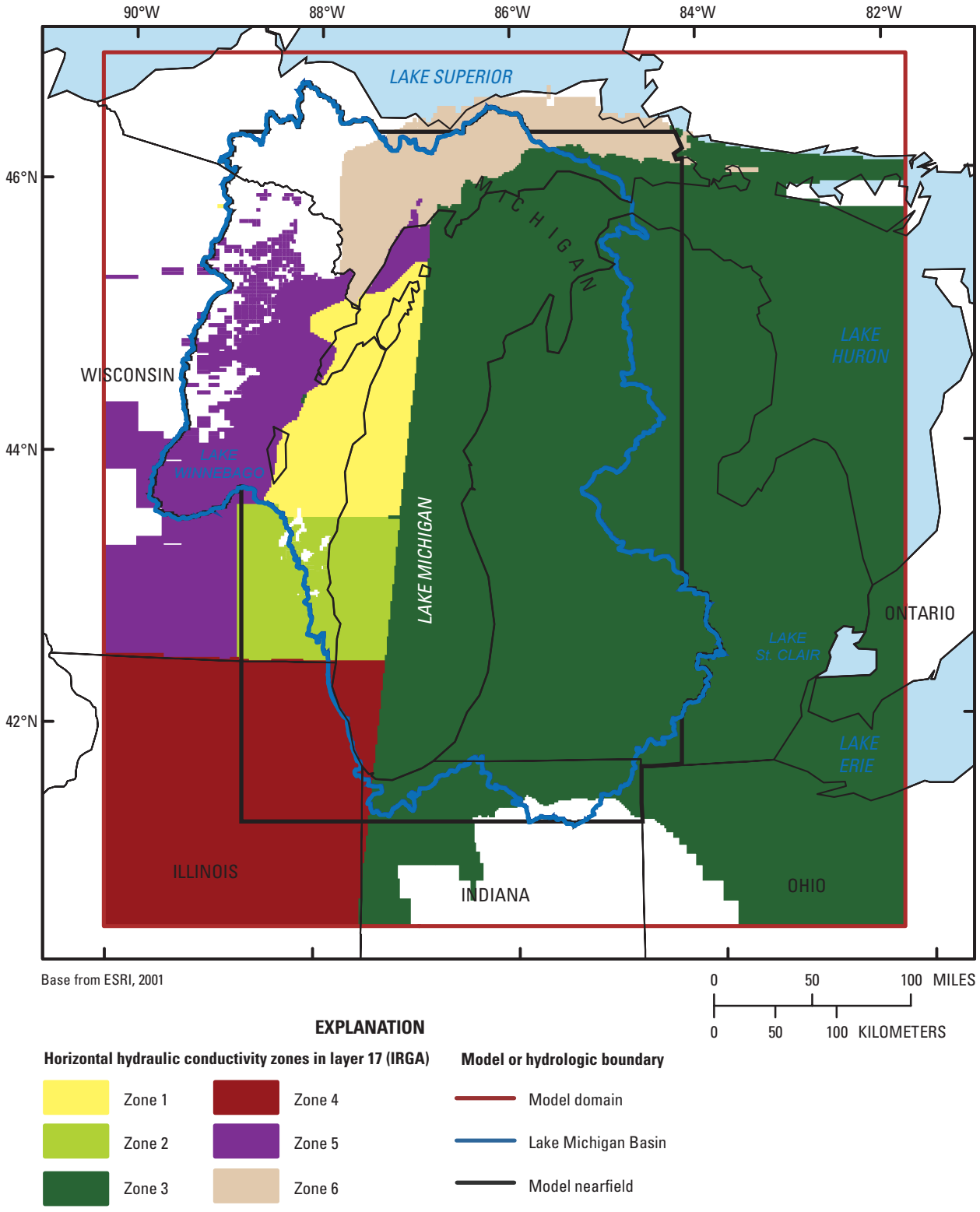

Figure 6*A*–8*A*. Horizontal hydraulic conductivity, IRGA: zonation.

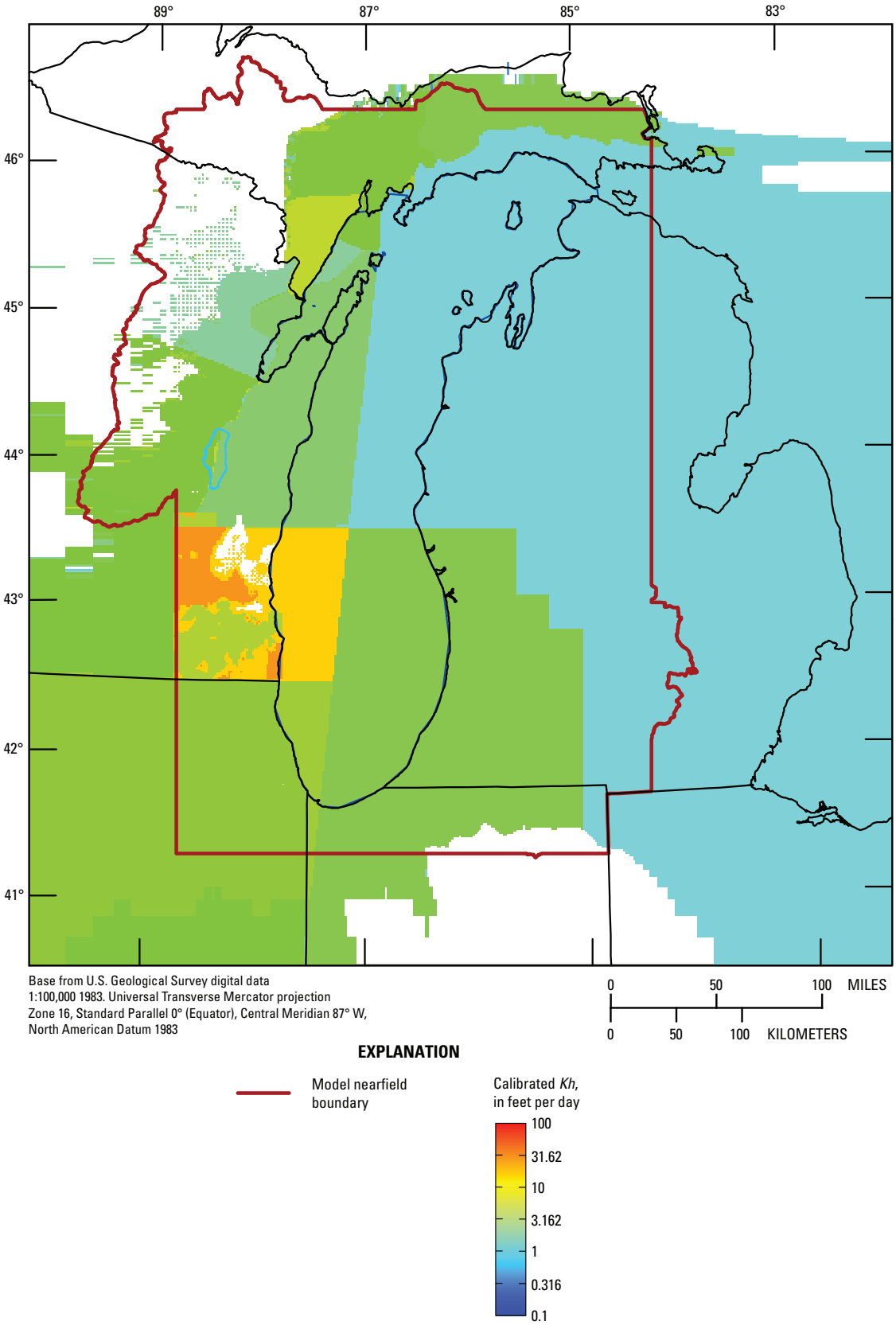

Figure 6*A*–8*B*. Horizontal hydraulic conductivity, IRGA: calibrated input.

Table 6*A*–9. Horizontal hydraulic conductivity of MTSM-L19 (upper Mount Simon sandstone: aquifer).

[Kh, horizontal hydraulic conductivity. Statistics limited to nearfield (including under Lake Michigan)]

Initial Kh (feet per day)								
Zone	1	2	3	4	5	6	7	8
Number nearfield cells	4,738	2,939	3,597	6,107	57,294	8,356	297	482
Number nearfield values	1	3	Gradational	5	2	3	1	2
Ave_thickness	300	67	223	102	280	175	300	105
Median_Kh	.43	1.00	1.92	2.76	3.00	1.50	1.40	6.00
Geometric_mean_Kh	.43	1.03	1.97	3.02	2.43	1.52	1.40	6.95
Min_Kh	.43	1.00	1.19	1.29	1.00	1.29	1.40	6.00
Max_Kh	.43	3.00	3.97	8.92	3.00	7.50	1.40	8.50
Calibrated Kh (feet per day)								
Zone	1	2	3	4	5	6	7	8
PEST inversion multiplier	6.898276	1.315855	1.502177	1.520838	0.1	0.1	0.9244557	1.075758
Median_Kh	2.97	1.32	2.88	4.19	.30	.15	1.29	6.45
Geometric_mean_Kh	2.97	1.36	2.96	4.59	.24	.15	1.29	7.48
Min_Kh	2.97	1.32	1.79	1.96	.10	.13	1.29	6.45
Max_Kh	2.97	3.95	5.96	13.57	.30	.75	1.29	9.14

Thickness units are feet; Kh units are feet per day. Statistics calculated only for nearfield cells where thickness is equal to at least 1 foot.

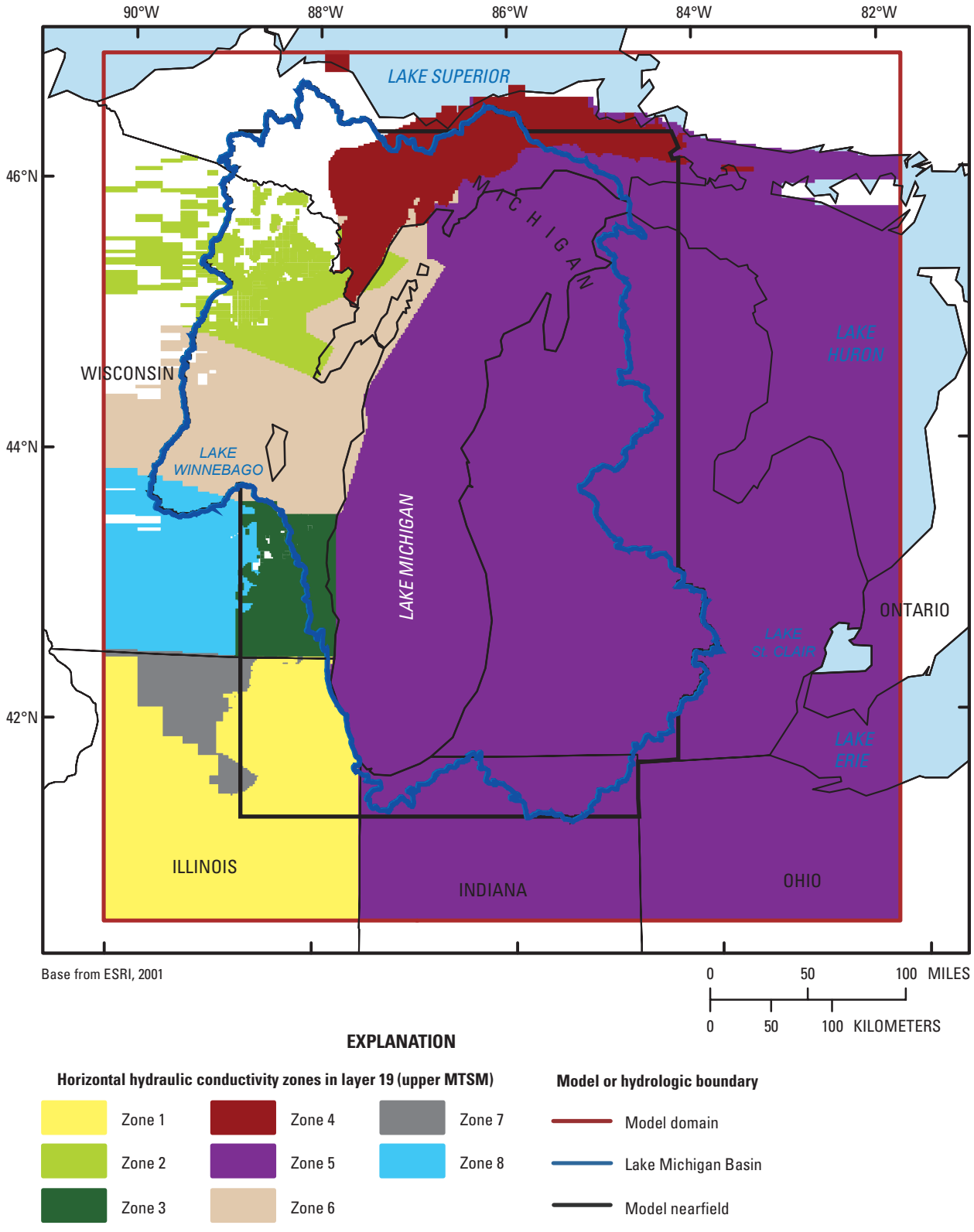

Figure 6*A*–9*A*. Horizontal hydraulic conductivity, upper MTSM: zonation.

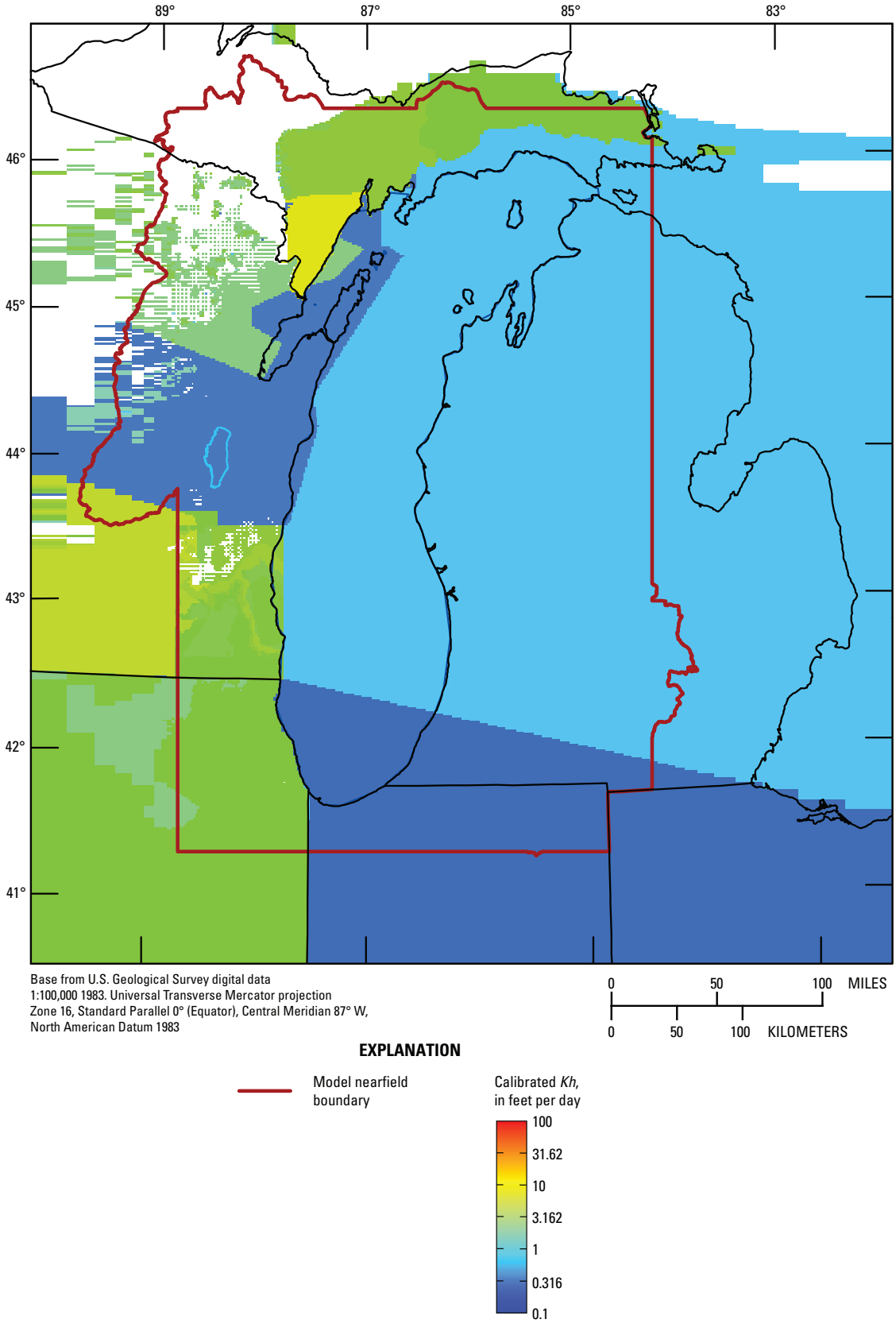

Figure 6*A*–9*B*. Horizontal hydraulic conductivity, upper MTSM: calibrated input.

Table 6*B*–1. Vertical hydraulic conductivity of QRNR-L1 (upper Quaternary: aquifer or confining unit depending on location).

[Kv, vertical hydraulic conductivity. Statistics limited to nearfield (including under Lake Michigan)]

Zone or statistic	Clayey till	Loamy till	Sandy till	Fine stratified	Medium-coarse stratified	Lake Michigan bed			
Initial Kv (feet per day)									
Zone	1	2	3	4	5	6	7	8	9
Number nearfield cells	10,260	20,874	167	4,051	23,727	217	6,102	420	18,210
Number nearfield values	Vary by cell	Vary by cell	Vary by cell	Vary by cell	Vary by cell	1	1	1	1
Ave_thickness (feet)	88	78	90	76	88	52	55	84	56
Median_Kv	5.00E−02	1.82E−01	5.88E−01	1.36E−01	3.47E+00	1.00E−03	1.00E−02	1.00E−01	1.00E−03
Geometric_mean_Kv	5.33E−02	2.05E−01	6.05E−01	2.05E−01	3.59E+00	1.00E−03	1.00E−02	1.00E−01	1.00E−03
Min_Kv	1.00E−02	5.00E−02	1.73E−01	2.00E−02	1.00E+00	1.00E−03	1.00E−02	1.00E−01	1.00E−03
Max_Kv	5.00E−01	2.50E+00	2.22E+00	1.00E+00	1.46E+01	1.00E−03	1.00E−02	1.00E−01	1.00E−03
Calibrated Kv (feet per day)									
Zone	1	2	3	4	5	6	7	8	9
PEST inversion multipliers	0.8901941	1.37701	1.045449	1.356127	1.108223	1.08354	1.08354	1.08354	1.08354
Median_Kv	4.45E−02	2.50E−01	6.14E−01	1.85E−01	3.84E+00	1.08E−03	1.08E−02	1.08E−01	1.08E−03
Geometric_mean_Kv	4.74E−02	2.82E−01	6.33E−01	2.78E−01	3.98E+00	1.08E−03	1.08E−02	1.08E−01	1.08E−03
Min_Kv	8.90E−03	6.89E−02	1.81E−01	2.71E−02	1.11E+00	1.08E−03	1.08E−02	1.08E−01	1.08E−03
Max_Kv	4.45E−01	3.44E+00	2.32E+00	1.36E+00	1.61E+01	1.08E−03	1.08E−02	1.08E−01	1.08E−03

Thickness units are feet; Kv units are feet per day. Statistics calculated only for nearfield cells where thickness is equal to at least 1 foot.

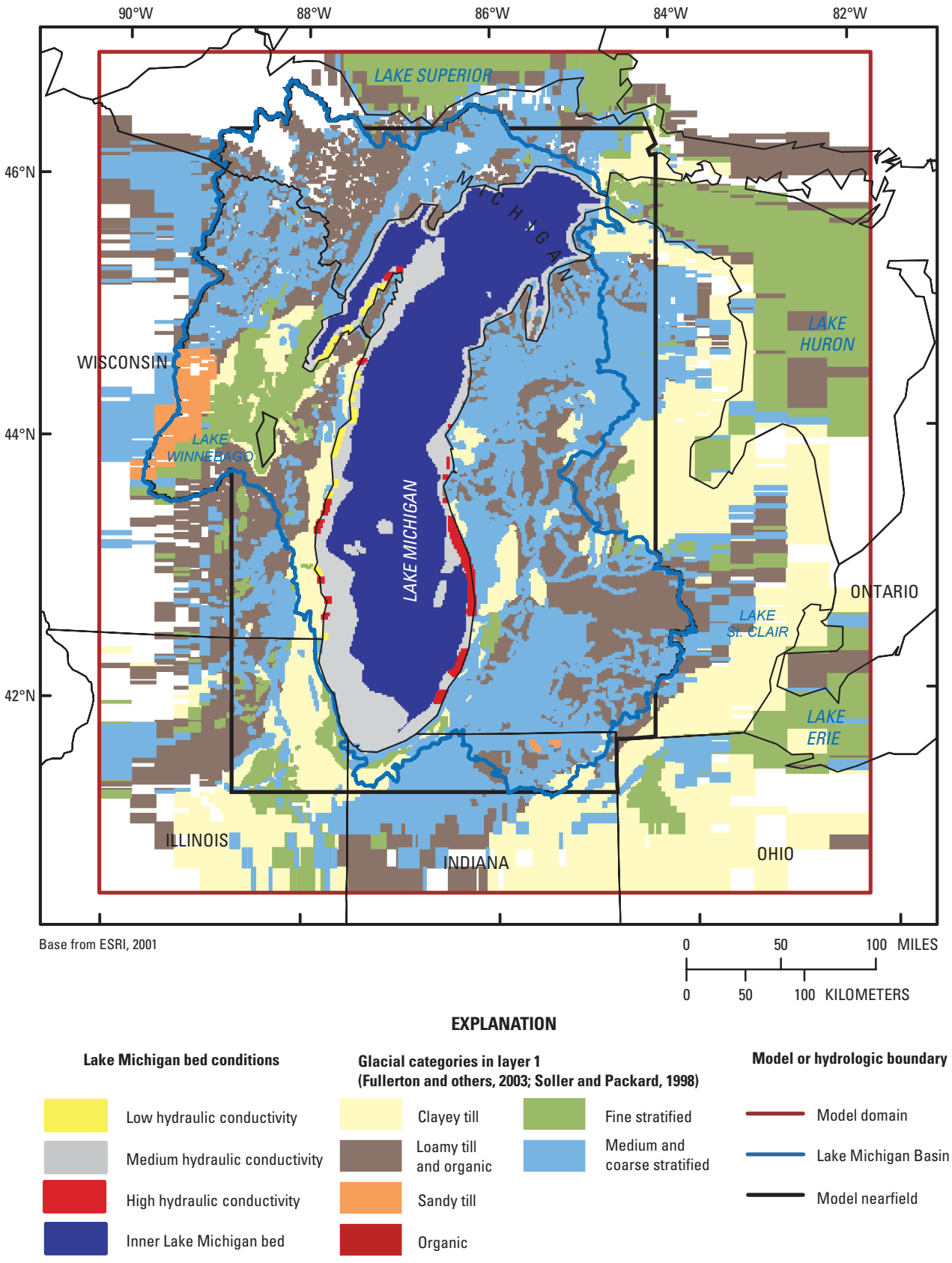

Figure 6*B*–1*A*. Vertical hydraulic conductivity, upper QRNR including Lake Michigan lakebed: zonation.

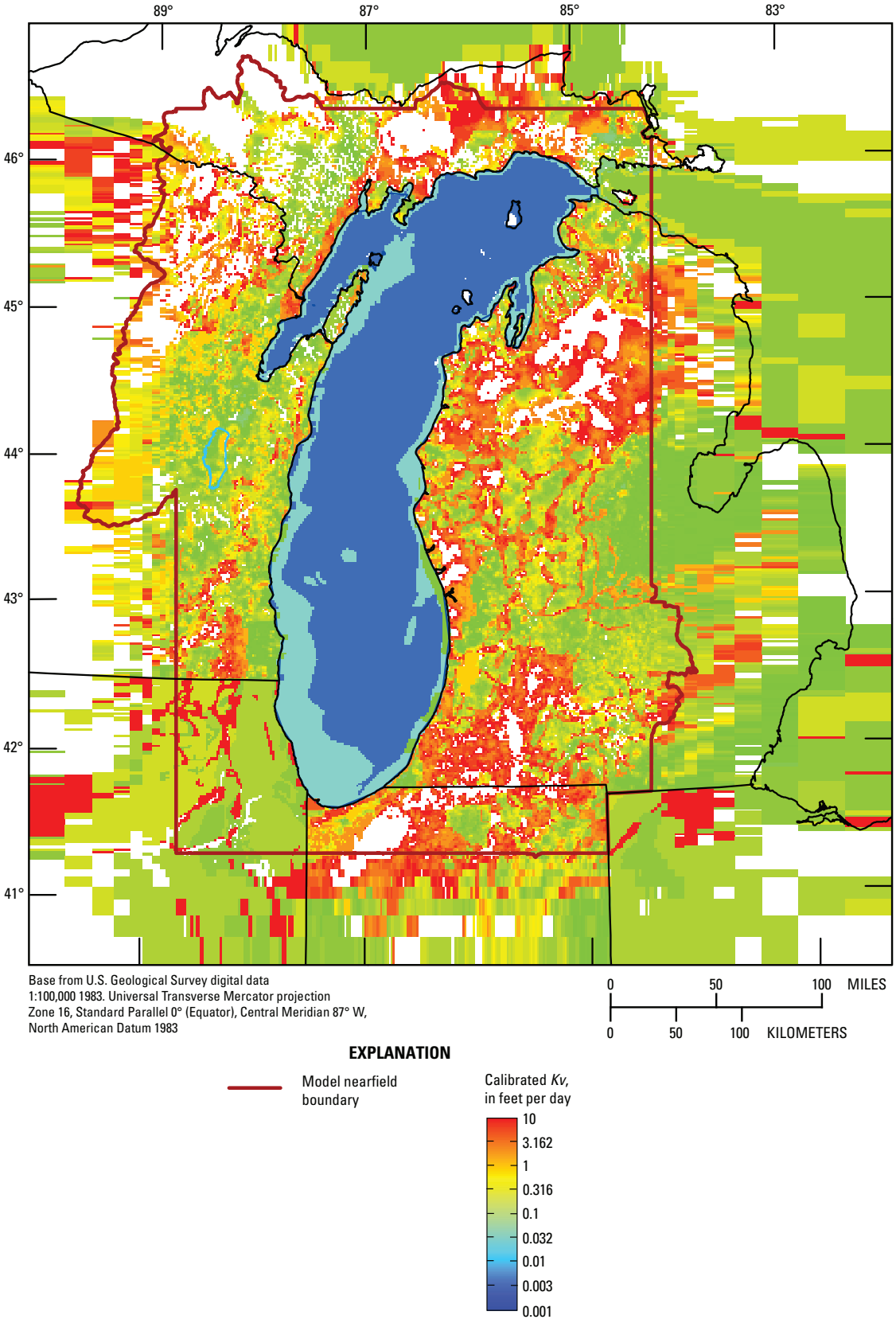

Figure 6*B*–1*B*. Vertical hydraulic conductivity, upper QRNR including Lake Michigan lakebed: calibrated input.

Table 6*B*–2. Vertical hydraulic conductivity of QRNR-L2 (middle Quaternary: aquifer or confining unit depending on location).

[Kv, vertical hydraulic conductivity. Statistics limited to nearfield (including under Lake Michigan)]

Zone or statistic	Clayey till	Loamy till	Sandy till	Fine stratified	Medium-coarse stratified	Unknown
Initial Kv (feet per day)						
Zone	1	2	3	4	5	6
Number nearfield cells	2,379	1,612	58	1,529	2,381	29,993
Number nearfield values	Vary by cell	Vary by cell	Vary by cell	Vary by cell	Vary by cell	Vary by cell
Ave_thickness (ft)	58	65	42	56	55	149
Median_Kv	5.00 E−02	2.50 E−01	6.50 E−01	3.25 E−01	2.93 E+00	1.83 E−01
Geometric_mean_Kv	4.61 E−02	2.14 E−01	6.71 E−01	2.81 E−01	3.01 E+00	2.52 E−01
Min_Kv	1.00 E−03	5.05 E−02	1.52 E−01	2.00 E−02	1.00 E−03	1.00 E−03
Max_Kv	5.00 E−01	2.13 E+00	1.75 E+00	1.00 E+00	1.42 E+01	1.00 E+01
Calibrated Kv (feet per day)						
Zone	1	2	3	4	5	6
PEST inversion multipliers	0.8901941	1.37701	1.045449	1.356127	1.108223	1.328345
Median_Kv	4.45 E−02	3.44 E−01	6.80 E−01	4.40 E−01	3.24 E+00	2.43 E−01
Geometric_mean_Kv	4.10 E−02	2.95 E−01	7.01 E−01	3.81 E−01	3.34 E+00	3.35 E−01
Min_Kv	8.90 E−04	6.95 E−02	1.59 E−01	2.71 E−02	1.11 E−03	1.33 E−03
Max_Kv	4.45 E−01	2.94 E+00	1.83 E+00	1.36 E+00	1.57 E+01	1.33 E+01

Thickness units are feet; Kv units are feet per day. Statistics calculated only for nearfield cells where thickness is equal to at least 1 foot.

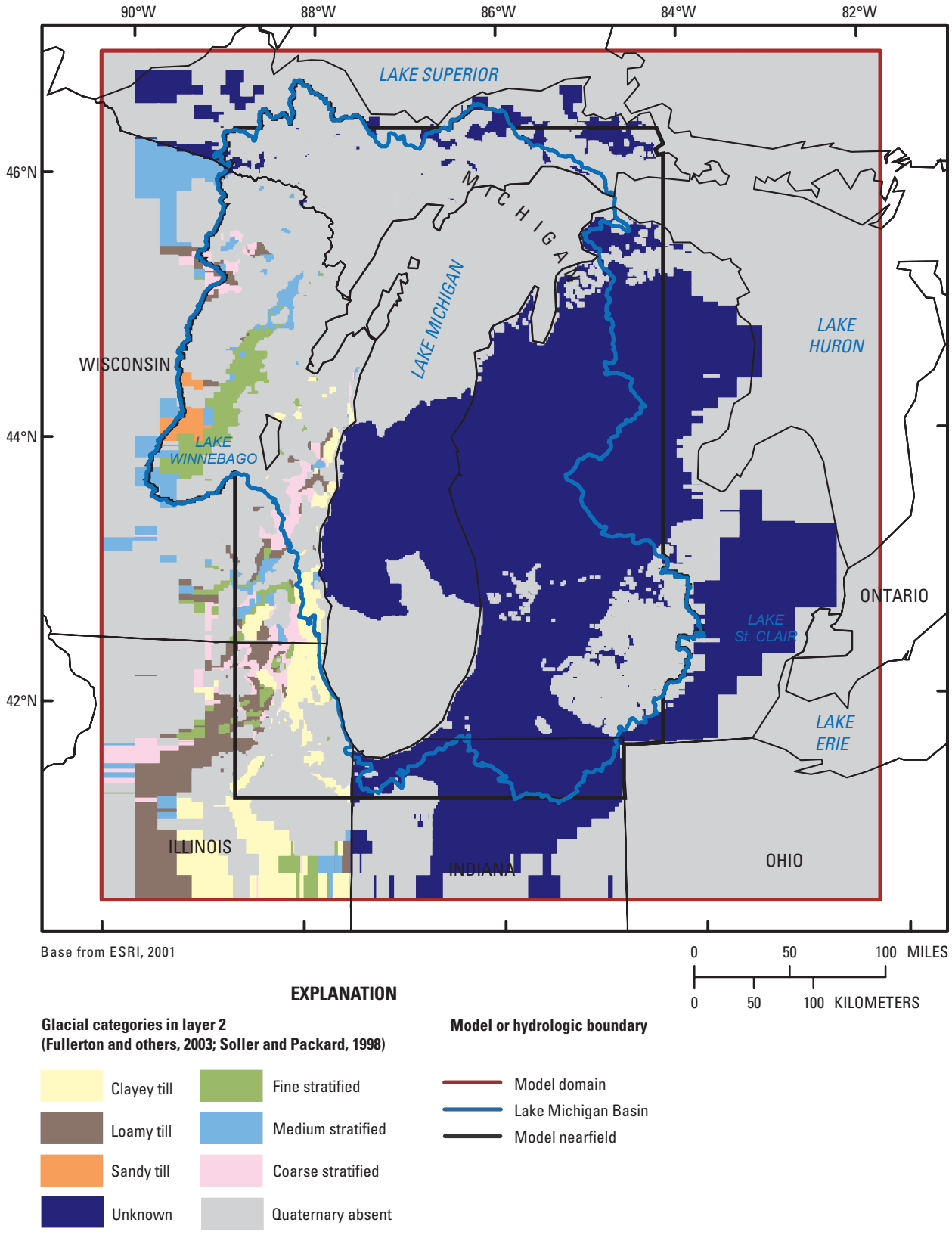

Figure 6*B*–2*A*. Vertical hydraulic conductivity, middle QRNR: zonation.

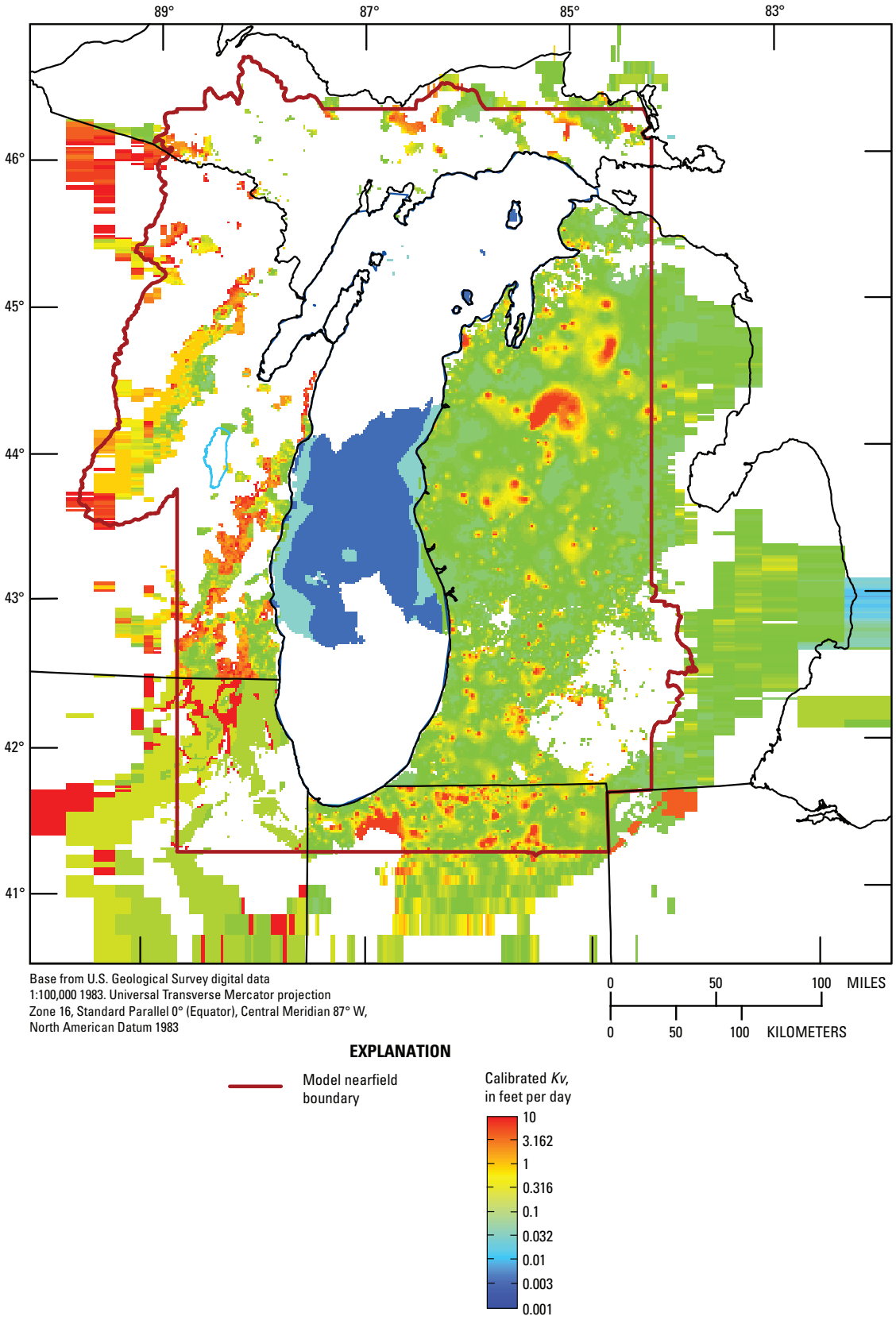

Figure 6*B*–2*B*. Vertical hydraulic conductivity, middle QRNR: calibrated input.

Table 6*B*–3. Vertical hydraulic conductivity of QRNR-L3 (lower Quaternary: aquifer or confining unit depending on location).

[Kv, vertical hydraulic conductivity; --, not applicable. Statistics limited to nearfield (including under Lake Michigan)]

Zone or statistic	Clayey till	Loamy till	Sandy till	Fine stratified	Medium-coarse stratified	Unknown
	Initial Kv (feet per day)					
Zone	1	2	3	4	5	6
Number nearfield cells	21	40	0	33	42	15,330
Number nearfield values	Vary by cell	Vary by cell	--	Vary by cell	Vary by cell	Vary by cell
Ave_thickness (feet)	16	43	--	23	23	199
Median_Kv	2.12 E−02	2.50 E−01	--	1.17 E−01	3.66 E+00	2.71 E−01
Geometric_mean_Kv	2.29 E−02	2.80 E−01	--	2.24 E−01	3.45 E+00	3.59 E−01
Min_Kv	1.14 E−02	1.24 E−01	--	8.45 E−02	1.33 E+00	1.00 E−02
Max_Kv	5.00 E−02	6.76 E−01	--	1.00 E+00	8.97 E+00	1.00 E+00
	Calibrated Kv (feet per day)					
Zone	1	2	3	4	5	6
PEST inversion multipliers	0.8901941	1.37701	--	1.356127	1.108223	1.328345
Median_Kv	1.89 E−02	3.44 E−01	--	1.59 E−01	4.06 E+00	3.60 E−01
Geometric_mean_Kv	2.04 E−02	3.86 E−01	--	3.04 E−01	3.83 E+00	4.77 E−01
Min_Kv	1.02 E−02	1.71 E−01	--	1.15 E−01	1.48 E+00	1.33 E−02
Max_Kv	4.45 E−02	9.30 E−01	--	1.36 E+00	9.94 E+00	1.33 E+00

Thickness units are feet; Kv units are feet per day. Statistics calculated only for nearfield cells where thickness is equal to at least 1 foot.

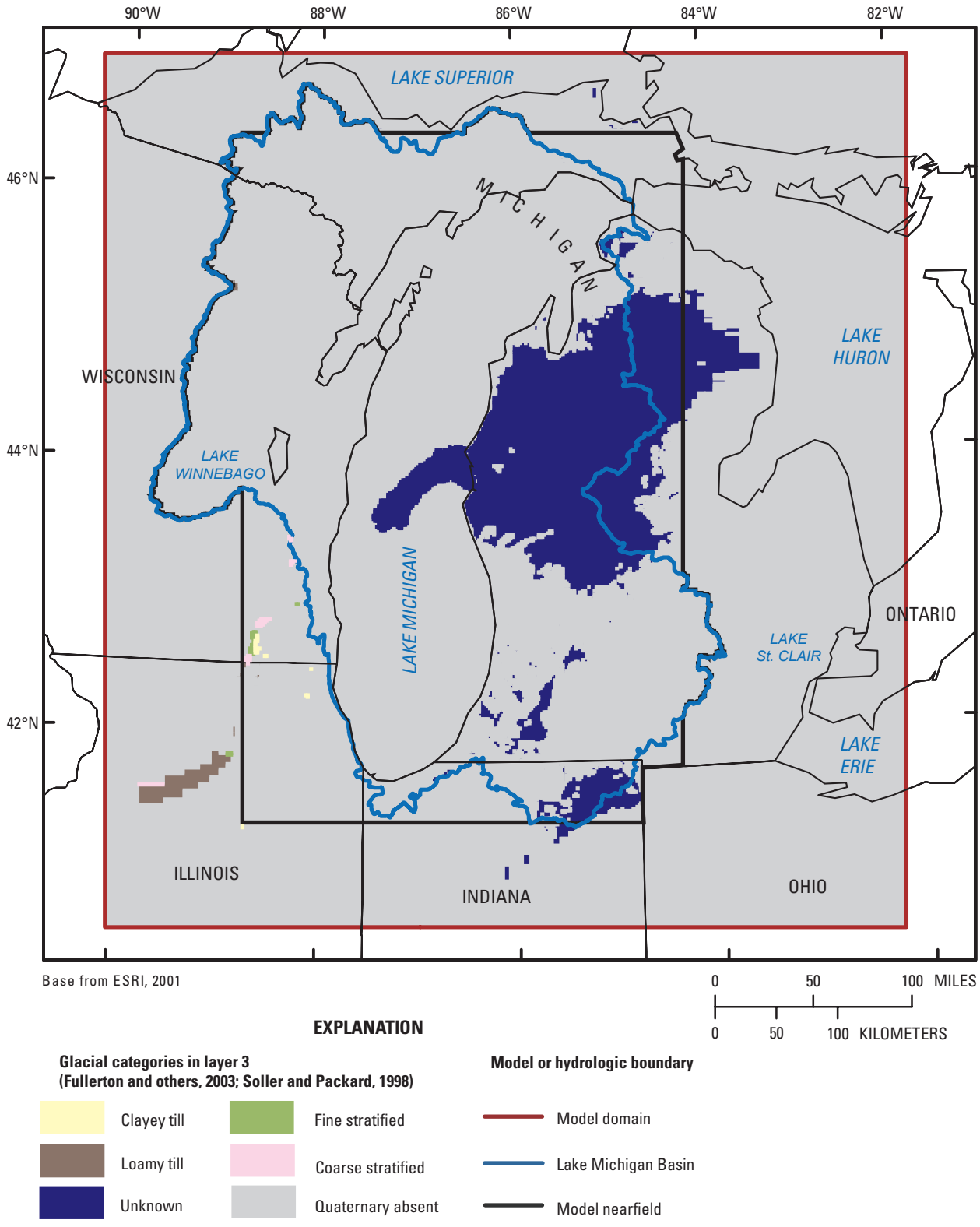

Figure 6*B*–3*A*. Vertical hydraulic conductivity, lower QRNR: zonation.

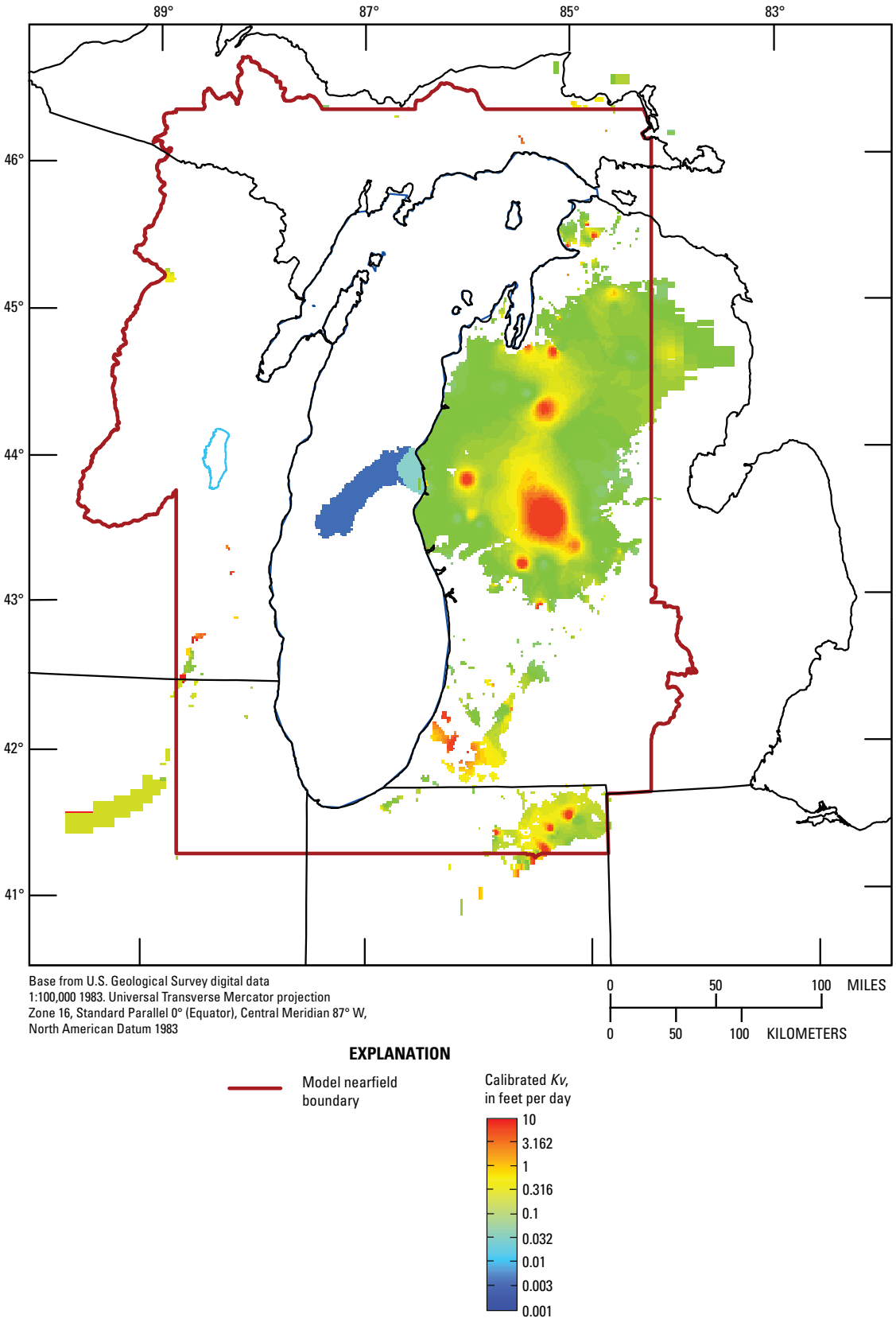

Figure 6*B*–3*B*. Vertical hydraulic conductivity, lower QRNR: calibrated input.

Table 6*B*–4. Vertical hydraulic conductivity of PEN2-L6 (Parma Sandstone aquifer, Bayport Limestone aquifer, Saginaw shale: aquifer or confining unit depending on location).

[Kv, vertical hydraulic conductivity; Gradational, number of nearfield values implies values are interpolated across cells. Statistics limited to nearfield (including under Lake Michigan)]

Initial Kv (feet per day)					
Zone	1	2	3	4	5
Number nearfield cells	1,648	4,786	3,199	70	215
Number nearfield values	Gradational	Gradational	Gradational	Gradational	1
Ave_thickness (feet)	148	192	148	226	29
Median_Kv	4.74 E−04	8.43 E−04	1.52 E−03	2.59 E−03	7.00 E−02
Geometric_mean_Kv	4.40 E−04	8.54 E−04	1.54 E−03	2.62 E−03	7.00 E−02
Min_Kv	3.00 E−04	6.01 E−04	1.21 E−03	2.44 E−03	7.00 E−02
Max_Kv	6.00 E−04	1.20 E−03	2.42 E−03	3.34 E−03	7.00 E−02
Calibrated Kv (feet per day)					
Zone	1	2	3	4	5
PEST inversion multipliers	0.9875861	1.795126	1.136216	1.571383	0.7712138
Median_Kv	4.68 E−04	1.51 E−03	1.73 E−03	4.07 E−03	5.40 E−02
Geometric_mean_Kv	4.35 E−04	1.53 E−03	1.75 E−03	4.11 E−03	5.40 E−02
Min_Kv	2.96 E−04	1.08 E−03	1.37 E−03	3.84 E−03	5.40 E−02
Max_Kv	5.93 E−04	2.16 E−03	2.75 E−03	5.24 E−03	5.40 E−02

Thickness units are feet, Kv units are feet perday. Statistics calculated only for nearfield cells where thickness is equal to at least 1 foot.

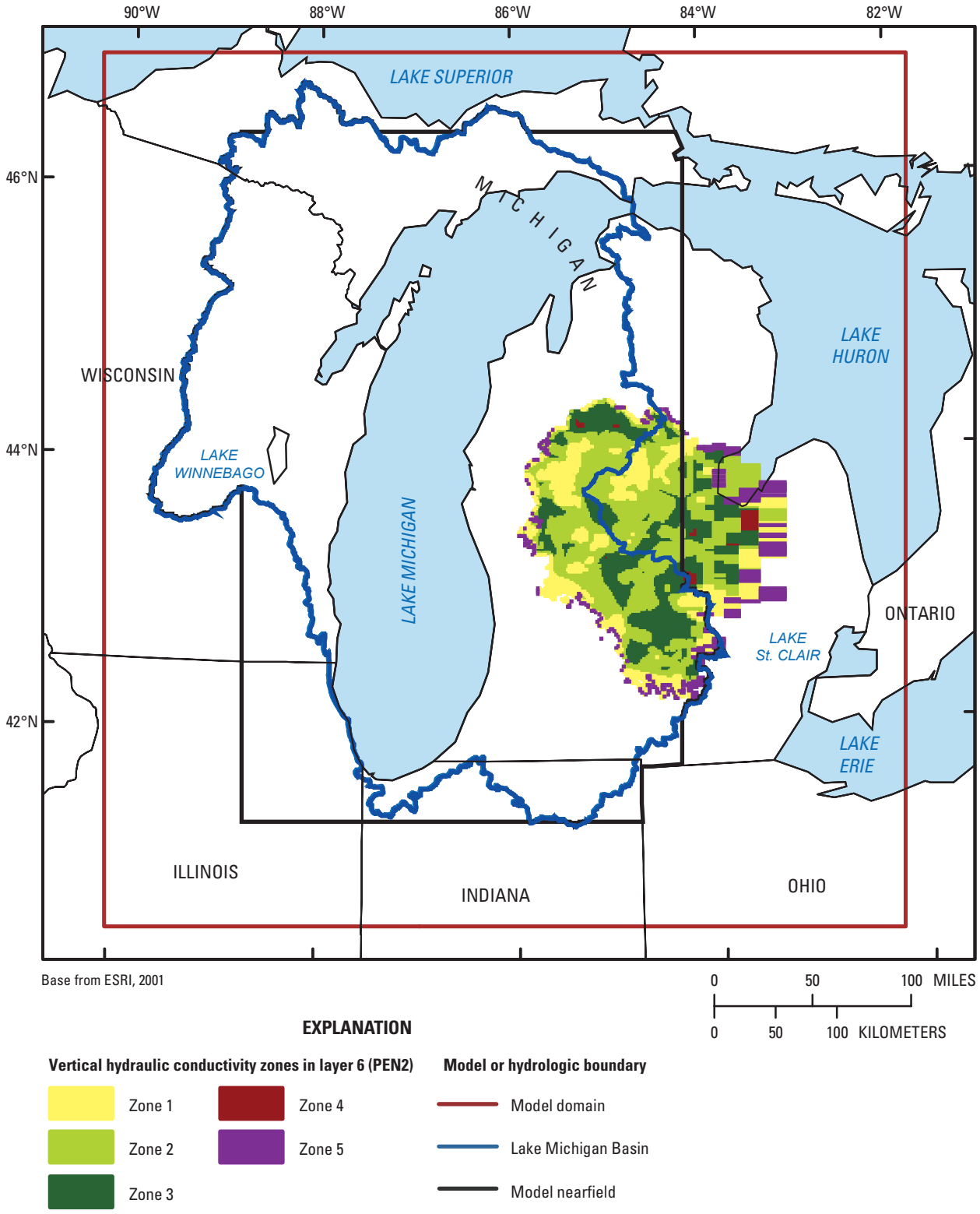

Figure 6*B*–4*A*. Vertical hydraulic conductivity, PEN2: zonation.

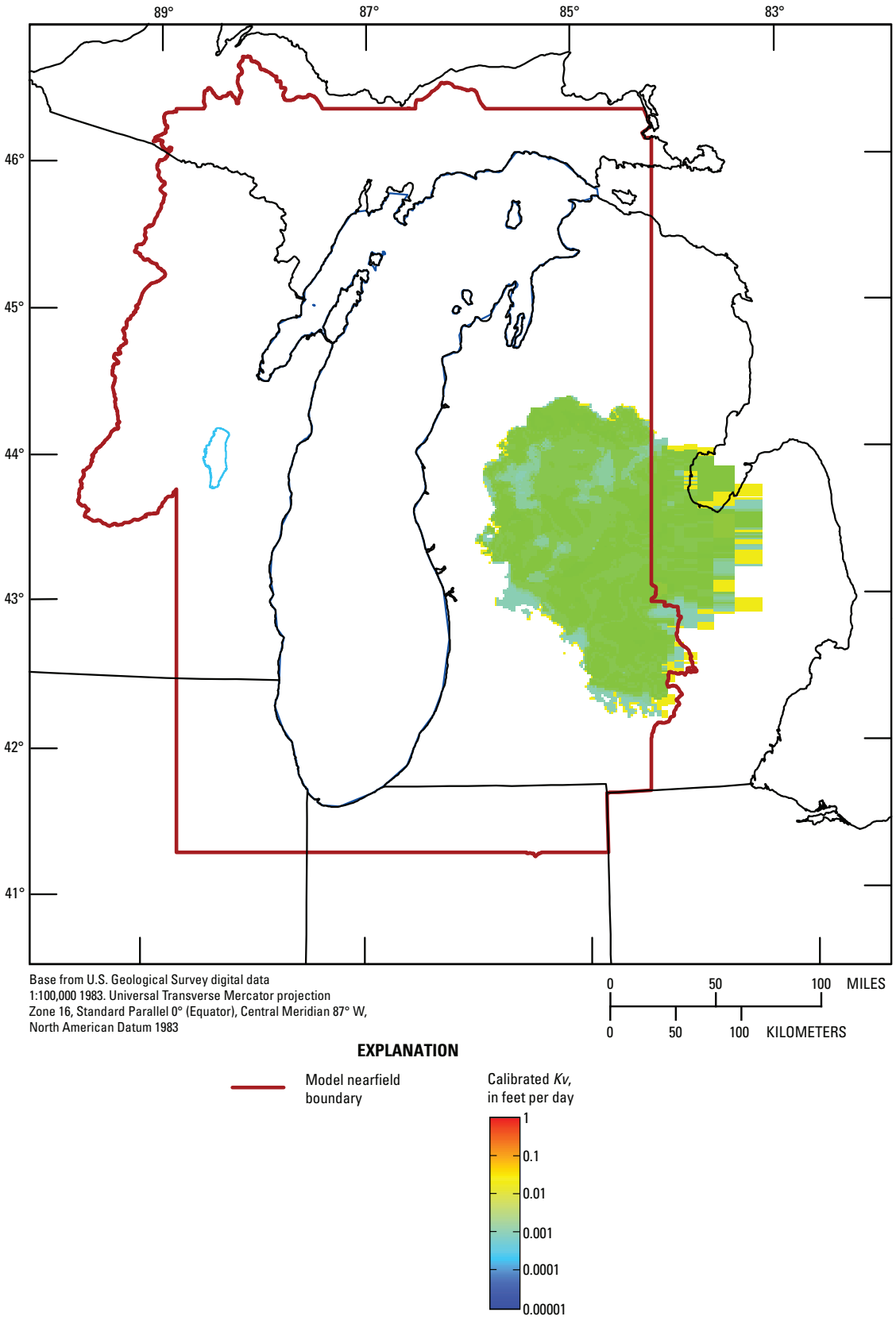

Figure 6*B*–4*B*. Vertical hydraulic conductivity, PEN2: calibrated input.

Table 6*B*–5. Vertical hydraulic conductivity of MICH-L7 (Michigan shale: confining unit).

[Kv, vertical hydraulic conductivity. Statistics limited to nearfield (including under Lake Michigan)]

Initial Kv (feet per day)	
Zone	1
Number nearfield cells	13,647
Number nearfield values	1
Ave_thickness (feet)	255
Median_Kv	1.00 E−04
Geometric_mean_Kv	1.00 E−04
Min_Kv	1.00 E−04
Max_Kv	1.00 E−04
Calibrated Kv (feet per day)	
Zone	1
PEST inversion multipliers	1.196813
Median_Kv	1.20 E−04
Geometric_mean_Kv	1.20 E−04
Min_Kv	1.20 E−04
Max_Kv	1.20 E−04

Thickness units are feet, Kv units are feet per day. Statistics calculated only for nearfield cells where thickness is equal to at least 1 foot.

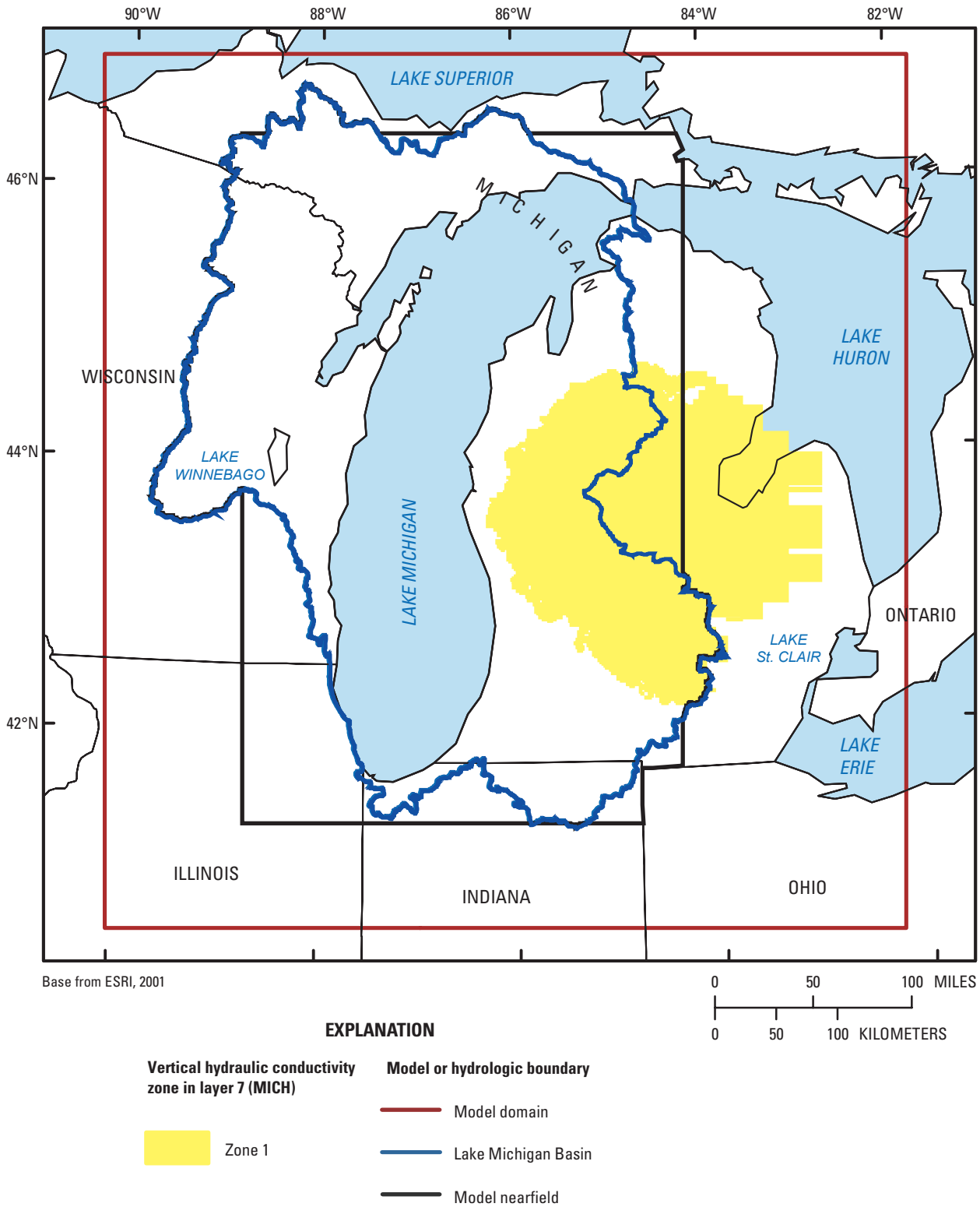

Figure 6*B*–5*A*. Vertical hydraulic conductivity, MICH: zonation.

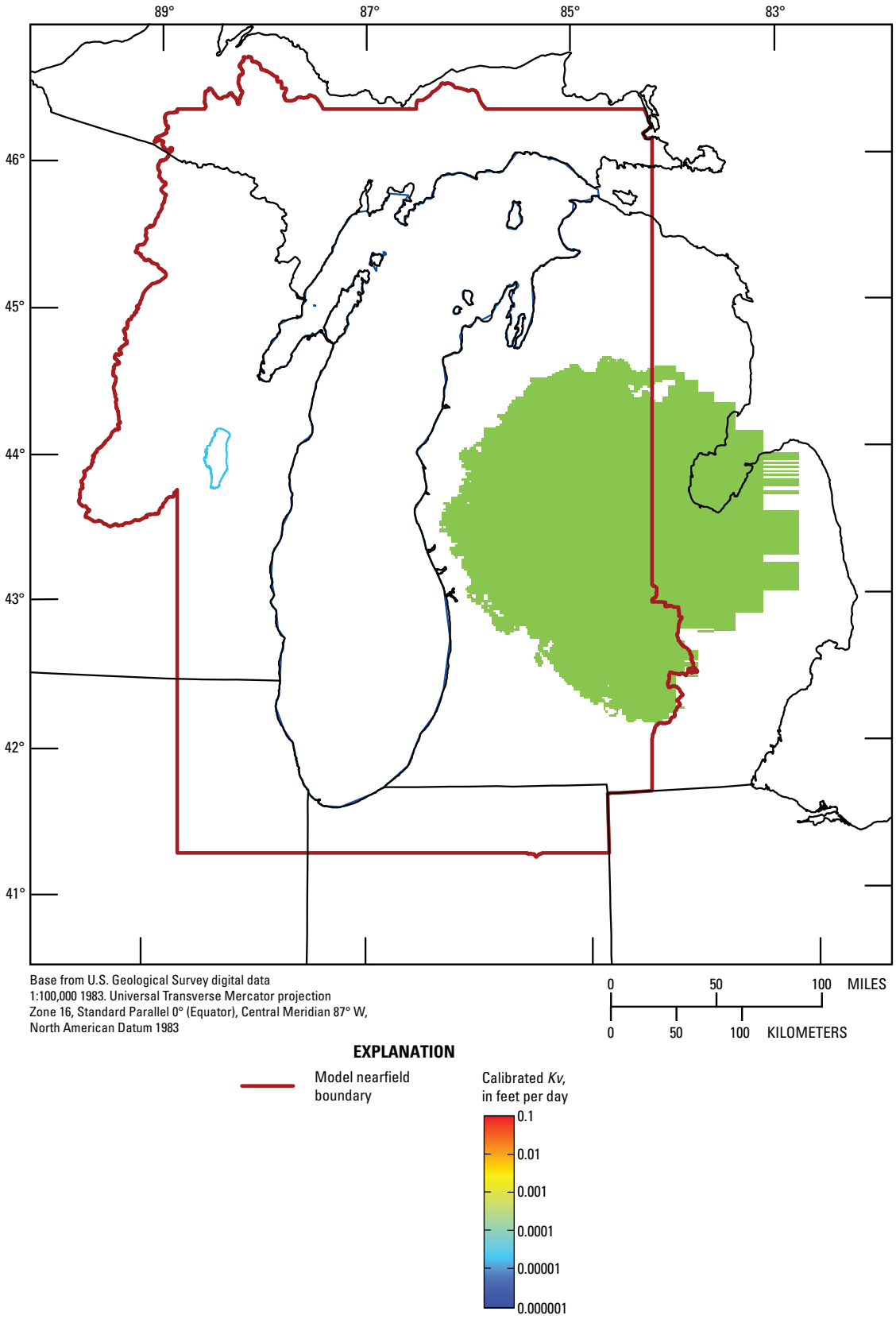

Figure 6*B*–5*B*. Vertical hydraulic conductivity, MICH: calibrated input.

Table 6*B*–6. Vertical hydraulic conductivity of DVMS-L9 (Devonian-Mississippian, including Antrim and Coldwater shales: confining unit).

[Kv, vertical hydraulic conductivity; --, not applicable. Statistics limited to nearfield (including under Lake Michigan)]

Initial Kv (feet per day)			
Zone	1	2	3
Number nearfield cells	200	40,340	0
Number nearfield values	1	1	0; Only farfield
Ave_thickness (feet)	58	927	--
Median_Kv	2.20 E−06	5.00 E−06	--
Geometric_mean_Kv	2.20 E−06	5.00 E−06	--
Min_Kv	2.20 E−06	5.00 E−06	--
Max_Kv	2.20 E−06	5.00 E−06	--
Calibrated Kv (feet per day)			
Zone	1	2	3
PEST inversion multipliers	1.367526	0.8558034	--
Median_Kv	3.01 E−06	4.28 E−06	--
Geometric_mean_Kv	3.01 E−06	4.28 E−06	--
Min_Kv	3.01 E−06	4.28 E−06	--
Max_Kv	3.01 E−06	4.28 E−06	--

Thickness units are feet, Kv units are feet per day. Statistics calculated only for nearfield cells where thickness is equal to at least 1 foot.

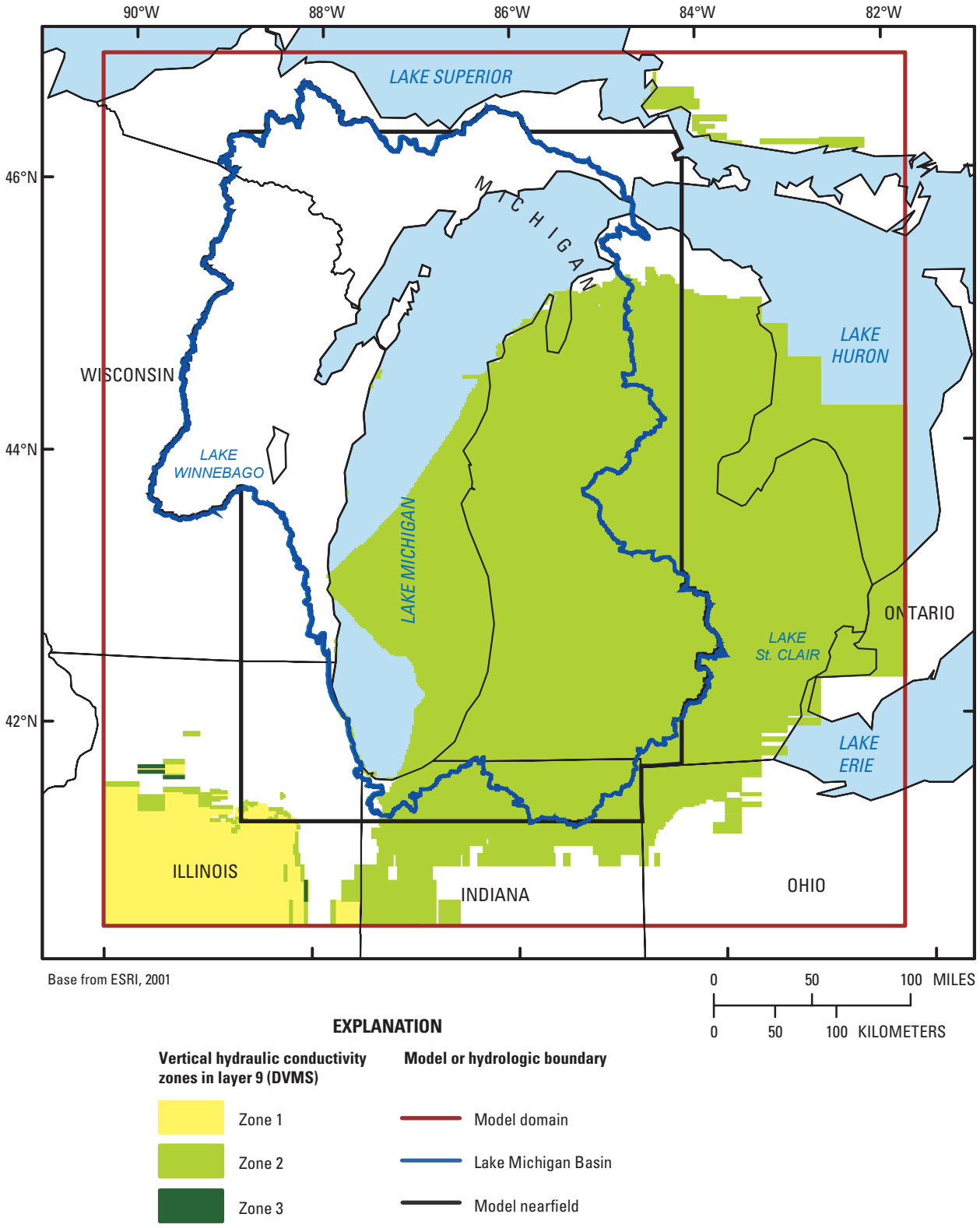

Figure 6*B*–6*A*. Vertical hydraulic conductivity, DVMS: zonation.

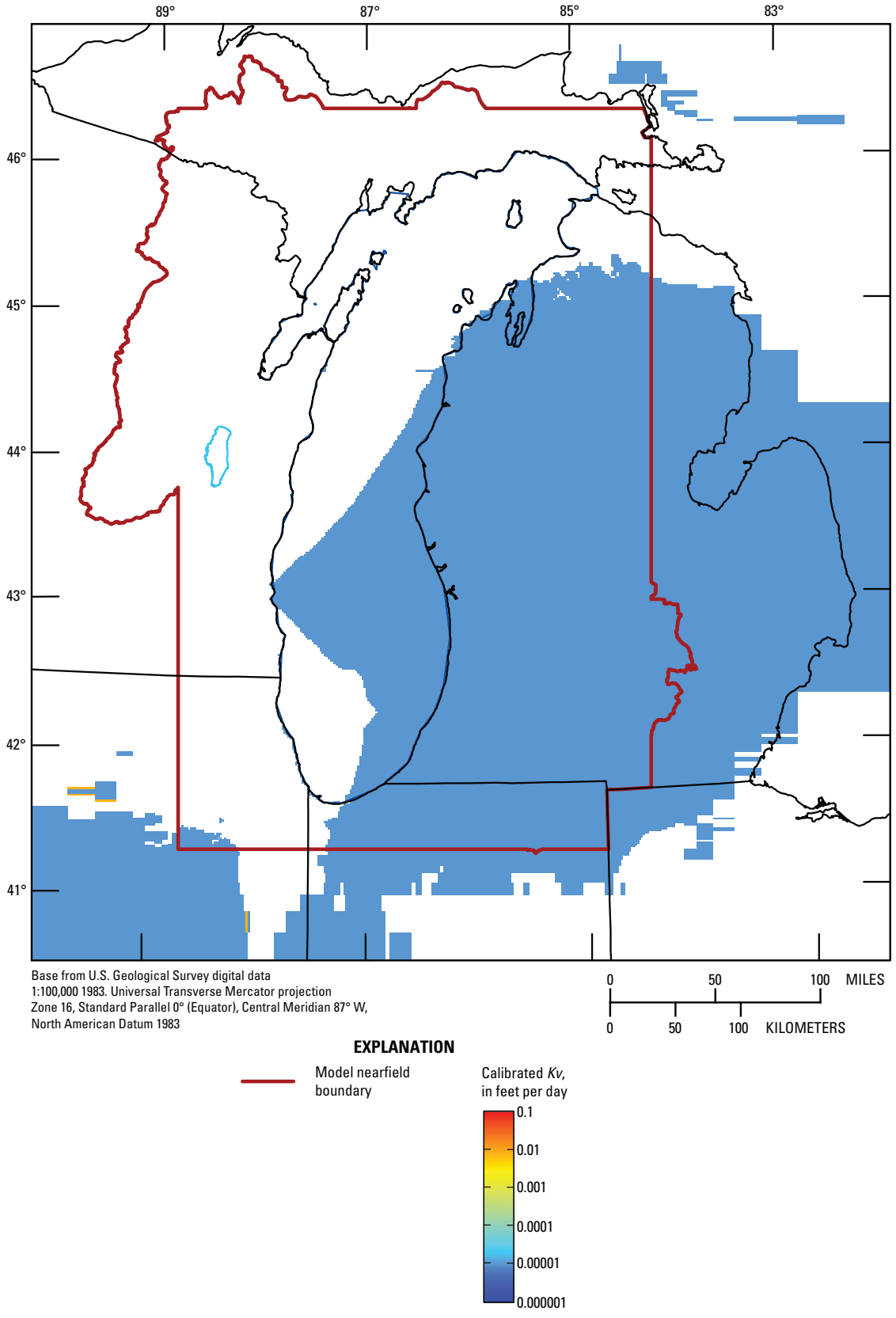

Figure 6*B*–6*B*. Vertical hydraulic conductivity, DVMS: calibrated input.

Table 6*B*–7. Vertical hydraulic conductivity of SLDV-L11 (middle Silurian-Devonian, including Salina Group evaporites: aquifer or confining unit depending on location).

[Kv, vertical hydraulic conductivity. Statistics limited to nearfield (including under Lake Michigan)]

Initial Kv (feet per day)					
Zone	1	2	3	4	5
Number nearfield cells	16,488	14,292	34,334	645	1,420
Number nearfield values	1	1	1	3	1
Ave_thickness (feet)	1,415	931	450	196	183
Median_Kv	1.00 E−07	1.00 E−04	1.00E−03	8.00E−03	1.67E−02
Geometric_mean_Kv	1.00 E−07	1.00 E−04	1.00E−03	8.36E−03	1.67E−02
Min_Kv	1.00 E−07	1.00 E−04	1.00E−03	5.30E−03	1.67E−02
Max_Kv	1.00 E−07	1.00 E−04	1.00E−03	1.00E−02	1.67E−02
Calibrated Kv (feet per day)					
Zone	1	2	3	4	5
PEST inversion multipliers	1.144564	1.443614	2.833561	1.457894	1.121505
Median_Kv	1.14 E−07	1.44 E−04	2.83 E−03	1.17 E−02	1.87 E−02
Geometric_mean_Kv	1.14 E−07	1.44 E−04	2.83 E−03	1.22 E−02	1.87 E−02
Min_Kv	1.14 E−07	1.44 E−04	2.83 E−03	7.73 E−03	1.87 E−02
Max_Kv	1.14 E−07	1.44 E−04	2.83 E−03	1.46 E−02	1.87 E−02

Thickness units are feet, Kv units are feet per day. Statistics calculated only for nearfield cells where thickness is equal to at least 1 foot.

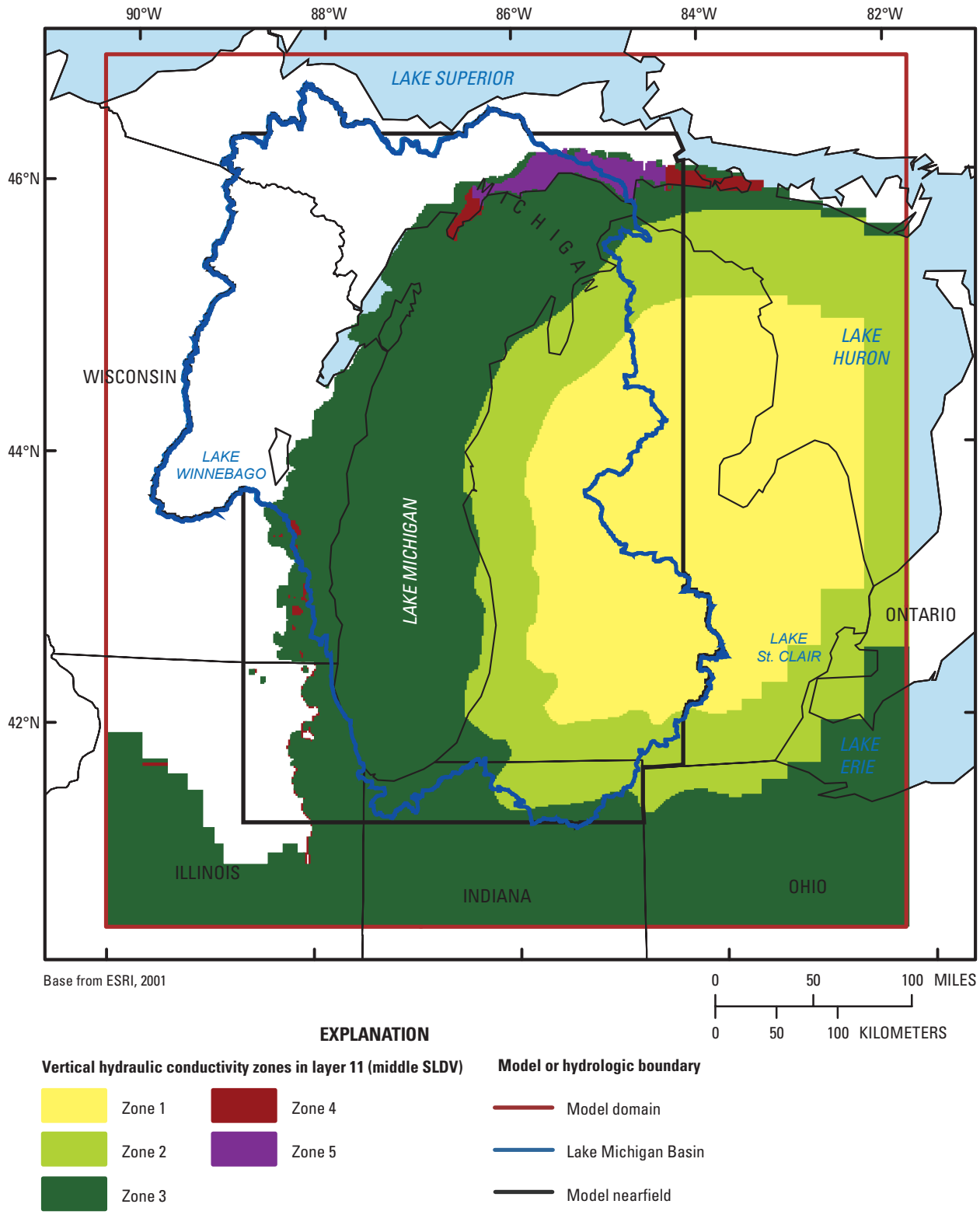

Figure 6*B*–7*A*. Vertical hydraulic conductivity, middle SLDV: zonation.

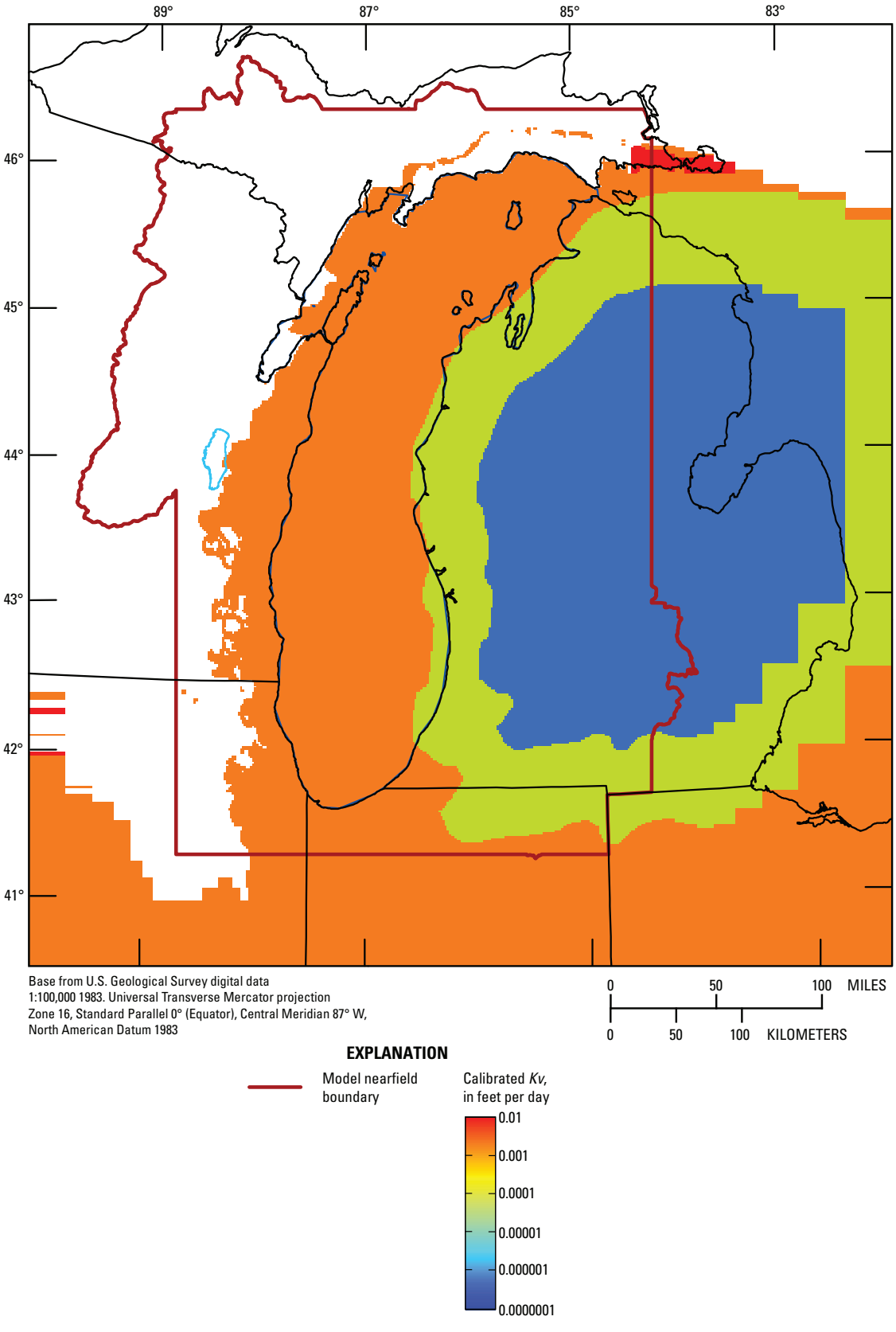

Figure 6*B*–7*B*. Vertical hydraulic conductivity, middle SLDV: calibrated input.

Table 6*B*–8. Vertical hydraulic conductivity of MAQU-L13 (Maquoketa shale: confining unit).

[Kv, vertical hydraulic conductivity. Pilot point application. Statistics limited to nearfield (including under Lake Michigan)]

Initial Kv (feet per day)							
Zone	1	2	3	4	5	6	7
Number nearfield cells	47,537	6,863	7,798	8,815	1,058	859	389
Number nearfield values	1	Gradational	Gradational	2	3	4	2
Ave_thickness (ft)	527	228	214	292	76	22	27
Median_Kv	6.70 E−06	6.70 E−06	6.70 E−06	2.00 E−05	1.00 E−03	1.00 E−03	3.00 E−03
Geometric_mean_Kv	6.70 E−06	7.80 E−06	7.40 E−06	1.31 E−05	5.07 E−04	9.08 E−04	1.42 E−03
Min_Kv	6.70 E−06	6.70 E−06	6.70 E−06	6.70 E−06	5.00 E−05	5.00 E−05	5.00 E−05
Max_Kv	6.70 E−06	3.39 E−05	1.33 E−05	2.00 E−05	3.00 E−03	3.00 E−03	3.00 E−03
Calibrated Kv (feet per day)							
Zone	1	2	3	4	5	6	7
PEST inversion multipliers	0.3	Pilot points	Pilot points	0.8675809	2.802746	1.10739	1.737369
Median_Kv	2.01 E−06			1.74 E−05	2.80 E−03	1.11 E−03	5.21 E−03
Geometric_mean_Kv	2.01 E−06			1.14 E−05	1.42 E−03	1.01 E−03	2.47 E−03
Min_Kv	2.01 E−06			5.81 E−06	1.40 E−04	5.54 E−05	8.69 E−05
Max_Kv	2.01 E−06			1.74 E−05	8.41 E−03	3.32 E−03	5.21 E−03

Geometric mean for zones 2 and zone 3 with pilot points:	
All Maquoketa cells	9.57 E−06
“Subcropping” cells	2.61 E−05
“Buried” cells	6.30 E−06

Thickness units are feet; Kv units are feet per day. Statistics calculated only for nearfield cells where thickness is equal to at least 1 foot.

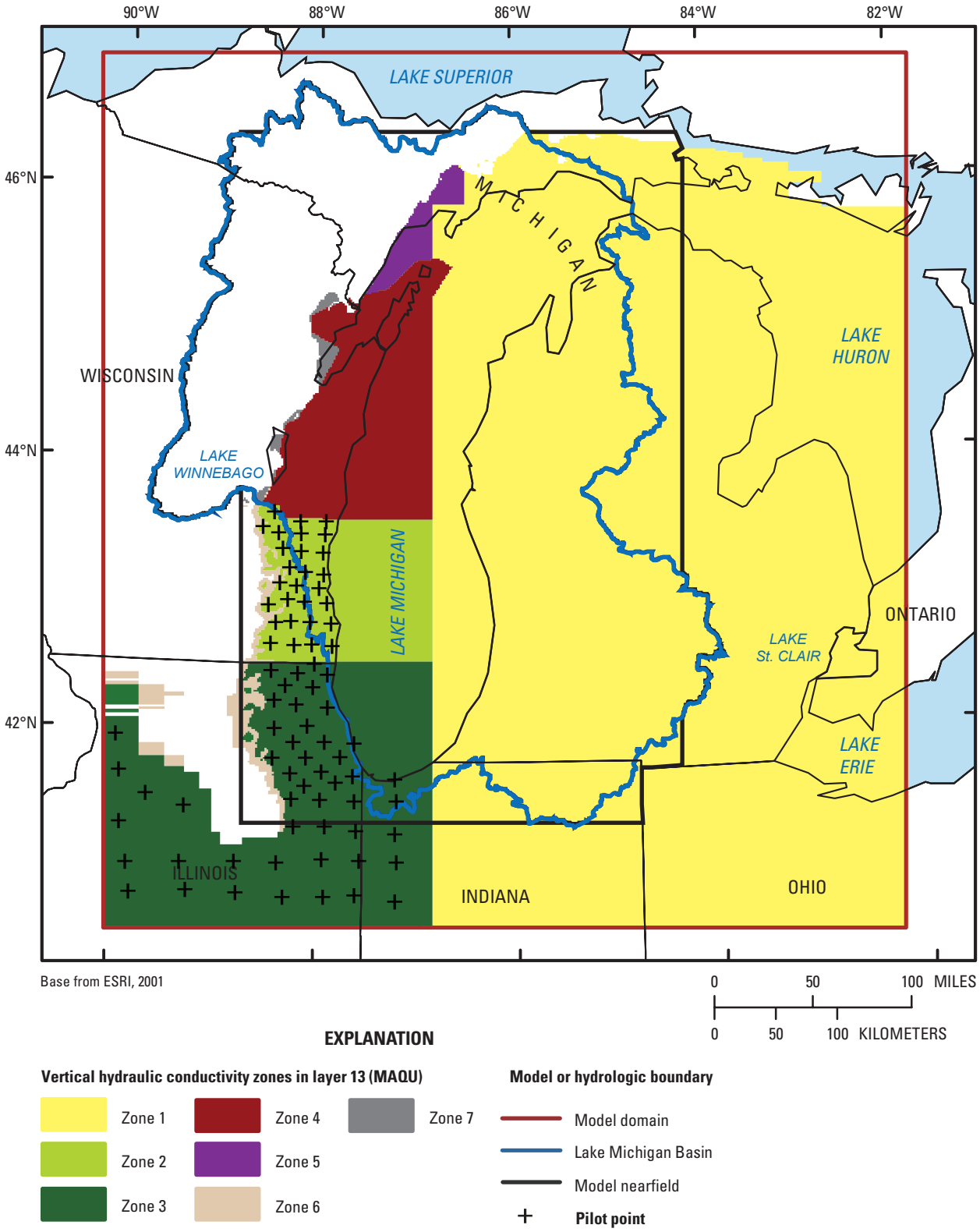

Figure 6*B*–8*A*. Vertical hydraulic conductivity, MAQU: zonation.

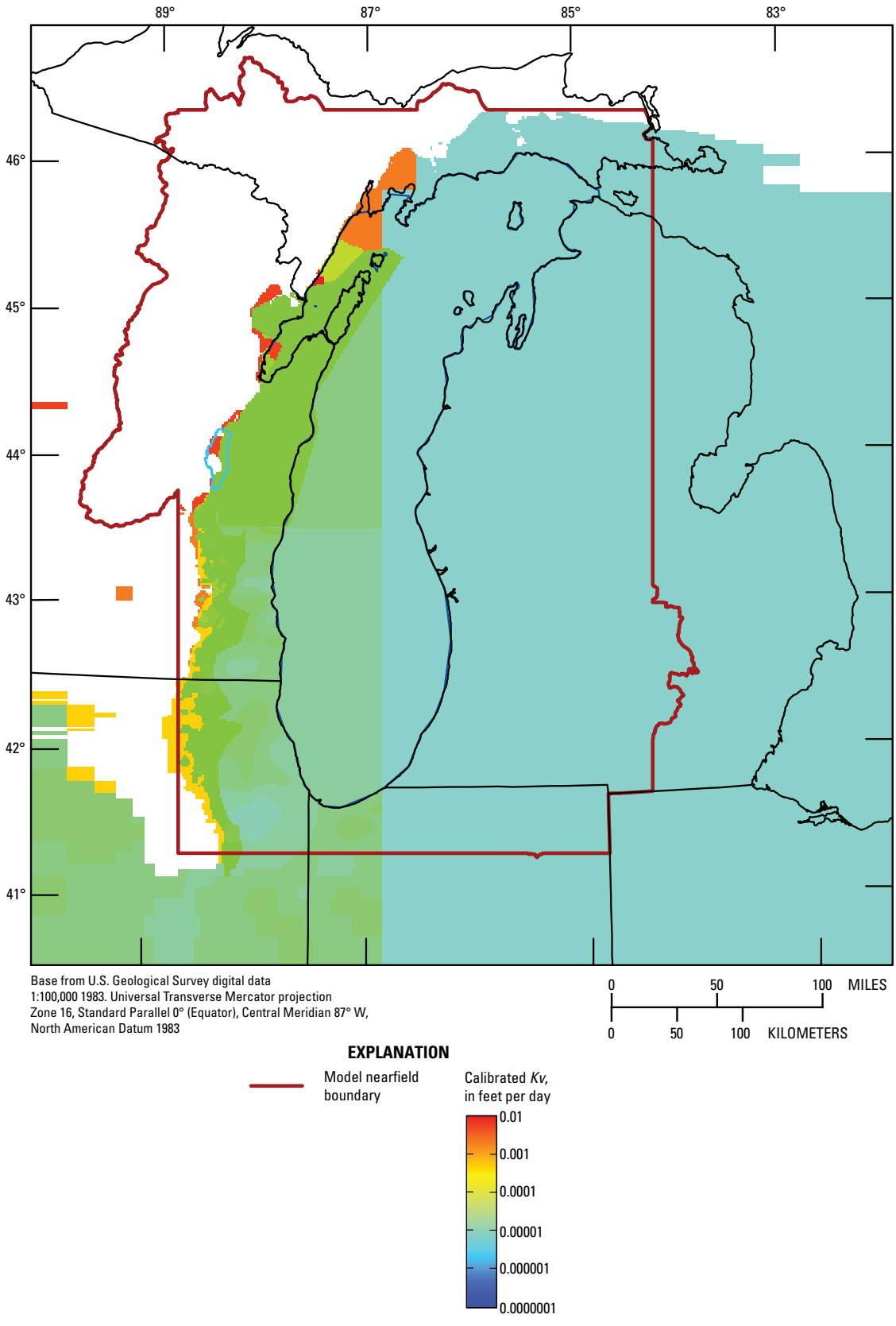

Figure 6*B*–8*B*. Vertical hydraulic conductivity, MAQU: calibrated input.

Table 6*B*–9. Vertical hydraulic conductivity of EACL-L18 (Eau Claire sandstone and siltstone: aquifer or confining unit depending on location).

[Kv, vertical hydraulic conductivity. Statistics limited to nearfield (including under Lake Michigan)]

Initial Kv (feet per day)							
Zone	1	2	3	4	5	6	7
Number nearfield cells	60,310	3,543	2,055	4,061	5,894	4,741	1,142
Number nearfield values	1	1	2	1	3	2	1
Ave_thickness (feet)	359	310	103	30	46	77	80
Median_Kv	1.00 E−05	4.00 E−05	4.00 E−04	6.00 E−04	5.00 E−03	2.76 E−02	8.92 E−02
Geometric_mean_Kv	1.00 E−05	4.00 E−05	4.06 E−04	6.00 E−04	4.91 E−03	2.37 E−02	8.92 E−02
Min_Kv	1.00 E−05	4.00 E−05	4.00 E−04	6.00 E−04	4.00 E−03	1.93 E−02	8.92 E−02
Max_Kv	1.00 E−05	4.00 E−05	4.30 E−04	6.00 E−04	6.00 E−03	2.76 E−02	8.92 E−02
Calibrated Kv (feet per day)							
Zone	1	2	3	4	5	6	7
PEST inversion multipliers	0.1147005	3.445694	0.541053	0.9397809	0.8709347	1.524785	1.483659
Median_Kv	1.15 E−06	1.38 E−04	2.16 E−04	5.64 E−04	4.35 E−03	4.20 E−02	1.32 E−01
Geometric_mean_Kv	1.15 E−06	1.38 E−04	2.20 E−04	5.64 E−04	4.27 E−03	3.62 E−02	1.32 E−01
Min_Kv	1.15 E−06	1.38 E−04	2.16 E−04	5.64 E−04	3.48 E−03	2.95 E−02	1.32 E−01
Max_Kv	1.15 E−06	1.38 E−04	2.33 E−04	5.64 E−04	5.23 E−03	4.20 E−02	1.32 E−01

Thickness units are feet, Kv units are feet per day. Statistics calculated only for nearfield cells where thickness is equal to at least 1 foot.

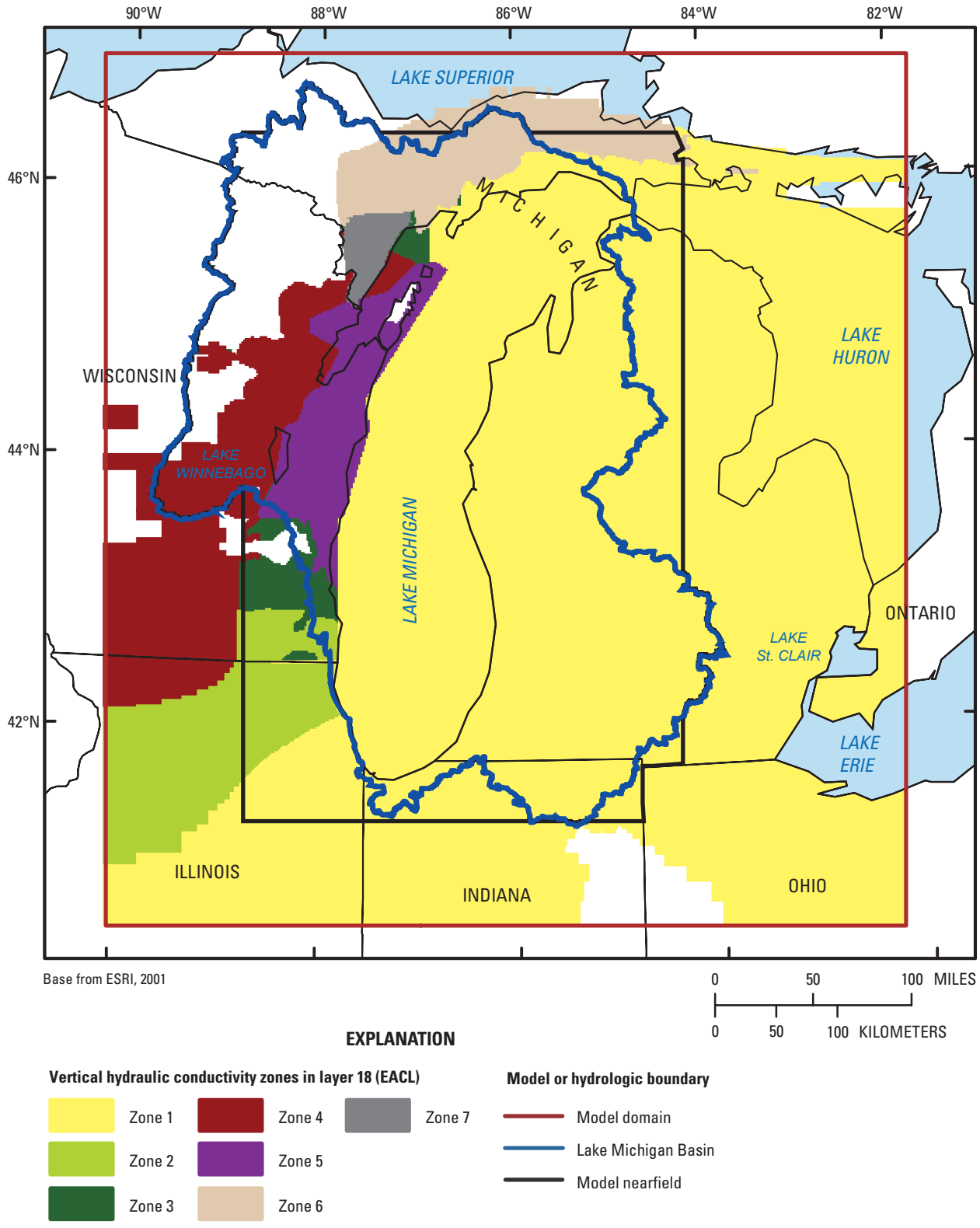

Figure 6*B*–9*A*. Vertical hydraulic conductivity, EACL: zonation.

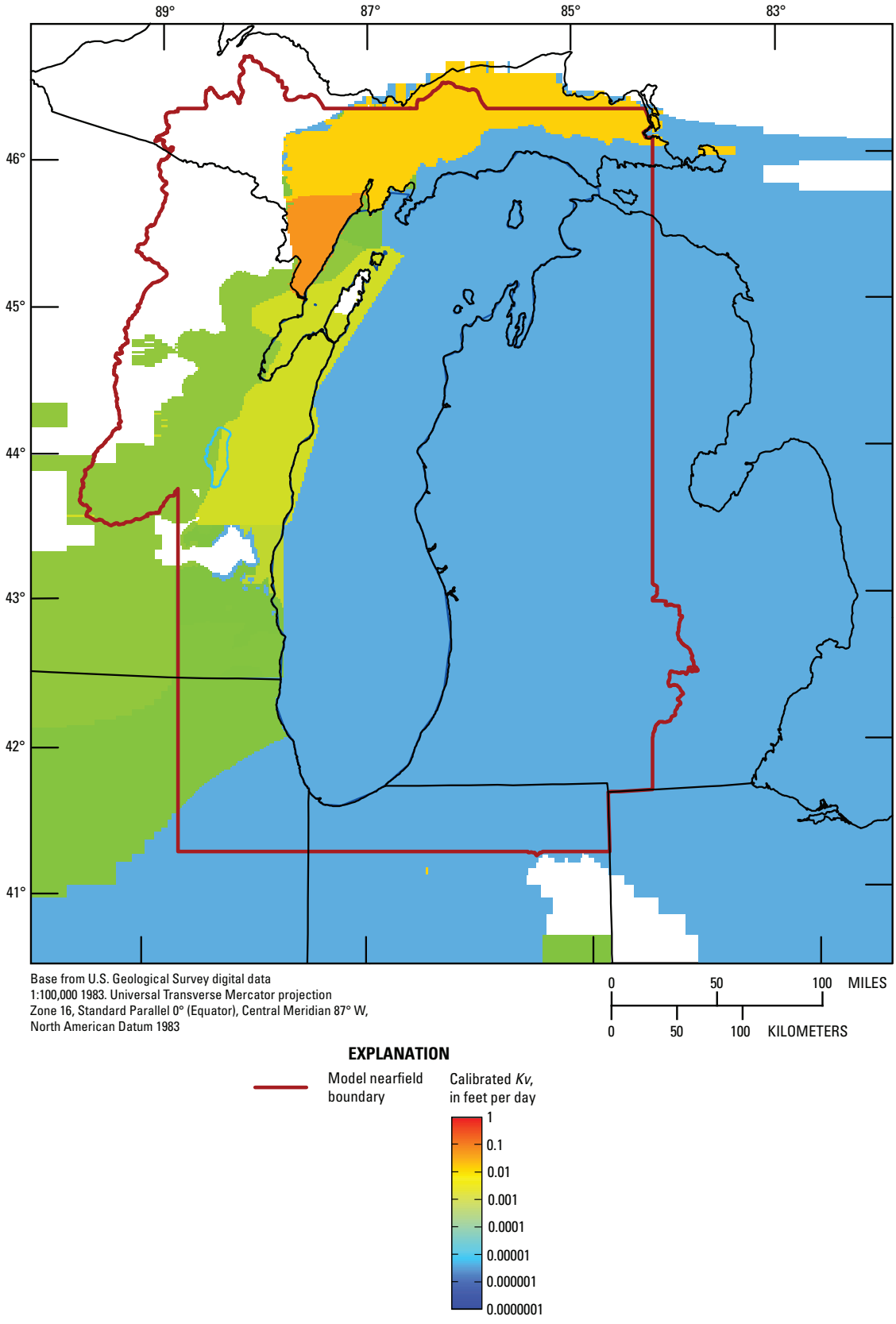

Figure 6*B*–9*B*. Vertical hydraulic conductivity, EACL: calibrated input.

Appendix 7. Base-Flow Calibration Targets

The groundwater component of streamflow, base flow, was estimated at 62 locations in the nearfield and farfield parts of the LMB model domain, which served as calibration targets. Model inputs were adjusted during the calibration process to improve the match between the base-flow estimates presented in this appendix and the base-flow values simulated by the model at the target locations.

7.1 Equations for Estimating Base Flow at Streamgage Locations

Base flow was estimated by using regression equations relating average annual base flow to drainage area and a base-flow factor, a term proportional to the 90 percent flow-duration value[1]. For streamgages in Wisconsin and the Upper Peninsula of Michigan, the statewide equation established by Gebert and others (2007) was used:

$$Q_b = 0.906A^{1.02}B_f^{0.52} \quad (1)$$

where

Q_b is average annual base flow (ft^3/s),

A is drainage area (square miles), and

B_f is the base-flow factor, defined as the 90 percent flow-duration value (Q_{90}, in cubic feet per second) divided by the drainage area (square miles).

For this statistically significant regression ($p < 0.001$), the average standard error of estimate was 12 percent, and the R^2 was 0.992. A total of 25 streamgages in Wisconsin and the Upper Peninsula of Michigan were chosen as base-flow targets; values of the base-flow factor were estimated for these streamgages by calculating the 90 percent flow-duration value (Q_{90}) based on daily discharges for each stress period, which were then used with equation 1 to estimate average annual base-flow targets for the selected gages.

For sites in Indiana, Illinois, and the Lower Peninsula of Michigan, a separate regression relation was established. Several automated base-flow-separation algorithms were used to determine average annual base flow for the period of record for selected streamgages in the Lake Michigan Basin (Neff and others, 2005). The base-flow-separation algorithms chosen did not include the method used by Gebert and others (2007). Consequently, average annual base flow using equation 1 was compared to results from Neff and others (2005) for streamgages in Wisconsin; results from the UK Institute of Hydrology method (Piggott and others, 2005) most closely match base flow computed by equation 1, so this method was used to represent average annual base flow. Streamgages in Indiana, Illinois, and the Lower Peninsula of Michigan with at least 27 years of record during the 1970–99 period were chosen, resulting in 46 gages available for the regression analysis. Q_{90} values were calculated from the daily discharges for the 46 selected sites for the 1970–99 period. Base-flow-factor values were computed for this period by using established drainage areas for the streamgages, and a multiple linear regression on log-transformed variables was used to establish the following regression equation:

$$Q_b = 1.06A^{0.986}B_f^{0.446} \quad (2)$$

The regression defined by equation 2 was statistically significant at the 5-percent level ($p < 0.001$), with an average standard error of estimate of 17 percent and an R^2 of 0.991.

A total of 37 streamgages in Indiana, Illinois, and the Lower Peninsula of Michigan were chosen as base-flow targets for the model; values of the base-flow factor were estimated for these selected gages by calculating the 90 percent flow-duration value (Q_{90}) using daily discharges for each stress period, which were then used with equation 2 to estimate average annual base-flow targets for the selected gages.

7.2 Data Sources

The source for the Q_{90} flows and basin drainage area at target locations was the U.S. Geological Survey NWISWeb database at (*http://waterdata.usgs.gov/nwis/dv/?referred_module=sw*, accessed June 2007). The geographical extent of the basin area upstream from each streamgage was mapped on the basis of GIS coverages derived from Horizon Systems Corporation (2006; accessed April 17, 2007) and from Neff and others (2005). The upstream areas were overlaid on the model grid to define the cells over which simulated base flow to RIV cells was accumulated in order to compare to base-flow targets estimated by means of the Gebert regression equations. These target estimates were compared to alternative estimates based on hydrograph-separation techniques performed by Neff and others (2005). That study applied multiple hydrograph-separation methods to daily average streamflow records for 3,936 streamgages in the Great Lakes Basin. The hydrograph-separation methods included the fixed-interval method (HYSEP1), sliding-interval method (HYSEP2), and local minimum method (HYSEP3) developed by Sloto and Crouse (1996); the PART method developed by Rutledge (1998); and the BFLOW method developed by Arnold and Allen (1999).

[1] The flow-duration curve is a plot that shows the percentage of time that flow in a stream is likely to equal or exceed some specified value. Accordingly, the 50-percent value (Q_{50}) defines the flow exceeded 50 percent of the time, the 75-percent value (Q_{75}) defines the flow exceeded 75 percent of the time, and the the 90-percent value (Q_{90}) defines the flow exceeded 90 percent of the time.

7.3 Tabulation of Base-Flow Targets

The following table lists the 62 streamgages where base flow was estimated (36 in the three subregions in Michigan, 17 in the two subregions in Wisconsin, 3 in the northern Indiana subregion, and 6 in the northeastern Illinois subregion). The gages are referenced to locations in figure 45*E* (in the main report text) and grouped by model subregion. Each target gage is accompanied by its upstream basin area, duration of record, the base-flow estimate used as the calibration target and based on the Gebert equations (identified in the table heading as **BF_Gebert**), base-flow estimates derived from five other methods that use hydrograph separation, and ratios of the Gebert results to the Q_{50}, Q_{75}, and Q_{90} values from the stream's flow-duration curve. Summary statistics for basin area, duration of record, and base-flow comparisons are listed at the bottom of the table.

Table 7–1. Base-flow calibration targets.

The criteria used to select gaged streams suitable as baseflow targets are the following:
• The stream has at least 10 years of discharge record.
• The drainage area of the stream is between 50 and 2,000 square miles.
• If one streamgage is nested within a larger streamgage, then the larger streamgage is used and the smaller nested gage is discarded.
• If a gaged location is known to be regulated by any type of control structure or dam, then the streamgage is not used to calculate base-flow targets.
Base-flow unit is cubic feet per second (ft^3/s).
The base-flow estimates listed under the heading "BF_Gebert" and printed in blue correspond to the base-flow targets used in model calibration.

Subregion	Number	Gage name	Gage_ID	Area (mi^2)	Begin date	End date	Yr_record	BF_ Gebert (ft^3/s)	BF_ HYSEP1 (ft^3/s)
SLP_MI (17)									
	1	St. Joseph River at Burlington, Mich.	4096405	206	10/1/1962	9/30/2001	39	**104.12**	158.5
	2	Coldwater River near Hodunk, Mich.	4096600	293	10/1/1962	9/30/1989	27	**125.87**	210.3
	3	Nottawa Creek nNear Athens, Mich.	4096900	162	10/1/1966	9/30/1997	31	**102.64**	131.5
	4	Prairie River near Nottawa, Mich.	4097540	106	10/1/1962	9/30/2001	39	**65.13**	88.5
	5	Fawn River near White Pigeon, Mich.	4098500	192	10/1/1957	9/30/1975	18	**118.99**	147.1
	6	Paw Paw River at Riverside, Mich.	4102500	390	10/1/1951	9/30/2001	50	**301.17**	398.2
	7	South Branch Black River near Bangor, Mich.	4102700	83.6	6/1/1966	9/30/2001	35	**55.55**	79.33
	8	Kalamazoo River near Battle Creek, Mich.	4105500	824	7/27/1937	9/30/2001	64	**505.90**	563.2
	9	Rabbit River near Hopkins, Mich.	4108600	71.4	10/1/1965	9/30/2001	36	**39.74**	44.31
	10	Red Cedar River at East Lansing, Mich.	4112500	355	8/31/1902	9/30/2001	71	**115.31**	140.8
	11	Looking Glass River at Hinman Rd near Eagle, Mich.	4114500	281	8/1/1944	9/30/1996	52	**105.79**	148.4
	12	Maple River at Maple Rapids, Mich.	4115000	434	8/1/1944	9/30/2001	57	**115.46**	199.1
	13	Flat River at Smyrna, Mich.	4116500	528	10/1/1950	9/30/1986	36	**331.88**	360.9
	14	Thornapple River near Caledonia, Mich.	4118000	773	10/1/1951	9/30/1994	41	**429.71**	512.7
	15	White River near Whitehall, Mich.	4122200	406	8/1/1957	9/30/2001	44	**320.33**	390.2
	16	Chippewa River near Midland, Mich.	4154500	597	10/1/1947	12/31/1972	25	**309.64**	316.2
	17	Pine River near Midland, Mich.	4155500	390	5/31/1934	9/30/2001	54	**191.28**	219.8

Number	BF_ HYSEP3 (ft^3/s)	BF_ PART (ft^3/s)	BF_ BFLOW (ft^3/s)	BF_ median (ft^3/s)	BF_ mean (ft^3/s)	Q_{90} (ft^3/s)	Q_{75} (ft^3/s)	Q_{50} (ft^3/s)	Ratios		
									Gebert: BF_BFLOW	Gebert: Q_{50}	Gebert: Q_{75}
1	143.4	161	119	158.5	148.1	46.27	80.72	144.85	0.87	0.72	1.29
2	186.3	226.3	155.5	209.4	197.56	46.22	87.72	181.16	0.81	0.69	1.43
3	117.4	136.1	102.3	131.5	123.82	59.94	83.74	123.81	1.00	0.83	1.23
4	80.78	91.49	70.88	88.5	84.04	36.13	52.68	84.64	0.92	0.77	1.24
5	140.3	147.5	121.6	147.1	140.74	67.97	98.86	141.14	0.98	0.84	1.20
6	367.3	411	342.2	398.2	383.48	231.19	291.15	401.62	0.88	0.75	1.03
7	72.02	83.93	60.02	79.24	74.91	33.71	43.43	73.17	0.93	0.76	1.28
8	516.2	574.1	465.6	563.2	536.5	299.02	398.04	556.21	1.09	0.91	1.27
9	41.56	46.66	34.83	44.31	42.36	19.26	27.13	42.79	1.14	0.93	1.46
10	119.5	155.3	98.68	140.6	130.98	30.1	50.13	106.85	1.17	1.08	2.30
11	131.9	158.8	101.7	147.3	137.62	32.93	48.2	100.67	1.04	1.05	2.19
12	146.8	220.5	126.3	199.1	178.38	23.67	44.15	121.62	0.91	0.95	2.62
13	333.7	366.1	295.9	360.9	343.72	199.17	253.8	355.44	1.12	0.93	1.31
14	437.9	534.8	393	512.5	478.18	224.05	306.47	459.63	1.09	0.93	1.40
15	379.1	406.7	350.9	390.1	383.4	252.87	305.59	393.33	0.91	0.81	1.05
16	286.4	330.2	242.2	311.5	297.3	146.92	191.44	275.21	1.28	1.13	1.62
17	195.4	230.6	161.3	219.8	205.64	83.55	124.93	204.16	1.19	0.94	1.53

Table 7–1. Base-flow calibration targets.—Continued

The criteria used to select gaged streams suitable as baseflow targets are the following:
• The stream has at least 10 years of discharge record.
• The drainage area of the stream is between 50 and 2,000 square miles.
• If one streamgage is nested within a larger streamgage, then the larger streamgage is used and the smaller nested gage is discarded.
• If a gaged location is known to be regulated by any type of control structure or dam, then the streamgage is not used to calculate base-flow targets.
Base-flow unit is cubic feet per second (ft^3/s).
The base-flow estimates listed under the heading "BF_Gebert" and printed in blue correspond to the base-flow targets used in model calibration.

Subregion	Number	Gage name	Gage_ID	Area (mi^2)	Begin date	End date	Yr_record	BF_ Gebert (ft^3/s)	BF_ HYSEP1 (ft^3/s)
NLP_MI (11)									
	18	Muskegon River near Merritt, Mich.	4121000	355	10/1/1946	12/31/1973	27	**171.41**	205.1
	19	Pere Marquette River at Scottville, Mich.	4122500	681	8/1/1939	9/30/2001	62	**535.56**	638.9
	20	Big Sable River near Freesoil, Mich.	4123000	115	6/1/1942	12/31/1973	31	**106.80**	131.1
	21	Little Manistee River near Freesoil, Mich.	4126200	178	10/1/1956	9/30/1975	19	**152.66**	164.1
	22	Platte River at Honor, Mich.	4126740	118	3/27/1990	9/30/2001	11	**108.15**	119.6
	23	Boardman River near Mayfield, Mich.	4127000	182	10/1/1952	9/30/1989	37	**159.62**	174.3
	24	Cheboygan River near Cheboygan, Mich.	4130000	889	10/1/1942	9/30/1982	40	**649.27**	725.9
	25	Black River near Cheboygan, Mich.	4132000	558	12/1/1942	9/30/2001	31	**281.85**	332.9
	26	Au Sable River near Red Oak, Mich.	4136000	1108	10/1/1908	9/30/2001	12	**799.05**	761.2
	27	Tobacco River at Beaverton, Mich.	4152500	487	7/1/1948	9/30/1982	34	**289.23**	258.3
	28	Salt River near North Bradley, Mich.	4153500	138	6/1/1934	9/30/1971	37	**36.07**	40.73
UP_MI (8)									
	29	Manistique River near Blaney, Mich.	4055000	704	4/1/1938	9/30/1970	32	**494.86**	731.2
	30	W Br Manistique River near Manistique, Mich.	4056000	322	4/1/1938	9/30/1956	18	**220.09**	348.3
	31	Indian River near Manistique, Mich.	4057000	302	4/1/1938	9/30/1993	34	**256.46**	357.8
	32	Sturgeon River near Nahma Junction, Mich.	4057510	183	10/1/1966	9/30/2001	35	**113.73**	158.9
	33	Escanaba River at Cornell, Mich.	4059000	870	9/1/1903	9/30/2001	51	**488.70**	605.3
	34	Ford River near Hyde, Mich.	4059500	450	10/1/1954	9/30/2001	47	**170.51**	267.4
	35	Sturgeon River near Foster City, Mich.	4065500	237	10/1/1954	9/30/1980	26	**109.51**	149.1
	36	Pine River near Rudyard, Mich.	4127918	184	4/1/1972	9/30/2001	29	**116.41**	167.4

Number	BF_ HYSEP3 (ft^3/s)	BF_ PART (ft^3/s)	BF_ BFLOW (ft^3/s)	BF_ median (ft^3/s)	BF_ mean (ft^3/s)	Q_{90} (ft^3/s)	Q_{75} (ft^3/s)	Q_{50} (ft^3/s)	Ratios		
									Gebert: BF_BFLOW	Gebert: Q_{50}	Gebert: Q_{75}
18	193.2	211.6	167.4	204.4	196.34	73.21	122.79	186	1.02	0.92	1.40
19	618.3	652.8	576.3	638.8	625.02	427.95	502.47	633.73	0.93	0.85	1.07
20	127.7	133.3	118.5	131	128.32	99.22	110.59	129.28	0.90	0.83	0.97
21	160.4	165	149.8	164.1	160.68	130.26	143	162.38	1.02	0.94	1.07
22	119.2	120.5	115.5	119.6	118.88	98.92	109.04	125.03	0.94	0.86	0.99
23	170.4	172.8	154	172.8	169.18	140.12	156.36	180.92	1.04	0.88	1.02
24	706.1	688.5	617.4	706.1	692.64	477.23	622.95	804.97	1.05	0.81	1.04
25	281.7	314.7	229.9	314.7	298.48	129.14	233.75	380.12	1.23	0.74	1.21
26	756.2	786	707	761.2	754.44	582.19	660.48	755.3	1.13	1.06	1.21
27	242.3	255.9	205.7	255.9	243.9	161.35	200.2	259.92	1.41	1.11	1.44
28	34.79	39.36	23.89	39.36	35.89	6.98	11.03	21.4	1.51	1.69	3.27
29	661.9	759.3	579	731.1	692.5	344.32	463.04	624.82	0.85	0.79	1.07
30	298.6	368.4	259.4	348.3	324.74	144.32	189.19	268.92	0.85	0.82	1.16
31	337.3	362.5	300	357.4	343	219.76	279.55	348.89	0.85	0.74	0.92
32	141.7	164.7	113.1	158.9	147.56	65.1	85.61	126.69	1.01	0.90	1.33
33	524.7	611.5	434.7	605.3	556.34	259.09	339.61	507.48	1.12	0.96	1.44
34	206	287.2	170.9	267.4	240.02	54.3	91.06	176.28	1.00	0.97	1.87
35	121.7	150.2	96.5	149.1	133.4	43.73	65.98	106.29	1.13	1.03	1.66
36	151.7	169.1	116	167.4	154.46	68.13	84.43	124.85	1.00	0.93	1.38

Table 7–1. Base-flow calibration targets.—Continued

The criteria used to select gaged streams suitable as baseflow targets are the following:
• The stream has at least 10 years of discharge record.
• The drainage area of the stream is between 50 and 2,000 square miles.
• If one streamgage is nested within a larger streamgage, then the larger streamgage is used and the smaller nested gage is discarded.
• If a gaged location is known to be regulated by any type of control structure or dam, then the streamgage is not used to calculate base-flow targets.
Base-flow unit is cubic feet per second (ft^3/s).
The base-flow estimates listed under the heading "BF_Gebert" and printed in blue correspond to the base-flow targets used in model calibration.

Subregion	Number	Gage name	Gage_ID	Area (mi^2)	Begin date	End date	Yr_record	BF_ Gebert (ft^3/s)	BF_ HYSEP1 (ft^3/s)
NE_WI (13)									
	37	Brule River near Florence, Wis.	4061000	389	2/1/1914	9/7/1994	50	**285.45**	301.1
	38	Pike River at Amberg, Wis.	4066500	255	2/26/1914	9/30/2001	57	**158.10**	176.2
	39	Peshtigo River at Peshtigo, Wis.	4069500	1080	6/1/1953	9/30/2001	48	**625.94**	636.4
	40	Pensaukee River near Pensaukee, Wis.	4071858	134	10/1/1972	9/30/1996	24	**27.03**	54.99
	41	Duck Creek near Howard, Wis.	4072150	108	5/1/1988	9/30/2001	13	**3.98**	23.6
	42	Wolf River near Shawano, Wis.	4077400	816	10/1/1985	6/30/2001	89	**594.75**	664.2
	43	Embarrass River near Embarrass, Wis.	4078500	384	6/1/1919	9/30/2001	73	**188.85**	212.8
	44	Little Wolf River at Royalton, Wis.	4080000	507	1/1/1914	9/30/1985	59	**278.69**	302.1
	45	Waupaca River near Waupaca, Wis.	4081000	265	6/28/1916	9/30/1985	51	**200.65**	201.2
	46	Kewaunee River near Kewaunee, Wis.	4085200	127	9/1/1964	9/30/2001	32	**38.16**	48.78
	47	East Twin River at Mishicot, Wis.	4085281	110	7/25/1972	9/30/1996	24	**33.68**	51.15
	48	Manitowoc River at Manitowoc, Wis.	4085427	526	7/26/1972	9/30/2001	27	**121.82**	245.4
	49	Sheboygan River at Sheboygan, Wis.	4086000	418	6/30/1916	9/30/2001	59	**122.35**	172.8
SE_WI (4)									
	50	Menomonee River at Wauwatosa, Wis.	4087120	123	10/1/1961	9/30/2001	40	**39.66**	53.88
	51	Root River at Racine, Wis.	4087240	190	8/22/1963	9/30/2001	38	**40.00**	88.28
	52	Rock River at Watertown, Wis.	5425500	969	6/1/1931	9/30/2001	64	**189.85**	423.4
	53	Bark River near Rome, Wis.	5426250	122	10/18/1979	9/30/2001	20	**62.29**	79.28

Number	BF_ HYSEP3 (ft^3/s)	BF_ PART (ft^3/s)	BF_ BFLOW (ft^3/s)	BF_ median (ft^3/s)	BF_ mean (ft^3/s)	Q_{90} (ft^3/s)	Q_{75} (ft^3/s)	Q_{50} (ft^3/s)	Ratios		
									Gebert: BF_BFLOW	Gebert: Q_{50}	Gebert: Q_{75}
37	293.2	312.6	267.5	301.1	295.18	205.65	240.06	295.72	1.07	0.97	1.19
38	168.2	187.7	147.3	175.9	171.06	99.86	121.28	163.73	1.07	0.97	1.30
39	585.5	642.3	505.5	636.3	601.2	351.94	463.92	671.13	1.24	0.93	1.35
40	46.07	52.02	29.94	52.02	47.55	6.31	13.55	31.8	0.90	0.85	1.99
41	17.89	22.32	11.36	22.32	19.77	0.2	2.03	6.86	0.35	0.58	1.96
42	640.4	679.3	567.8	664.2	643.26	416.23	498.79	641.19	1.05	0.93	1.19
43	194.9	224.6	163.1	212.2	201.52	95.15	129.51	194.2	1.16	0.97	1.46
44	281.3	310.1	240.7	302.1	287.34	153.71	196.41	280.73	1.16	0.99	1.42
45	197.1	207.5	180.3	201	197.42	151.75	178.81	215.08	1.11	0.93	1.12
46	43.27	46.93	31.57	46.93	43.79	12.82	18.03	31.36	1.21	1.22	2.12
47	45.22	51.32	32.42	51.15	46.36	11.57	17.64	33.42	1.04	1.01	1.91
48	197.1	259	150.8	245.4	219.64	30.6	49.33	120.33	0.81	1.01	2.47
49	148.2	185.8	114.3	172.8	158.86	38.35	62.33	119.41	1.07	1.02	1.96
50	48.29	53.64	34.95	53.64	48.95	14.22	23.71	45.19	1.13	0.88	1.67
51	69.24	80.35	47.81	80.35	74.94	9.58	21.25	56.09	0.84	0.71	1.88
52	342.7	416.3	272.5	416.3	375.44	40.02	94.42	269.85	0.70	0.70	2.01
53	73.49	80.09	58.32	79.22	74.08	33.92	51.64	76.87	1.07	0.81	1.21

Table 7–1. Base-flow calibration targets.—Continued

The criteria used to select gaged streams suitable as baseflow targets are the following:
• The stream has at least 10 years of discharge record.
• The drainage area of the stream is between 50 and 2,000 square miles.
• If one streamgage is nested within a larger streamgage, then the larger streamgage is used and the smaller nested gage is discarded.
• If a gaged location is known to be regulated by any type of control structure or dam, then the streamgage is not used to calculate base-flow targets.
Base-flow unit is cubic feet per second (ft^3/s).
The base-flow estimates listed under the heading "BF_Gebert" and printed in blue correspond to the base-flow targets used in model calibration.

Subregion	Number	Gage name	Gage_ID	Area (mi^2)	Begin date	End date	Yr_record	BF_ Gebert (ft^3/s)	BF_ HYSEP1 (ft^3/s)
N_IND (3)									
	54	Pigeon River near Scott, Ind.	4099750	361	6/1/1968	9/30/2001	33	**236.55**	315.9
	55	Kankakee River at Davis, Ind.	5515500	537	10/1/1925	9/30/2001	73	**389.28**	466
	56	Yellow River at Plymouth, Ind.	5516500	294	10/1/1948	9/30/2001	53	**117.72**	155.8
NE_ILL (6)									
	57	Coon Creek at Riley, Ill.	5438250	85.1	8/1/1961	10/20/1982	21	**23.11**	41
	58	Des Plaines River at Lemont, Ill.	5533500	684	11/4/1914	9/30/1944	29	**91.95**	264.3
	59	Little Calumet River at Harvey, Ill.	5536325	252	10/1/1916	9/30/1933	17	**80.47**	187.4
	60	Hickory Creek at Joliet, Ill.	5539000	107	10/1/1944	9/30/2001	57	**26.67**	41.9
	61	Du Page River at Shorewood, Ill.	5540500	324	10/1/1940	9/30/2001	61	**120.67**	179.8
	62	Fox River at South Elgin, Ill.	5551000	1556	10/1/1989	9/30/1998	11	**801.41**	1023

Total = 62

Statistic	Area (mi^2)	Statistic	Years
Ave_Area	401	Ave_Record	40
Median	323	Median	36.5
Min	71	Min	11
Max	1556	Max	89
Standard deviation	305	Standard deviation	17

Number	BF_ HYSEP3 (ft^3/s)	BF_ PART (ft^3/s)	BF_ BFLOW (ft^3/s)	BF_ median (ft^3/s)	BF_ mean (ft^3/s)	Q_{90} (ft^3/s)	Q_{75} (ft^3/s)	Q_{50} (ft^3/s)	Ratios		
									Gebert: BF_BFLOW	Gebert: Q_{50}	Gebert: Q_{75}
54	286	331.4	252.9	315.9	300.48	147.72	193.15	293.98	0.94	0.80	1.22
55	446.8	484.2	409.1	465.8	454.38	279.04	344.42	453.22	0.95	0.86	1.13
56	135.6	165.1	112.1	155.8	144.96	39.61	64.02	132.82	1.05	0.89	1.84
57	37.14	44.22	27.64	41	38.23	7.19	14.78	30.83	0.84	0.75	1.56
58	198.2	282.6	151.8	262.3	231.84	13.95	39.13	162.19	0.61	0.57	2.35
59	173.9	204.2	130.4	186.4	176.46	27.83	63.38	115.77	0.62	0.70	1.27
60	35.62	42	25.82	41.9	37.45	7.61	13.41	30.34	1.03	0.88	1.99
61	165.1	200	139.5	179.7	172.82	47.54	92.24	173.82	0.87	0.69	1.31
62	901.1	1069	758.7	1,008	951.96	399.18	579.15	962.45	1.06	0.83	1.38

Statistic	Gebert: BF_BFLOW	Gebert: Q_{50}	Gebert: Q_{75}
Ave_Ratio	1.00	0.89	1.50
Median	1.03	0.88	1.36
Min	0.35	0.57	0.92
Max	1.51	1.69	3.27
Standard deviation	0.18	0.16	0.47

References

Arnold, J.G., and Allen, P.M., 1999, Automated methods for estimating baseflow and ground water recharge from streamflow records: Journal of the American Water Resources Association, v. 35, no. 2, p. 411–424.

Gebert, W.A., Radloff, M.J., Considine, E.J., and Kennedy, J.L., 2007, Use of streamflow data to estimate base flow/ground-water recharge for Wisconsin: Journal of the American Water Resources Association, v. 43, no. 1, p. 220–236. (Also available at *http://www3.interscience.wiley.com/cgi-bin/fulltext/118544614/PDFSTART*).

Horizon Systems Corporation, 2006, National Hydrography Dataset Plus, accessed April 17, 2007, at *http://www.horizon-systems.com/nhdplus/data.php.*

Neff, B.P., Day, S.M., Piggott, A.R., and Fuller, L.M., 2005, Base flow in the Great Lakes Basin: U.S. Geological Survey Scientific Investigations Report 2005–5217, 23 p.

Piggott, A.R., Moin, S., and Southam, C., 2005, A revised approach to the UKIH method for the calculation of base flow: Hydrological Sciences Journal, v. 50, no. 5, p. 911–920.

Rutledge, A.T., 1998, Computer programs for describing the recession of ground-water discharge and for estimating mean ground-water recharge and discharge from streamflow data—Update: U.S. Geological Survey Water-Resources Investigations Report 98–4148, 43 p.

Sloto, R.A., and Crouse, M.Y., 1996, HYSEP—A computer program for streamflow hydrograph separation and analysis: U.S. Geological Survey Water-Resources Investigations Report 96–4040, 46 p.

U.S. Geological Survey, National Water Information System (NWIS), accessed June 2007 at *http://waterdata.usgs.gov/nwis/.*

Appendix 8. Comparison of Measured and Simulated Values at Calibration Targets

This appendix contains 22 scatterplots that illustrate the match between target values (measured or estimated) and the corresponding model-simulated values. Target locations are shown in figure 45 in the main report text. Calibration statistics derived from the plotted values are presented in table 12 in the main report text. The scatterplots show calibration results for the following target sets:

Predevelopment water levels (pre-1940, stress periods 1–4)

1. USGS network water levels
2. Driller-log water levels
3. Wisconsin Cambrian-Ordovician head contours, prepumping
4. Michigan Pennsylvanian head contours, prepumping
5. Michigan Marshall head contours, prepumping
6. Indiana miscellaneous water levels

Northeastern Illinois

7. Predevelopment Illinois Cambrian-Ordovician head contours
8. 2000 Illinois Cambrian-Ordovician head contours
9. 1864–2000 Illinois Cambrian-Ordovician drawdown contours

Base flow

10. Base flow

Vertical head gradient

11. USGS network wells
12. USGS RASA packer tests

Postdevelopment water levels (post-1940, stress periods 5–13)

13. Southern Lower Peninsula, Mich., network water levels
14. Northern Lower Peninsula, Mich., network water levels
15. Upper Peninsula, Mich., network water levels
16. Northeastern Wisconsin network water levels
17. Southeastern Wisconsin network water levels
18. Northern Indiana network water levels
19. Farfield network water levels

Head-change set

20. Decadal head changes in USGS network wells
21. 1980–2000 recovery in Illinois Cambrian-Ordovician head contours

Unweighted postdevelopment household well targets (not included in calibration)

22. Water levels from nearfield driller logs for all time periods

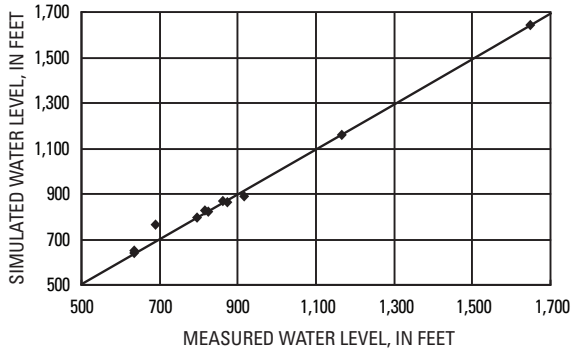

Figure 8–1. Predevelopment (pre-1940) water levels from USGS network wells.

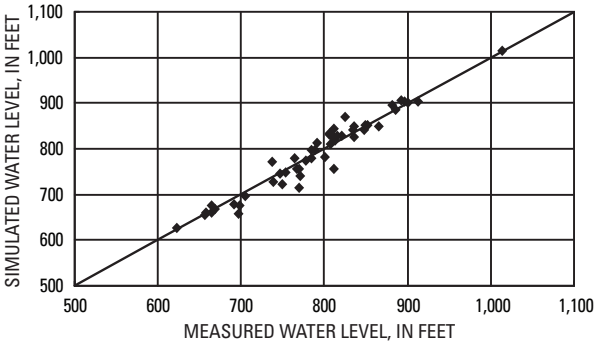

Figure 8–2. Predevelopment (pre-1940) water levels from driller logs.

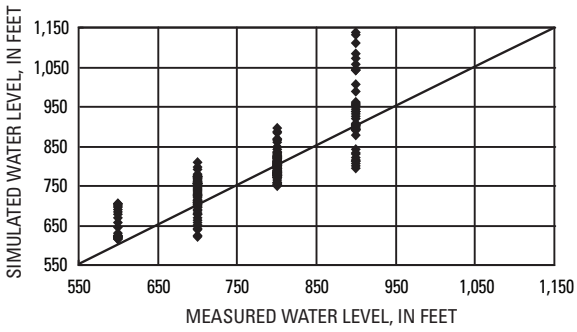

Figure 8–3. Predevelopment conditions for C-O aquifer system in Wisconsin from published map with contours.

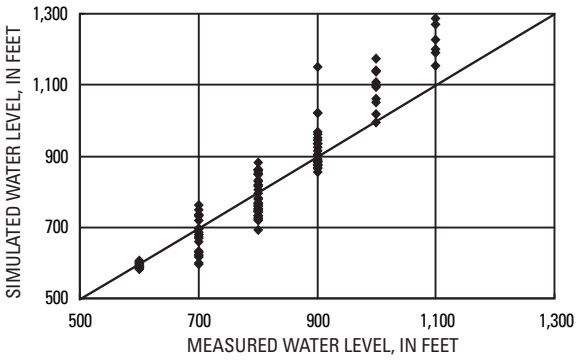

Figure 8–4. Predevelopment conditions for PENN aquifer system from published map with contours.

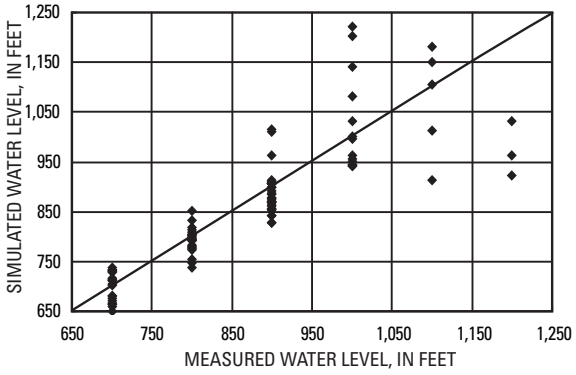

Figure 8–5. Predevelopment conditions for MSHL aquifer system from published map with contours.

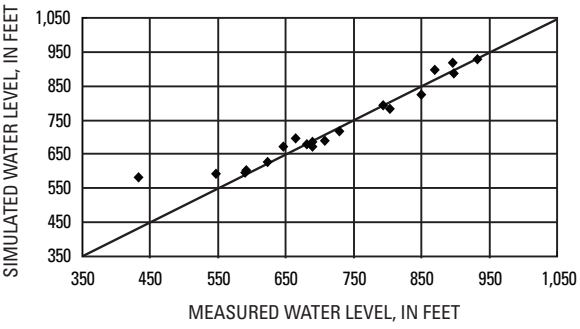

Figure 8–6. Predevelopment (pre-1940) water levels for Indiana from network wells and driller logs.

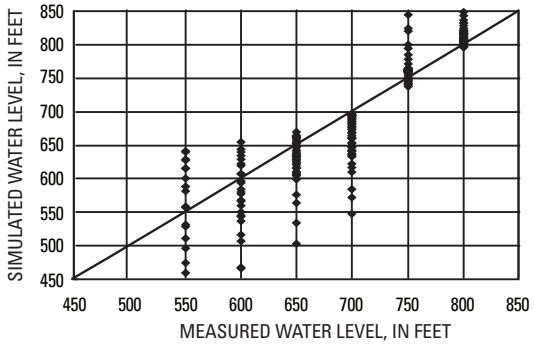

Figure 8–7. Predevelopment conditions for C-O aquifer system in northeastern Illinois from published map with contours.

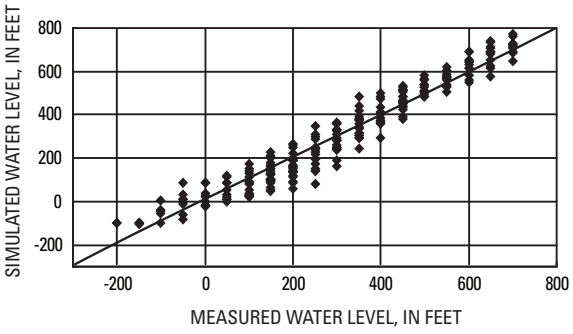

Figure 8–8. 2000 conditions for C-O aquifer system in northeastern Illinois from published map with contours.

Figures 8–1 through 8–8. Relation between measured and simulated values for 22 calibration-target groups. (The diagonal (1:1) line indicates perfect agreement between measured and simulated values.)

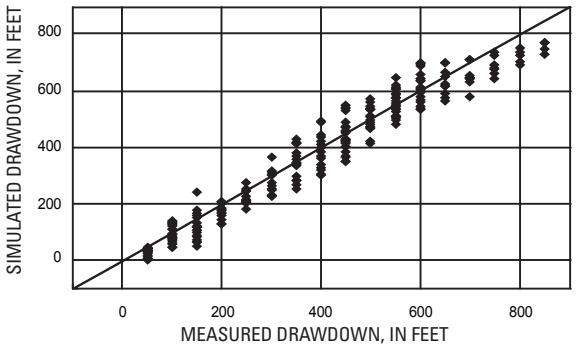

Figure 8–9. Drawdown and drawup calibration targets for C-O aquifer system for water-level changes between 1864 and 2000 based on published contour maps for northeastern Illinois.

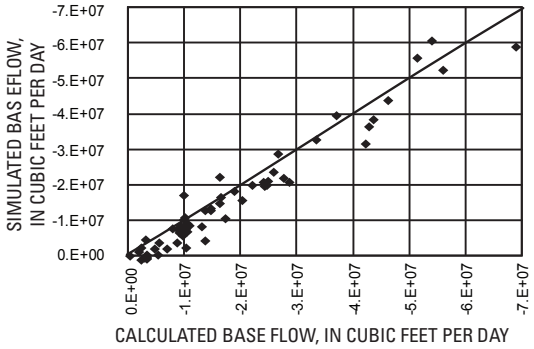

Figure 8–10. Base-flow calibration targets for 1990–2005 conditions at USGS streamgages (see appendix 7).

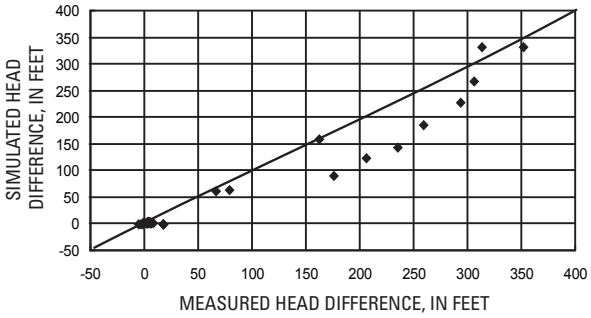

Figure 8–11. Vertical-head-difference calibration targets from pairs of network wells.

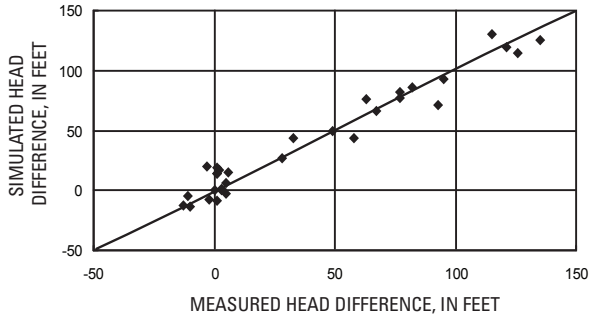

Figure 8–12. Vertical-head-difference calibration targets from pairs of packed intervals in RASA wells.

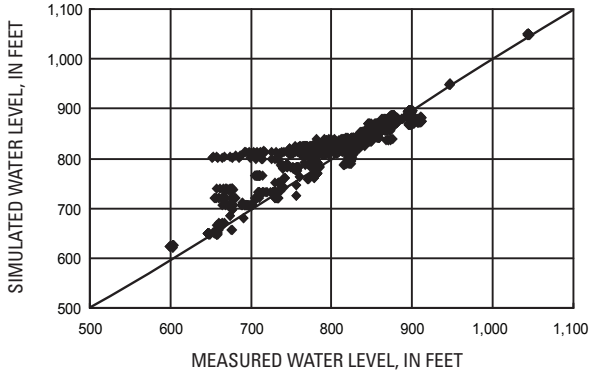

Figure 8–13. Post-1940 water levels in the Southern Lower Peninsula, Michigan, from network wells.

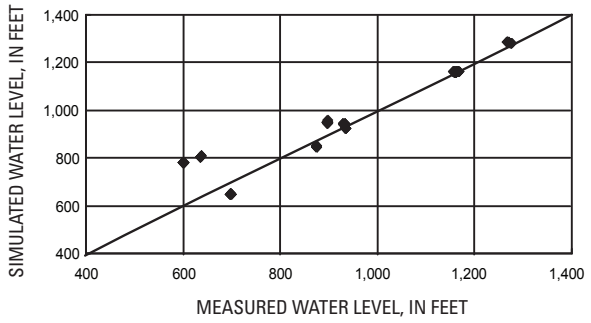

Figure 8–14. Post-1940 water levels in the Northern Lower Peninsula, Michigan, from network wells.

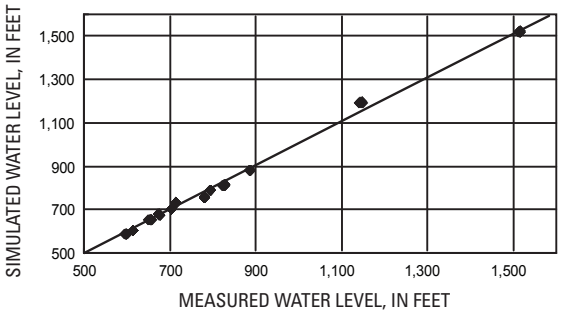

Figure 8–15. Post-1940 water levels in the Upper Peninsula, Michigan, from network wells.

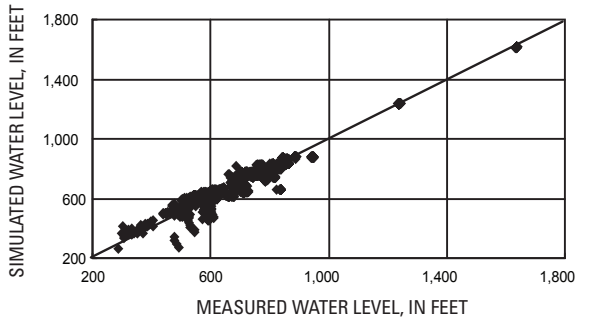

Figure 8–16. Post-1940 water levels for Northeastern Wisconsin from network wells.

Figures 8–9 through 8–16. Relation between measured and simulated values for 22 calibration-target groups. (The diagonal (1:1) line indicates perfect agreement between measured and simulated values.)

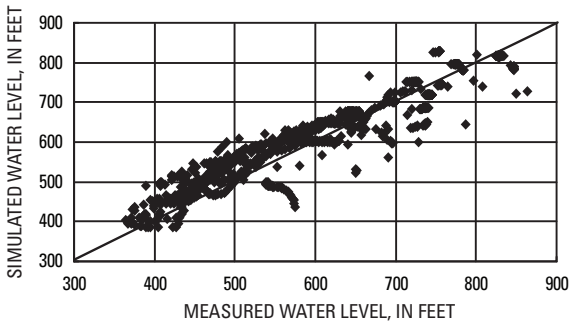

Figure 8–17. Post-1940 water levels in Southeastern Wisconsin from network wells.

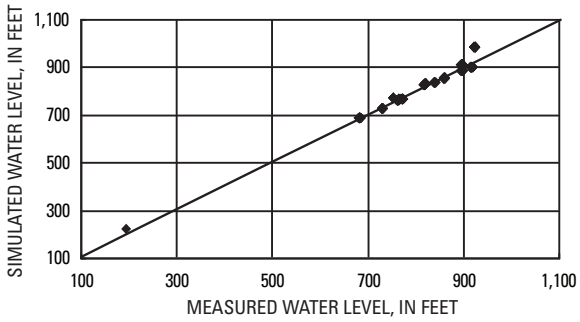

Figure 8–18. Post-1940 water levels in Northern Indiana from network wells.

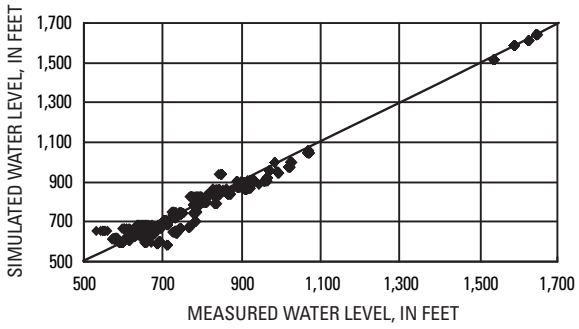

Figure 8–19. Post-1940 water levels in model FARFIELD from network wells.

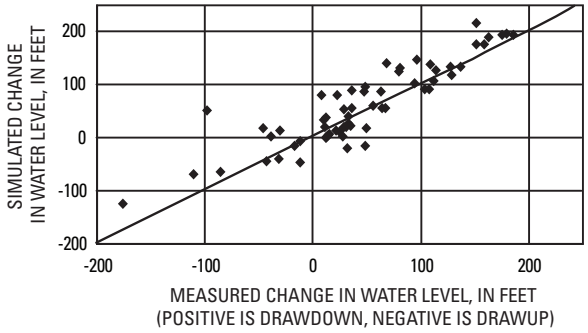

Figure 8–20. Drawdown and drawup calibration targets from USGS network wells.

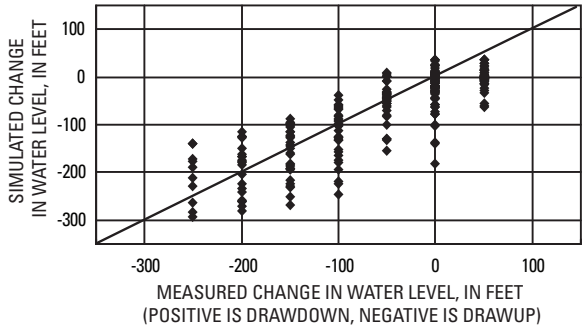

Figure 8–21. Drawdown and drawup calibration targets for C-O aquifer system for water-level changes between 1980 and 2000 based on published contour maps for northeastern Illinois.

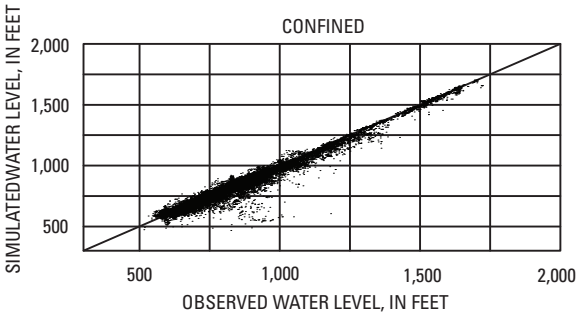

Figure 8–22. Post-1940 water levels from driller logs (not used in PEST inversion).

Figures 8–17 through 8–22. Relation between measured and simulated values for 22 calibration-target groups. (The diagonal (1:1) line indicates perfect agreement between measured and simulated values.)

Appendix 9. Geometric Means of Hydraulic-Conductivity Values, by Aquifer System, for Initial and Calibrated Models

The tables in this appendix show the arithmetic mean and geometric mean of K_h=*TRAN/THK* (as well as the range of K_h values) across active cells in *subregions*, by *aquifer*, where K_h is horizontal hydraulic conductivity (feet per day), *TRAN* is transmissivity (feet squared per day), and *THK* is thickness (feet).

To calculate the K_h across the vertical stack of cells within an aquifer system, the transmissivity for each layer belonging to the aquifer system is calculated as K_h multiplied by the thickness of the layer, the values are summed, and then the total is divided by the summed thickness of the layers. The set of aquifer-system K_h values from the cells in the subregion are then averaged by calculating the geometric mean across cells.

Aquifer or aquifer/confining unit	Aquifer system	Top layer	Bottom layer
Quaternary	QRNR	1	1
Grand River/Saginaw/Parma/Bayport	PENN	5	6
Marshall	MSHL	8	8
Silurian-Devonian	SLDV	10	12
Cambrian-Ordovician	C-O	14	20

(Confining units in layers 4, 7, 9, and 13 are excluded.)

For the initial version of the model (STF2sCFX) and for the confined version of the model (SLMB-C), *THK* is the stratigraphic thickness of cells because that is what is used in the model calculations. For the unconfined version of the model (SLMB-U), *THK* refers to the saturated thickness, which is equal either to the stratigraphic thickness of confined cells or to the *predevelopment* saturated thickness in cases where the water table is in the cell. For all models, only cells with *stratigraphic* thickness (for confined) or *saturated* thickness (for unconfined) greater than 1 foot are considered. No-flow cells are excluded for all models, and dry cells are excluded for the unconfined model. Because the analysis is limited to the nearfield and because almost all the nearfield cells are uniform in dimension, no area-weighted correction is applied to the calculation of the statistics.

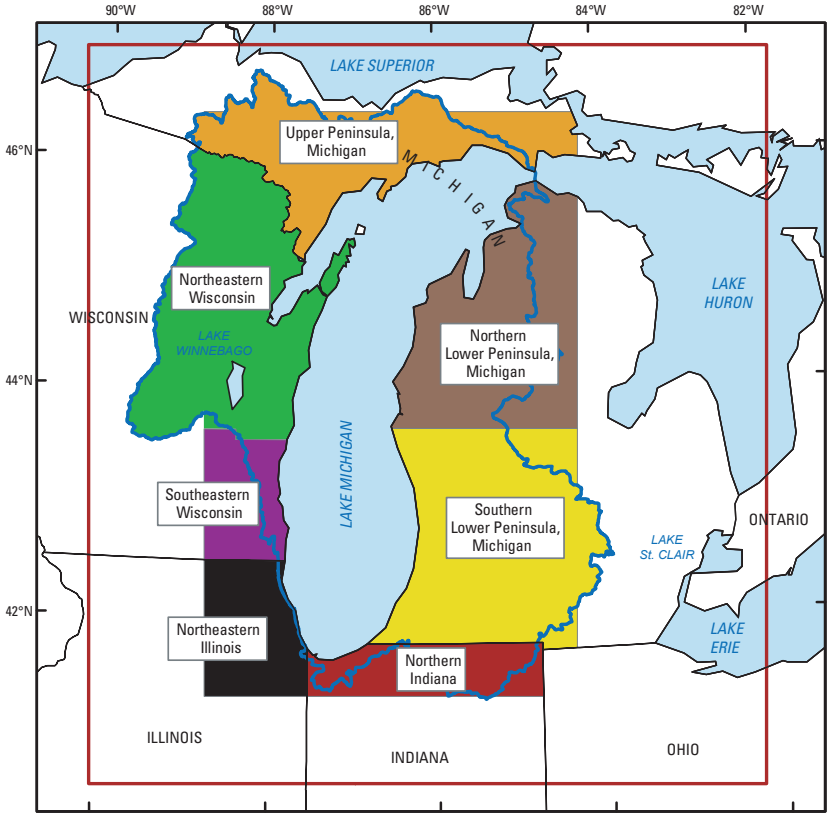

SUBREGIONS	
Southern Lower Peninsula, Michigan	(SLP_MI)
Northern Lower Peninsula, Michigan	(NLP_MI)
Upper Peninsula, Michigan	(UP_MI)
Northeastern Wisconsin	(NE_WI)
Southeastern Wisconsin	(SE_WI)
Northern Indiana	(N_IND)
Northeastern Illinois	(NE_ILL)

Table 9–1. Quaternary aquifer layers.

Subregion	Minimum layer	Maximum layer	Number of cells	Geometric mean Kh	Minimum Kh	Maximum Kh	Average thickness
Initial confined (STF2sCFX)							
SLP_MI	1	3	15,357	7.064	0.00001	205.07	223
NLP_MI	1	3	13,388	7.262	0.00001	254.52	456
UP_MI	1	3	7,424	7.572	0.00001	251.67	61
NE_WI	1	3	10,855	5.712	0.00001	275.87	79
SE_WI	1	3	4,019	4.105	0.00001	120.96	127
N_IND	1	3	4,737	21.009	0.18290	270.46	230
NE_ILL	1	3	5,062	2.473	0.00001	100.00	120
Calibrated confined (SLMB-C)							
SLP_MI	1	3	15,357	12.410	0.00002	396.12	223
NLP_MI	1	3	13,388	9.982	0.00002	520.41	456
UP_MI	1	3	7,424	16.901	0.00002	514.57	61
NE_WI	1	3	10,855	14.132	0.00003	564.05	79
SE_WI	1	3	4,019	11.146	0.00003	247.33	127
N_IND	1	3	4,737	34.112	0.18290	553.00	230
NE_ILL	1	3	5,062	8.045	0.00002	204.46	120
Calibrated unconfined (SLMB-U)							
SLP_MI	1	3	15,477	12.874	0.30000	378.43	201
NLP_MI	1	3	13,570	9.881	0.10000	385.36	409
UP_MI	1	3	10,494	23.098	0.10000	440.19	50
NE_WI	1	3	11,756	20.729	0.10000	440.81	57
SE_WI	1	3	4,079	13.207	0.10000	265.35	103
N_IND	1	3	4,737	30.680	0.30000	440.51	211
NE_ILL	1	3	5,209	9.942	0.30000	151.41	100

Table 9–2. Pennsylvanian aquifer layers.

Subregion	Minimum layer	Maximum layer	Number of cells	Geometric mean Kh	Minimum Kh	Maximum Kh	Average thickness
Initial confined (STF2sCFX)							
SLP_MI	5	6	5,969	5.126	0.27140	17.25	305
NLP_MI.	5	6	3,948	6.788	0.30000	9.83	431
Calibrated confined (SLMB-C)							
SLP_MI	5	6	5,969	5.864	0.41068	23.95	305
NLP_MI	5	6	3,948	8.581	0.45396	12.15	431
Calibrated unconfined (SLMB-U)							
SLP_MI	5	6	5,969	4.749	0.35942	22.25	305
NLP_MI	5	6	3,948	8.793	0.35942	14.80	431

Table 9–3. Marshall aquifer layers.

Subregion	Minimum layer	Maximum layer	Number of cells	Geometric mean Kh	Minimum Kh	Maximum Kh	Average thickness
Initial confined (STF2sCFX)							
SLP_MI	8	8	10,150	10.047	0.00001	20.00	201
NLP_MI	8	8	6,714	5.011	5.00000	15.00	183
Calibrated confined (SLMB-C)							
SLP_MI	8	8	10,150	13.904	0.00001	38.55	201
NLP_MI	8	8	6,714	4.255	4.23592	38.55	183
Calibrated unconfined (SLMB-U)							
SLP_MI	8	8	10,150	12.112	3.94838	28.74	201
NLP_MI	8	8	6,714	3.964	3.94838	27.01	183

Table 9–4. Silurian-Devonian aquifer layers.

Subregion	Minimum layer	Maximum layer	Number of cells	Geometric mean Kh	Minimum Kh	Maximum Kh	Average thickness
Initial confined (STF2sCFX)							
SLP_MI	10	12	15,477	1.483	0.46691	1.96	2,312
NLP_MI	10	12	13,570	1.704	1.44081	1.97	4,898
UP_MI	10	12	2,605	1.449	0.00001	5.00	244
NE_WI	10	12	3,765	2.604	0.00001	9.09	285
SE_WI	10	12	2,995	3.170	0.44622	9.09	173
N_IND	10	12	4,737	1.142	0.88001	1.60	719
NE_ILL	10	12	5,184	3.364	0.00001	9.09	112
Calibrated confined (SLMB-C)							
SLP_MI	10	12	15,477	1.586	0.50908	2.06	2,312
NLP_MI	10	12	13,570	2.073	1.54374	4.25	4,898
UP_MI	10	12	2,605	2.604	0.33129	6.12	244
NE_WI	10	12	3,765	3.816	0.37803	9.50	285
SE_WI	10	12	2,995	3.467	0.40476	9.50	173
N_IND	10	12	4,737	1.122	0.70956	1.66	719
NE_ILL	10	12	5,184	3.392	0.00001	8.95	112
Calibrated unconfined (SLMB-U)							
SLP_MI	10	12	15,477	1.844	0.56456	2.38	2,312
NLP_MI	10	12	13,570	2.242	1.79693	3.28	4,898
UP_MI	10	12	2,604	2.507	0.45481	6.08	242
NE_WI	10	12	3,760	3.666	0.81918	10.09	285
SE_WI	10	12	2,995	3.277	1.09764	10.09	173
N_IND	10	12	4,737	1.328	0.66663	1.94	719
NE_ILL	10	12	5,183	3.676	1.01007	6.45	112

Table 9–5. Cambrian-Ordovician aquifer layers.

Subregion	Minimum layer	Maximum layer	Number of cells	Geometric mean Kh	Minimum Kh	Maximum Kh	Average thickness
Initial confined (STF2sCFX)							
SLP_MI	14	20	15,477	1.216	0.50049	1.79	2,909
NLP_MI	14	20	13,570	1.293	0.81217	1.68	3,911
UP_MI	14	20	10,148	1.871	0.06450	8.92	442
NE_W	14	20	11,750	1.786	0.22068	8.92	428
SE_WI	14	20	4,079	1.578	0.14693	5.60	1,216
N_IND	14	20	4,737	0.746	0.46799	1.20	2,679
NE_ILL	14	20	5,209	0.760	0.22586	2.45	3,578
Calibrated confined (SLMB-C)							
SLP_MI	14	20	15,477	0.774	0.25028	1.37	2,909
NLP_MI	14	20	13,570	0.595	0.19086	1.01	3,911
UP_MI	14	20	10,148	1.600	0.05670	14.67	442
NE_WI	14	20	11,750	1.694	0.13499	14.67	428
SE_WI	14	20	4,079	1.979	0.06284	18.34	1,216
N_IND	14	20	4,737	0.509	0.21511	1.38	2,679
NE_ILL	14	20	5,209	1.601	0.73435	3.86	3,578
Calibrated unconfined (SLMB-U)							
SLP_MI	14	20	15,477	0.705	0.26148	1.18	2,909
NLP_MI	14	20	13,570	0.574	0.20359	0.91	3,911
UP_MI	14	20	10,148	1.828	0.23072	18.23	438
NE_WI	14	20	11,750	1.692	0.15000	15.66	428
SE_WI	14	20	4,079	1.954	0.04506	20.49	1,216
N_IND	14	20	4,737	0.488	0.18389	1.68	2,679
NE_ILL	14	20	5,209	1.918	0.87250	3.56	3,578